LAMP PUMPED Nd:YAG LASER

Space-Qualificable Nd:YAG Laser For Optical Communications

Prepared by

Kevin B. Ward
Principal Investigator

Approved by

D.H. Pollock
Executive Director
Systems Group

Holobeam, Inc.
560 Winters Avenue
Paramus, New Jersey 07652

FINAL REPORT

May 1973

Prepared for

GODDARD SPACE FLIGHT CENTER
Greenbelt, Maryland 20771

FOREWARD

This report is the Final Engineering Report summarizing the work performed on NASA Contract NAS 5-11461 entitled "Lamp Pumped Nd:YAG Laser - Space Qualified Nd:YAG Laser for Optical Communications", covering the period 15 June 1971 to 21 July 1972. This report was prepared by the Systems Group of Holobeam, Inc., Paramus, New Jersey. The Principal Investigator on the program was Mr. Kevin B. Ward. Other contributers on the program were Mr. David H. Pollock, Executive Director of the Systems Group, Mr. Tobias Trifon, Lamp Fabrication Manager, Mr. Robert Kraushaar, Senior Scientist and Dr. Harlan Cook, Physicist.

The author wishes to acknowledge the contributions of Mr. Lee Gallagher for the development of the vapor pressure relationships between K-Rb mixtures and of Dr. James Boyden, Dr. Robert Pressley and Dr. James Murray of the Laser Products Group for their invaluable support and guidance during the cavity design and test phase. The author is also indebted to Mrs. Jean Tucker and Mrs. Suzanne Stagg who typed and corrected the drafts of this report and the monthly progress reports.

All the work performed under this contract was administered by the NASA Goddard Space Flight Center, Greenbelt, Maryland, Mr. T. Johnson was the Principal Technical Representative.

ABSTRACT

This report presents the results of a program concerned with the design, fabrication and evaluation of alkali pump lamps for eventual use in a space qualified Nd:YAG laser system. The study included evaluation of 2mm through 6mm bore devices. Early in the program it was determined that the 2 and 3mm lamp would be inadequate to meet the system performance requirements and therefore were not studied in depth as part of this contract effort. Work performed on another contract is presented summarily however for completeness. Primary emphasis was placed upon the optimization of the 4mm bore lamp and later on the 6mm bore lamp.

As part of this effort, reference was made to the Sylvania work concerned with the theoretical modeling of the Nd:YAG laser. Early in the program assumptions were made for the key parameters (α_o, P_o & dK) and anticipated performance levels were calculated. Based on actual measurements, these parameters were later reevaluated to match the observed performance. With the knowledge gained, a projection of laser performance was made based upon realistic lamp parameters which should easily be achieved during following developmental efforts.

Measurements were made on the lamp performance both in and out of the cavity configuration. One significant observation was that for a constant vapor pressure device, the spectral and fluorescent output did not vary for vacuum or argon environment. Therefore, the laser can be operated in an inert environment (eg. argon) with no degradation in output. Because of this observation, a slightly different interpretation was given to the parameter P_o.

Laser output power of 3.26 watts at 430 watts input was obtained for an optimized 4mm bore lamp. This data was obtained with a 4mm x 50mm rod and a 3% output mirror and had a transfer characteristic with a slope efficiency of 2.2%. Similar data taken with the same rod and a 2% mirror yielded 2.94 watts output for 435 watts input with a 1.55% slope efficiency. When a non-optimized 6mm bore lamp was used with the above combination (4mm x 50mm rod and 2% mirror), 3.7 watts output with 490 input and a slope efficiency of 1.65% was obtained.

For the above lamp, mirror and rod combinations, the laser threshold occurred between 120 and 200 watts with the higher output coupling (transmission) producing the higher thresholds. For 3mm rods and a 1% output coupling mirror laser thresholds between 70 and 90 watts was observed for lamps with optimum fills.

TABLE OF CONTENTS

TABLE OF CONTENTS (Cont'd.)

APPENDIX

LIST OF ILLUSTRATIONS

LIST OF ILLUSTRATIONS (Cont'd.)

LIST OF ILLUSTRATIONS (Cont'd.)

SECTION I

INTRODUCTION

1.1 General

An important advance required in the production of a space qualified Nd:YAG laser system is the development of a high efficiency pump lamp. This report covers the results of the research and development phase to produce such a lamp for this application.

The object of the program is to supply NASA with the data and results of the design, fabrication and test of high efficiency lamps for use in a mode locked Nd:YAG laser operating at an output wavelength of 1.06μ and an output of 4-10 watts. This program was to include:

a) Theoretical analysis of laser cavity performance using an alkali pump lamp.
b) Design and fabrication of several pump lamp configurations using various diameter envelopes.
c) Optimization of the potassium-rubidium alkali fill to the Nd:YAG absorption spectrum for high pumping efficiency.
d) Measurement of multi-mode output powers.
e) Measurement of single-mode output powers.

The above tasks were all performed and the results are presented in the following sections.

1.2 Technical Discussion

In this section the past developments in lamp pumping of Nd:YAG lasers will be highlighted and compared to the goals of this program. From this comparison, areas needing improvement will be discussed and realistic objectives will be established.

Since the discovery of 1.06 micron radiation from the Nd:YAG laser in 1964 there has been a continual effort to find more effective means of pumping this material. One of the early devices used for pumping of the Nd:YAG laser is the tungsten halogen filament lamp. These lamps operate typically with filament temperatures at 3200°K to 3400°K with only 3% of the output radiation below 1.0 microns being effective in pumping the Nd:YAG crystal. Tungsten filament lamps are therefore relatively inefficient as pumps for this application. Efficiencies in the

region of 1.5% and lasing thresholds between 400 and 600 watts have been reported.[1] One advantage in the use of tungsten-halogen lamps is the low cost per unit. This is offset however by the short lifetime (100 hours) and the nature of the long delicate filament which is vulnerable to vibration failure. Therefore, the tungsten filament lamp is unacceptable for a space borne application.

The next pump lamps considered were the inert gases which are rich in line structure in the near infrared. Xenon has the highest overall conversion efficiency and is commonly used in arc lamps. However, the infrared line spectra of xenon misses all of the Nd:YAG pump bands. Krypton was shown to be superior for pumping Nd:YAG by Reed[2] since two of its strongest emission lines (7600Å and 8110Å) are strongly absorbed by the laser crystal. At low input powers a 3.3% laser efficiency has been attained while at input power levels of 3 to 4 kilowatts efficiencies in the range of 4% have been reported. These lamps also typically have laser thresholds of 400 to 600 watts. Krypton lamps also are not useful for space applications because of their short operating life (less than 100 hours) and their need for a water cooled environment.

With the widespread introduction of metal halide lamps for commercial lighting applications, researchers were given a new tool with which to work. Investigations by Reiling[3] and Waymouth et al[4] demonstrated the changes in spectral output that could be achieved by adding various metal iodides to mercury arcs. A study of metal halides and alkali metals for use in pumping Nd:YAG lasers was carried out by Liberman, Church, Schlecht et al[5, 6, 7]. Their findings showed that the alkali iodide additives (potassium and rubidium in particular) when operated at pressures to produce broadening of the self resonance lines closely matched the Nd:YAG absorption bands at 0.73 to 0.76 microns and at 0.79 - 0.82 microns. These lamps yielded efficiencies of 2.5-3.5% and laser thresholds between 300 and 400 watts.

The above lamps had to use iodide forms of the alkali metals since they were quartz enveloped devices and could not withstand direct alkali attack. For most metals, it is preferable to use the halogen form since it has a lower vapor pressure than the corresponding pure metal. In the case of alkali metals however, the reverse is true, namely, the pure metal has a lower vapor pressure than the halogen form. Therefore, it becomes more desirable to use the pure form since lower temperatures are required to produce equivalent vapor pressures. As had previously been stated, the pure form of the alkali metal can not be contained in a quartz device because of the corrosive attack on the envelope. A suitable material for containment of the alkali discharge is pure alumina (Al_2O_3). This material is available in two forms polycrystalline and

single crystal (sapphire). The polycrystalline form is unacceptable becuase the diffuse envelope scatters the radiation passing through it and reduces the brightness of the lamp. A transparent single crystal sapphire envelope must therefore be used to achieve low threshold pumping of the Nd:YAG crystal.

This is the current status of lamp development for pumping of Nd:YAG lasers and forms the primary objective for this program. The foremost goal of this program is to develop a sapphire enveloped alkali pump lamp and by careful matching of the fill material to yield high laser efficiencies.

The program which was undertaken to fulfill this goal is described in detail in the following sections.

SECTION II

LASER CAVITY CONSIDERATIONS

2.1 Theoretical Optimum Cavity Performance

In view of the revised estimates of efficiency for the Rb-K pumping lamp, it is necessary to review the choice of laser parameters to optimize laser performance. To facilitate comparison, the definitions employed in the Sylvania[8] work will be used here also.

From a simple rate equal approach, the following result can be obtained for CW laser output power in terms of laser and pump lamp parameters:

$$P_{out} = \left(\frac{\pi}{4A\beta}\right) (Kd) \left(\frac{Td}{\alpha}\right) \left(P_{in} - P_o - \frac{\alpha}{K}\right) \qquad (1)$$

where

$\frac{\pi}{4A\beta}$ = non-optimizable parameter depending on the transition cross-section of the 1.064μ lasing transition and its upper state lifetime.

Kd and P_o are the slope and linear intercept of the power out curve for the pumping lamp. The slope includes the efficiency of the pumping cavity as well as the effective overlap between the emission lines of the lamp and the absorption lines of the rod.

T = output mirror transmission
α = total single pass loss in the laser resonation; $\frac{T}{2} + \alpha_o$
α_o = single pass dissipative loss
d = laser rod diameter
$P_{th} = P_o - \frac{\alpha}{K}$ = pump power required for laser to reach threshold
P_{in} = input power to pump lamp.

For optimum laser performance, we will maximize lamp efficiency, Kd, and minimize P_o and dissipative losses, α_o. Therefore, the only optimizable parameters remaining are d and T, the rod diameter and output coupling, respectively.

If both d and T are optimized for maximum output power, the following relation results:

$$P_{out} = \left(\frac{\pi}{32} \frac{1}{\beta A \alpha_o}\right) (dK)^2 \left(P_{in} - P_o\right)^2 \qquad (2)$$

This clearly indicates the importance of the lamp characteristics on the laser performance. The optimum choice of the other parameters depends very strongly on these pump characteristics. The best estimate of the characteristics of the new K-Rb lamps is

$Kd = 0.15 cm/KW$
$P_o = 23$ watts.

This is almost twice the efficiency of the pure K lamp on which Sylvania based their design. The linear intercept, P_o, is assumed to be the same, since the heat loss should be about the same for the new lamp. Assuming the parameters for this lamp, equation (2) is plotted (dashed curve) in Figure 1. A dissipative cavity loss of 0.6% per pass has also been assumed; this is the estimated minimum we can achieve. From this figure we can obtain the minimum power input required to attain a desired output power with a pumping lamp of these characteristics. It should be emphasized that this gives total output power at 1.06μ, with unrestricted mode structure and polarization. Also, each point on the dashed curve represents different rod diameter and output transmission.

The three solid curves in Figure 1 are optimized curves for 3 different fixed rod diameters 2, 4, and 8mm. Again, each point on these curves represents a different optimized output transmission. For comparison, Figure 2 shows power out as a function of power in only, for the same three rod diameters, and with the transmission optimized for 150 watts input.

To illustrate the dependence on rod diameter more clearly, Figure 3 shows power output vs rod diameter for two values of dissipative cavity loss and at a fixed input power of 150 watts. The difference in these two curves indicates the relative sensitivity of the laser to increases in dissipative loss due to, for instance, degradation of the optical components. Thus, a 4 or 6mm rod will give considerably more output, but will also be much more sensitive to increases in α_o than a 2mm rod.

An indicator of this sensitivity to increases in α_o is provided by the magnitude of the unsaturated gain relative to α_o. The larger this relative difference, the less sensitive the laser is. The unsaturated gain is also plotted in Figure 3. It is the unmarked curve, and its values are given by the right hand ordinate.

Figure 3 shows that the optimum rod diameter for maximum power output is different for the two values of α_o. Thus, α_o also effects the choice of rod diameter. Figure 4 shows the variation of output power with α_o for the three rod diameters. Again the characteristics of the new lamp were used at an input power of 150 watts, and the output coupling is assumed optimized.

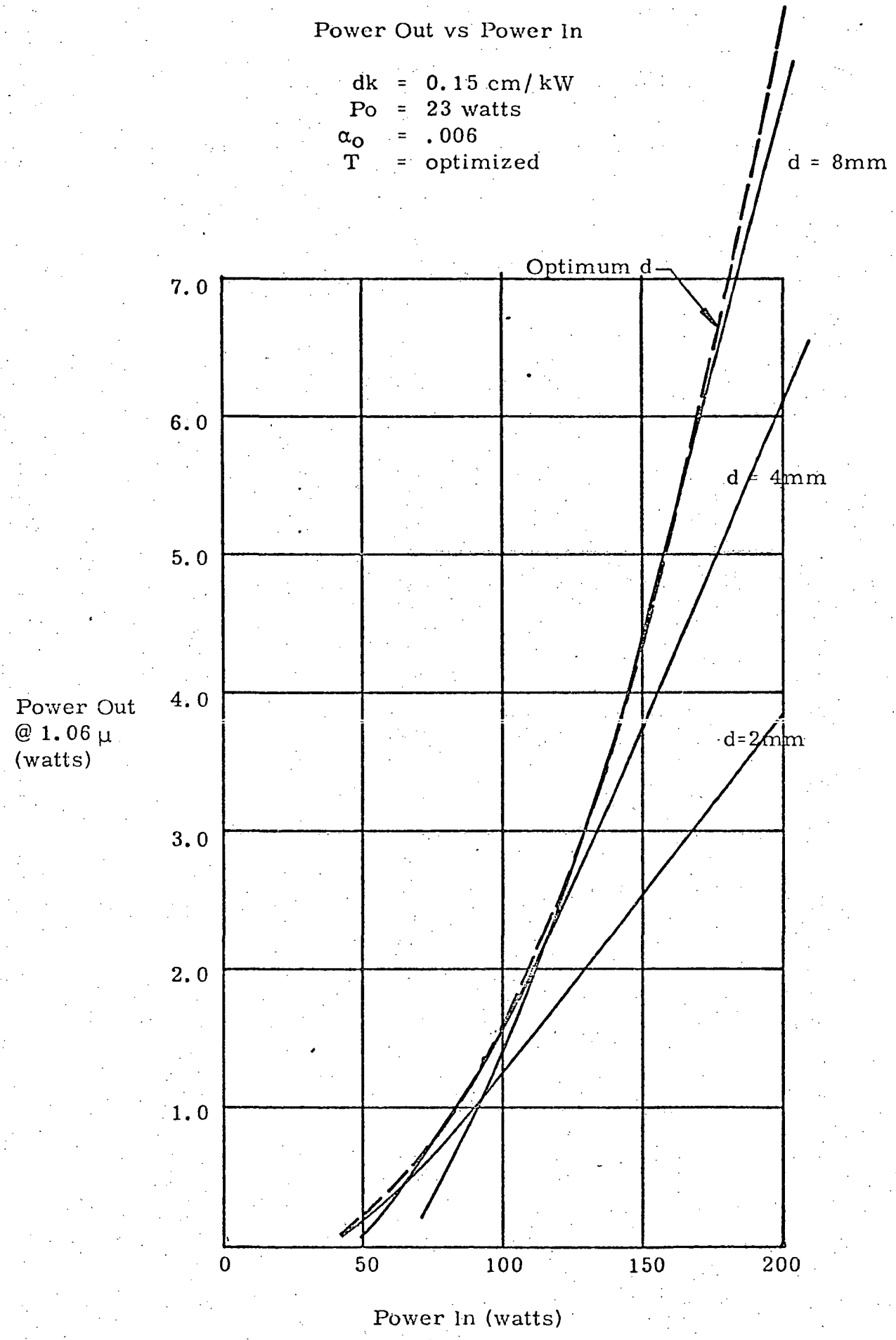

Figure 1 Power Transference

Power Out vs Power In

dk = 0.15 cm/kW
Po = 23 watts
α_o = .006
T optimized for Pn = 150 watts

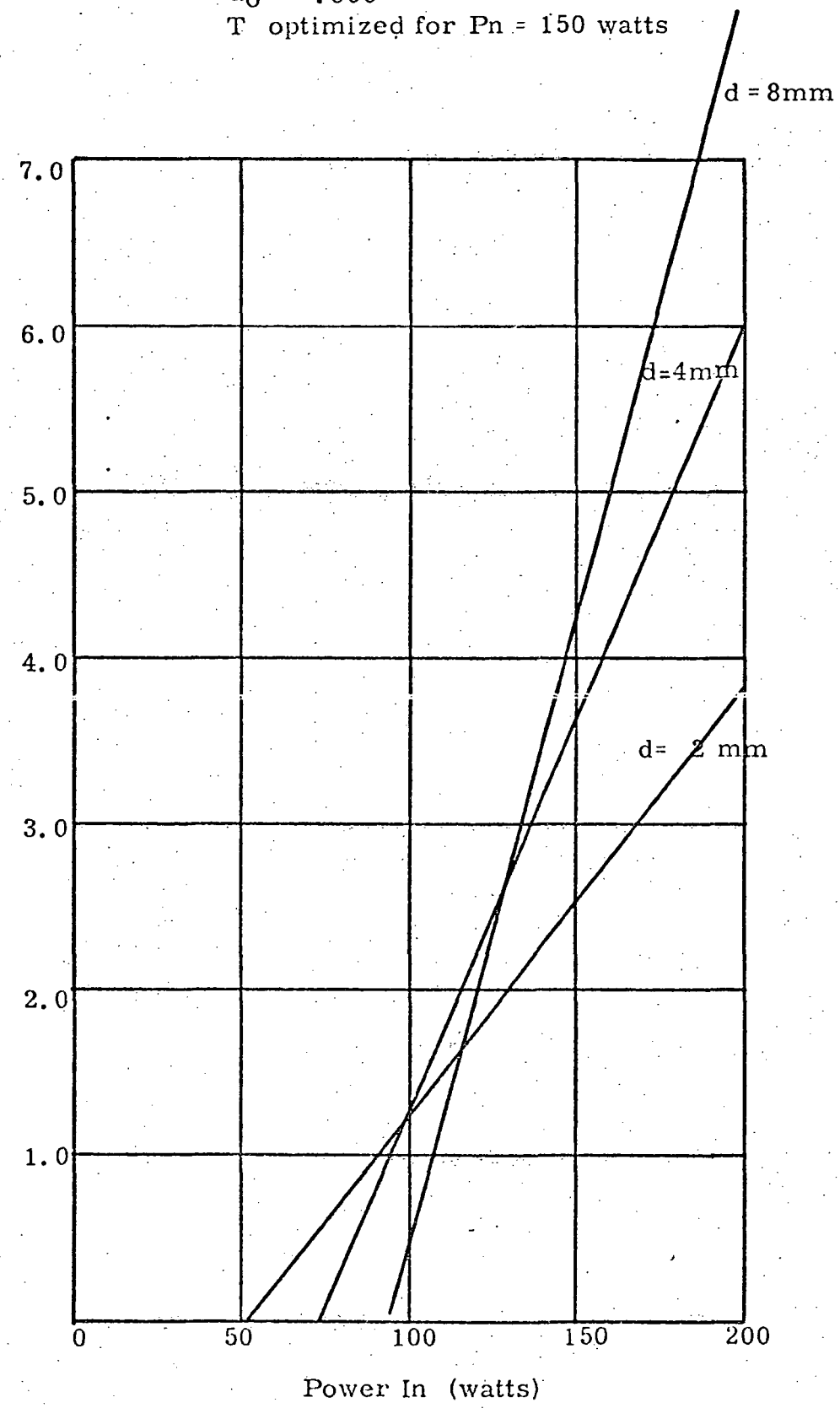

Figure 2 Optimized Power Curves

Power Out vs Rod Diameter

for dk = 0.15 cm/kW
α = .006 @.008
Pin = 150 watt
Po = 23 watt

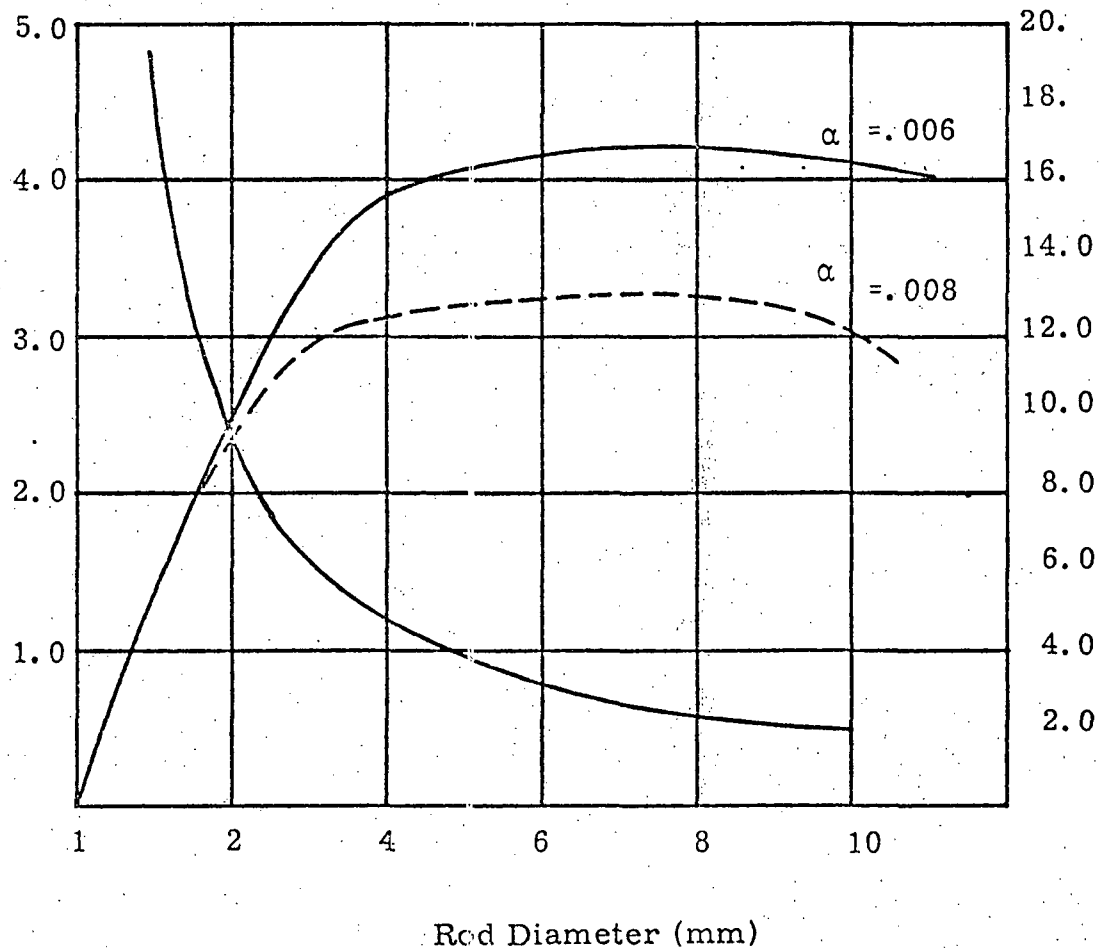

Figure 3 Unsaturated Gain

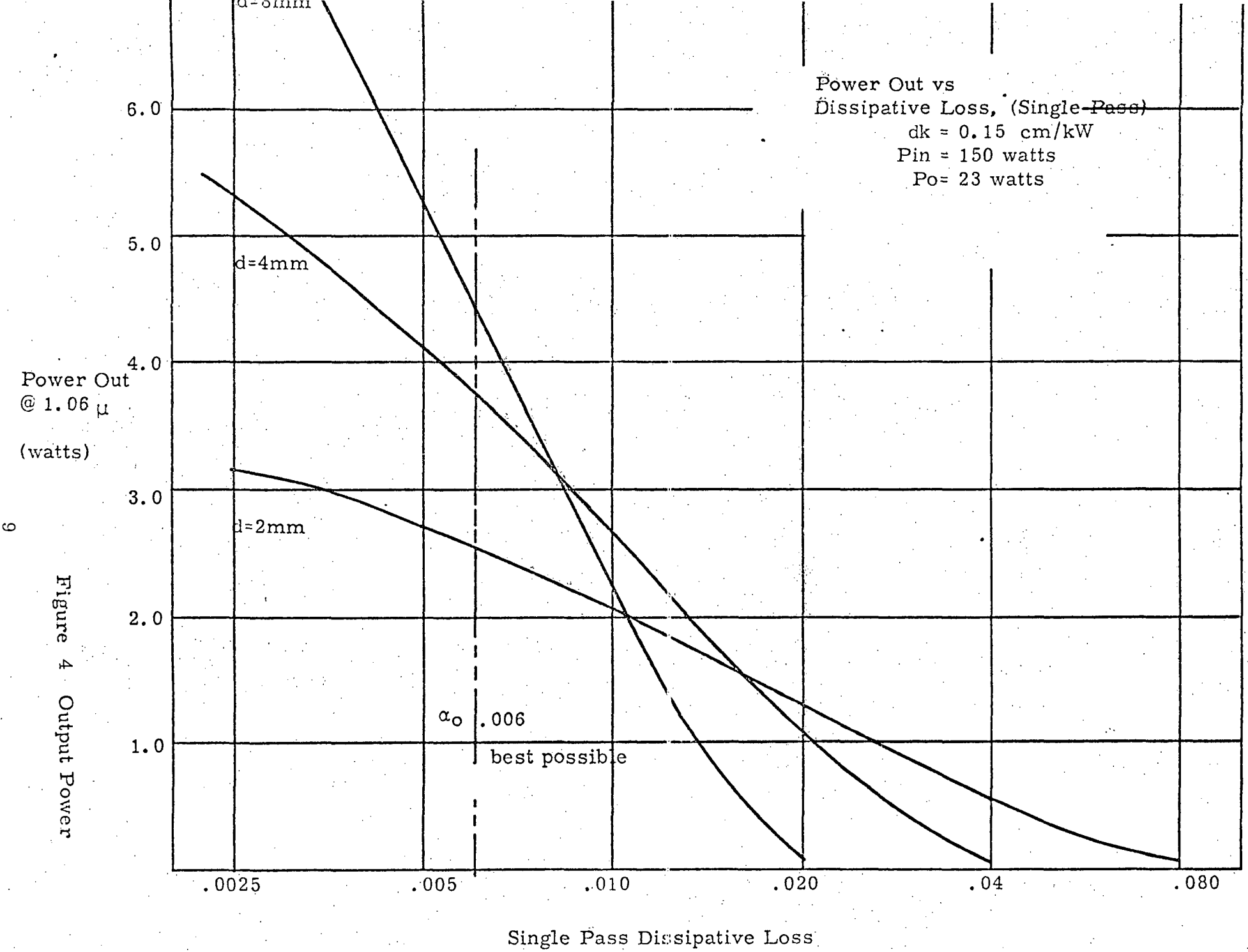

Figure 4 Output Power

In conclusion, a choice of 4mm for the rod diameter seems to provide a good compromise between power out and sensitivity to increases in α_o for this new pumping lamp. For 150 watts input and a dissipative loss of 0.6% per pass, this rod should give an unpolarized, multi-mode output of 3.8 watts.

The above discussion represents the results of a tradeoff analysis conducted during the first few weeks of the contract. All of the conclusions reached and data presented was based on assumptions related to anticipated lamp performance and capabilities. These assumptions were very ambitious goals for the lamp to achieve. Section 6.4 presents a comparison of the data shown here to actual measured data and discusses their differences.

2.2 Laser Performance Test Facility

The laser test facility is composed of two basis systems. The first system consists of a stainless steel vacuum/inert atmosphere chamber measuring 14 inches in diameter and 39 inches long. This chamber is connected to a 1000 liter/minute mechanical pump by a 4" line. In the line is a 4 inch right angle liquid nitrogen cold trap. The vacuum pump-cold trap combination permits the chamber to be pumped below 1 micron. Once the chamber is evacuated, a small valve allows the chamber to be backfilled with any desired inert gas.

Incorporated in the chamber are four viewing ports. Two of these ports are pyrex and are located in such a manner as to allow for the viewing of the front and rear of the laser cavity. This feature is useful for monitoring the operating condition of the lamp and allows one to visually monitor the output lamp spectra by use of a hand held spectrometer and an IR viewer. Using these instruments lamp spectra from 4000Å to 11,000Å was able to be visually observed. During lamp operation, the spectra between 7000Å and 8500Å was of greatest interest because of the change occurring in the potassium and rubidium resonance lines and therefore was the only region actually visually monitored. The remaining two ports are made of quartz and are aligned to the optical axis of the laser cavity. Output laser power is measured at the front port and lamp spectra can be recorded at the rear port.

The front cover of the chamber has feedthroughs for the connection of cooling water, lamp power, four heaters, eight thermocouples and one high voltage thermocouple. In addition, the front cover is mounted on sliding tracks which allows easy access to the laser cavity for mounting and adjustment.

The laser cavity is mounted to a guide rail attached to the sliding track and consists of two movable mirror mounts, two adjustable lamp holders and the laser head. The two mirror mounts are capable of x-y axis alignment to the laser rod and also allow for ease of interchangeability of various reflectivity mirror elements. In order to optimally align the pump lamp to the laser rod, x-y axis position adjustments were also incorporated into the lamp holders. These features prove to be useful in maximizing the laser power output once threshold is achieved.

The laser head itself consists of a goldplated elliptical reflector and a suitable rod holder. The ellipse has a 3 inch major axis, a 2-5/8 inch minor axis and a 2 inch depth. To obtain optimum coupling, the laser rod and lamp are positioned at the conjugate foci with the rod held stationary inside a water cooled Uranium #3320 glass flow tube. Once the water passes the rod, it is circulated through two flat gold coated end plates which are used to complete the reflector enclosure. Since water is maintained at a temperature of 50^{o}F both the laser rod and cavity are sufficiently cooled to prevent thermally induced changes in laser threshold and power output. A full scale representation of the elliptical cavity is shown in Figure 5.

The original tests were performed in the cavity which contained a 1.25 inch lamp clearance hole in the end plates. This clearance hole was originally included so that the cavity could accommodate a wide variety of lamp configurations. As the program progressed and the lamp became standardized, it was determined that output power could be increased by minimizing the diameter of the clearance hole. Figure 6 presents data for a non optimum lamp showing the increase in output power for the closed down holes. This modified cavity configuration was used in all of the final lamp performance evaluations.

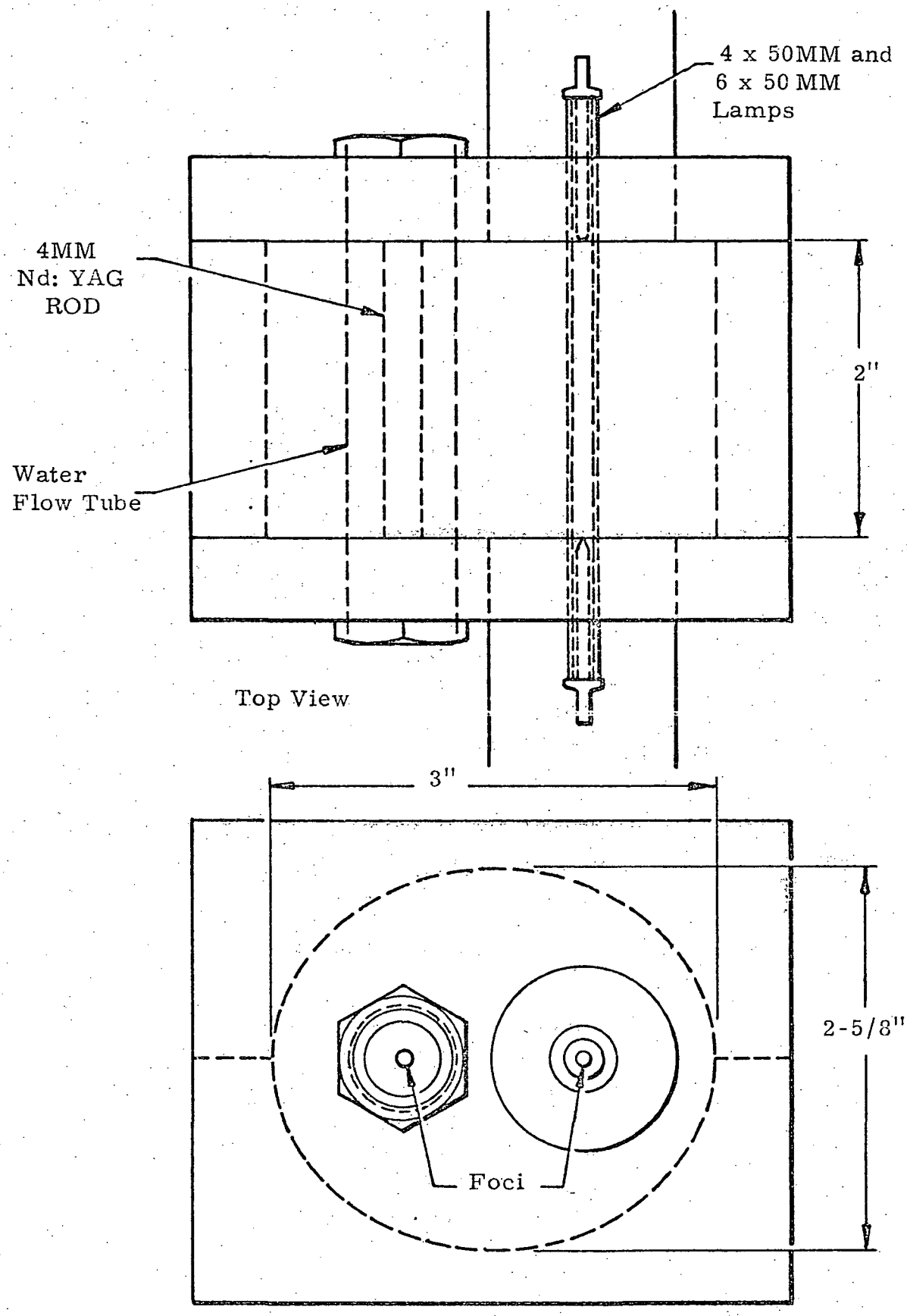

FIGURE 5 LASER CAVITY CONFIGURATION

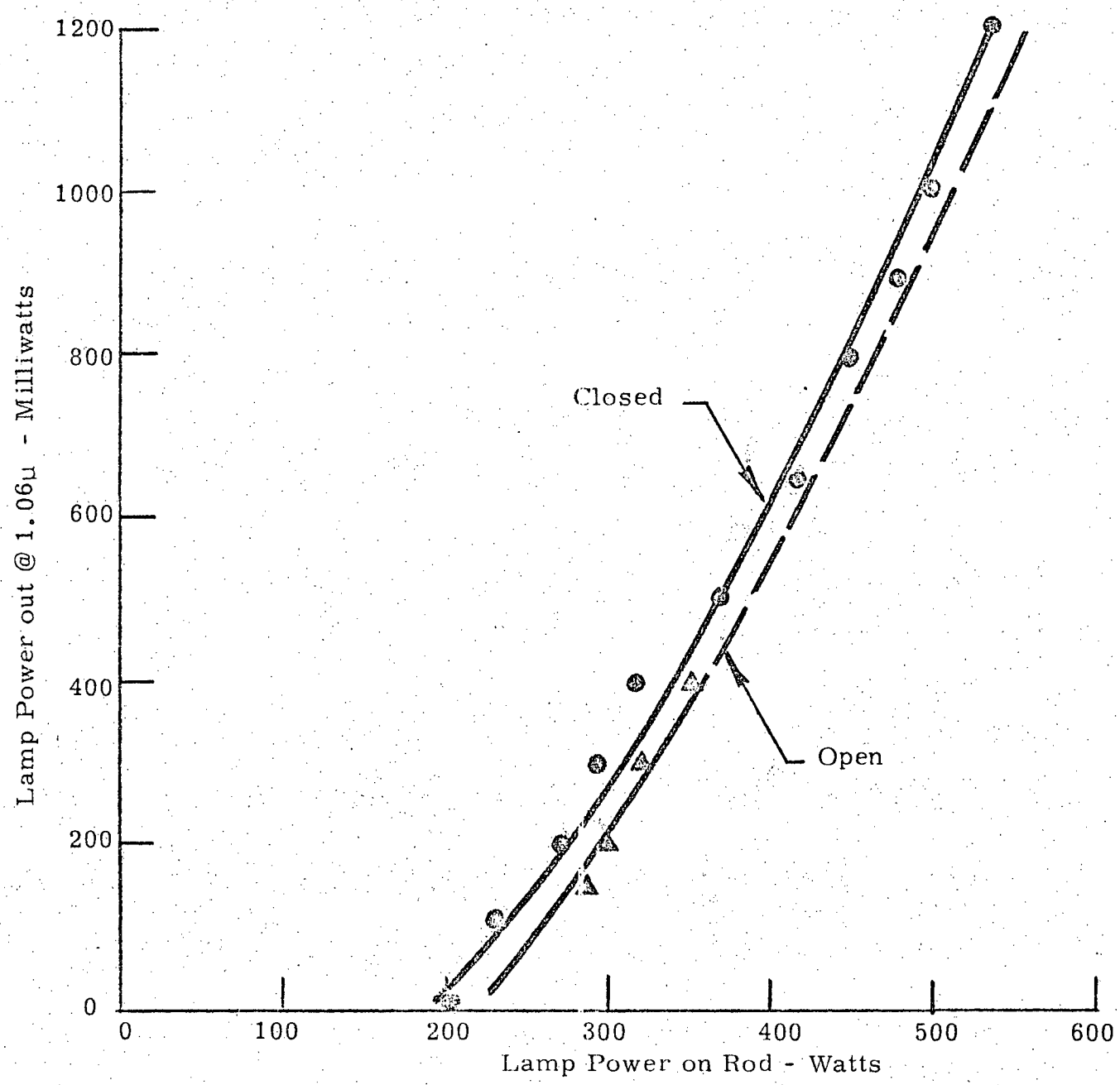

FIGURE 6 LASER POWER OUTPUT

SECTION III

LAMP DEVELOPMENT

3.1 Lamp Design and Construction

Figure 7 is a diagram of a typical sapphire frit sealed alkali pump lamp. All the lamp envelopes used in this effort were made from 4 and 6 mm bore sapphire tubing. The 4 mm bore had both tubular drawn (TDS) and core drilled (CDS) envelopes. The tubular drawn refers to the fact that the sapphire is grown in tubular form directly from the melt. Initially, the use of this tubing seemed to be an ideal solution to the envelope materials problem since it can be drawn to any required length and therefore eliminates the need for machining the lamp envelope from a solid boule of single crystal sapphire. However, as the program progressed, this sapphire presented several serious drawbacks which require additional investigations before an absolute determination can be made. These drawbacks will be presented in appropriate sections where their influences were most felt. The dominant advantage in the use of direct grown sapphire for lamp envelopes is cost since this material is considerably cheaper than using envelopes machined from boules of single crystal sapphire.

The electrodes used were fabricated from pure tungsten machined to the required shapes. A disadvantage in the use of pure tungsten is the higher work function of the pure material compared to the thoriated material. This higher work function initially results in a lamp which is slightly harder to start but does not affect operation once the stable condition of operation is achieved due to the alkali coating of the electrodes, which lowers their work function. The advantages in the use of pure tungsten are the ability to process the material at high temperature to achieve low gas poisoning and the material stability in an alkali environment. Typical electrodes are shown in Figure 8.

The last main component of the lamp is the flanges which are made of either nickel or niobium depending on the type of ceramic to metal seal being made. The flanges are discussed in greater detail under seal fabrication below.

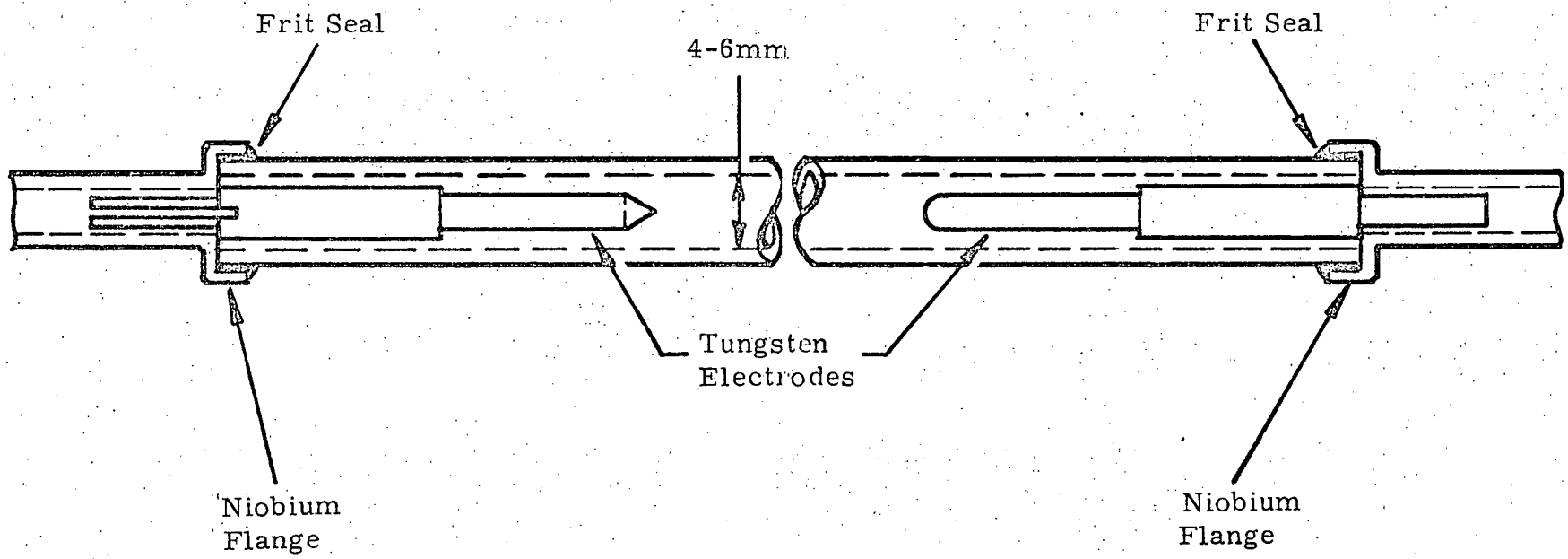

FIGURE 7 SAPPHIRE FRIT-SEALED ALKALI PUMP LAMP

ANODE

Pure Tungsten

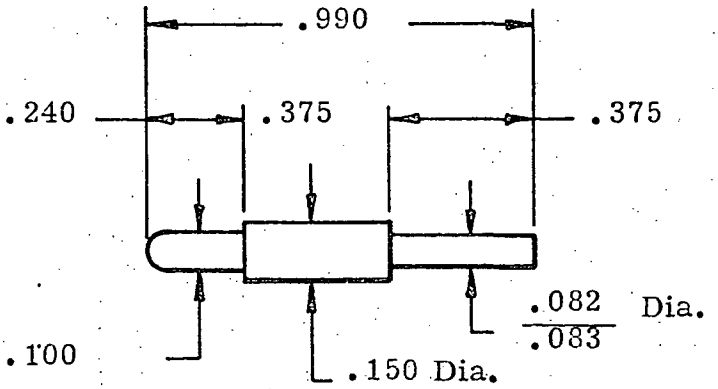

Ball Radius on Anode, must be polished, no ridges visible.

CATHODE

Pure Tungsten

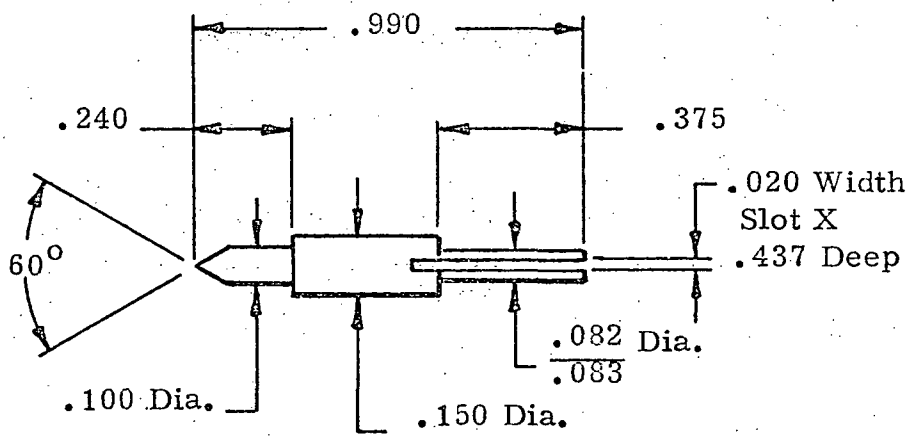

Cathode Tip must be free of chips, breaks, ridges must be polished.

Figure 8

Details of Typical Electrodes For 4mm Bore Lamp

3.2 Seal Investigations

During this contract effort, three types of seals were investigated for making the ceramic to metal bond.

(1) Copper Seals

The first bond used was the copper circumferential radial compression seal. In order to fabricate this seal, the envelopes must first have metalized bands applied to the sapphire. The metalization used was a tungsten-yttrium mixture. It was in this process, that the first problem area became evident. All the sapphire material sent for metalization cracked during the sintering process. This occurrence was considered unusual since sapphire tubes metalized on previous occasions were returned in satisfactory condition. Assuming this to be a one time breadkage, the sapphire tubes were replaced and another metalizing process was initiated. The results however were a repeat of the first attempt. Discussions with both the metalizer and the sapphire manufacturer produced no useful solution to the breakage problem. Since sapphire metalization is an integral step in the copper seal process. Holobeam has expended considerable effort in attempting to find another source of this service. Several potential vendors had been contacted and samples were sent for experimentation. In the beginning, these vendors were all hopeful and optimistic that either by using the same formulation or by using their own proprietary techniques, they could achieve the desired goals. However, at this time it must be reported that all attempts were unsuccessful and that at best metalization remains a risky process with only one company having demonstrated the ability to achieve limited success.

Since there was difficulty in obtaining satisfactory metalizing services, it was decided that lamps with copper seals would be fabricated only from previously metalized 4mm bore material on hand. The copper seal lamps use nickel or kovar flanges and nickel reservoirs. These devices are capable of air operation and therefore make for convenient experimental lamps. The primary advantage of air operation at this time is the ease of accessibility to the laser head for both external mirror adjustments and lamp position adjustments within the ellipse. The disadvantage of the copper seal is the limit of the temperature at which it can be maintained for extended periods of operation. The highest recommended temperature for long term operation is 600°C before degradation becomes a serious problem.

The failure mechanisms associated with a copper seal are hydrogen diffusion, grain growth and loss of mechanical strength. To minimize these effects and optimize seal lifetime, the seal should be operated at the lowest allowable temperature governed by the desired vapor pressure of the device. These vapor pressure requirements however often necessitate a reservoir temperature in the region of 500-575°C with a corresponding seal temperature of 525-600°C.

(2) Active Alloy Seals

Active alloy compensated butt seals have been successfully used by Holobeam on alkali devices incorporating polycrystalline alumina envelopes. These particular devices have survived average powers, pulse energies and seal temperatures far in excess of loading requirements anticipated for this program. However, the transition of the technologies previously developed to single crystal sapphire proved to be considerably more difficult than expected.

Efforts were undertaken to overcome the problems associated with achieving an active alloy seal since this type of bond offers several advantages over the copper seal. The first advantage is that the sapphire tubes do not have to be sent out for metalizing which eliminates one vendor operation. Another advantage is that the active alloy seal is stable in an alkali environment and therefore can operate at higher temperatures without concern about lamp contamination. The upper limit of operation of this seal has been determined to be between 900°C and 1000°C. One disadvantage to this type of lamp is that it incorporates niobium flanges which oxidize rapidly in an air environment at the operating temperatures associated with the lamp. Successful operation is only achieved when the lamp is running in either a vacuum or an inert atmosphere environment. This requirement places restriction on the adjustment which can be performed on the laser head with respect to mirror alignment and lamp position.

The active alloy braze is made as a compensated butt seal with a sandwich being formed by the sapphire tube, braze material, niobium flange, braze material and sapphire back-up ring. Because it would be extermely difficult to fabricate braze washers of the ternary alloy to the sizes required, it was decided to investigate ternary alloy dispersions available on transfer tapes. The two braze material combinations evaluated consisted of 60% Zr - 25% V-15% Cb and 65% Zr - 10% V - 25% Ti active ternary alloys.

During the early investigations, a successful braze and seal was not achieved since these materials did not properly "wet" the direct grown sapphire to form a reliable bond. This condition still resulted after many modifications were made to the time-temperature relationships used in the braze cycle. Sample brazes were then made utilizing Swiss manufactured single boule sapphire tubes. A successful leak tight braze was not achieved but there was excellent braze material flow and wetting of the sapphire. Vacuum tight seals should be achieved by determining the correct time-temperature cycle for the particular braze. It should also be noted at this time that the Swiss sapphire contains a small amount (1%) of titanium as an impurity. These impurities act as adhesion centers allowing the ternary bond and very good wetting of the sapphire. Since the direct grown sapphire is specified as being pure, it contains no impurities to act as adhesion centers for the active alloy. Continued investigations during the program did however produce evidence and promise that an active alloy seal could be developed for use with the direct gorwn sapphire. During one of the braze cycles, two pieces of 6mm bore by .030" wall sapphire were successfully bonded together to form a leak light seal using Holobeam's ternary alloy combination (56% Zr - 28% V - 16% Ti) and a greatly modified braze cycle. It should be emphasized that this was not a sapphire to metal seal but rather only a sapphire to sapphire seal. However, this development does show that wetting of the direct grown sapphire is possible and that with additional efforts, a successful active alloy seal could be mastered.

Because of the very limited success achieved with the active alloy sapphire seal further developmental efforts were discontinued.

(3) Frit Seals

With the active alloy lamp seal development being uncertain and the initial breakage rate associated with the copper seal lamp being excessively high at this time, it was decided to investigate an alternate ceramic to metal bond. The candidate chosen was a glass frit circumferential radial compression seal which turns out to be the easiest of the three to fabricate. The frit used initially on all lamps was type 1731, consisting of calcia-aluminate glass with a silica binder.

The first lamps fabricated for this program with the frit seal were made from 4mm bore sapphire tubes and niobium cup flanges. Details of a niobium cup flange are shown in Figure 9. The wall thickness of the flange material in contact with the sapphire tube was between .015 and .017 inch. During life test of these lamps,

seal failures occurred. Microscopic examination of the seal regions showed that the frit flow seemed to be undisturbed except for a small region where it may have parted from the niobium. In order to correct this mode of failure, the wall thickness of the niobium flange was decreased to between .008 and .010 inch. The decrease in thickness of the flange in the seal region should allow for greater material compliance during the thermal cycling of the seal and a corresponding reduction of thermally induced stresses in the frit interface. While these new lamps were being fabricated, a new occurrence developed. Some small longitudinal cracks appeared in several of the sapphire tubes just above the niobium flange. It was observed that these cracks did not always appear during the actual assembly but in some cases appeared several days later while the lamps were being stored in a warm oven prior to loading. When these lamps were examined, it was noted that some of the frit material had, because of capillary action, deposited itself in the annular space between the electrode and flange. To correct this problem and also to achieve greater material expansion matches, the wall thickness and shape of the flanges were again changed. These changes incorporated a reduction in wall thickness to between .004 and .005 inch, a closer fit of the niobium to the sapphire and a corner radius to reduce the chances of capillary action. The dimensions of the flange shown in Figure 9 reflects the above considerations. In addition, the method of applying the frit material was changed. The earlier lamps had the frit seal made in one step with additional material being applied only when a leak tight bond was not achieved. The new method is to apply the frit in four to six thin applications and gradually fill the voids to form a leak tight bond. Lamps fabricated using both the new flanges and frit application methodology have proved to be successful in solving the earlier problems.

The frit seal lamp offers many of the advantages of the active alloy lamp since the sapphire tubes do not have to be metalized and the seals can be operated at high temperatures. Another important advantage is the simplicity of fabrication associated with the frit seal. In addition, the frit seal can be repeatedly recycled and reworked until a leak tight bond is achieved which is unlike the copper and active alloy seals. In the copper seal, attempts to recycle a leaking seal has met with very limited success while with the active alloy seal, recycling is not feasible because of the chemical composition of the eutectics formed. The disadvantage is the same as for the active alloy seal since the niobium flange has to operate in either a vacuum or inert atmosphere environment. This only presents a problem in ease of ground based testing but has no effect on the final use and application of the device.

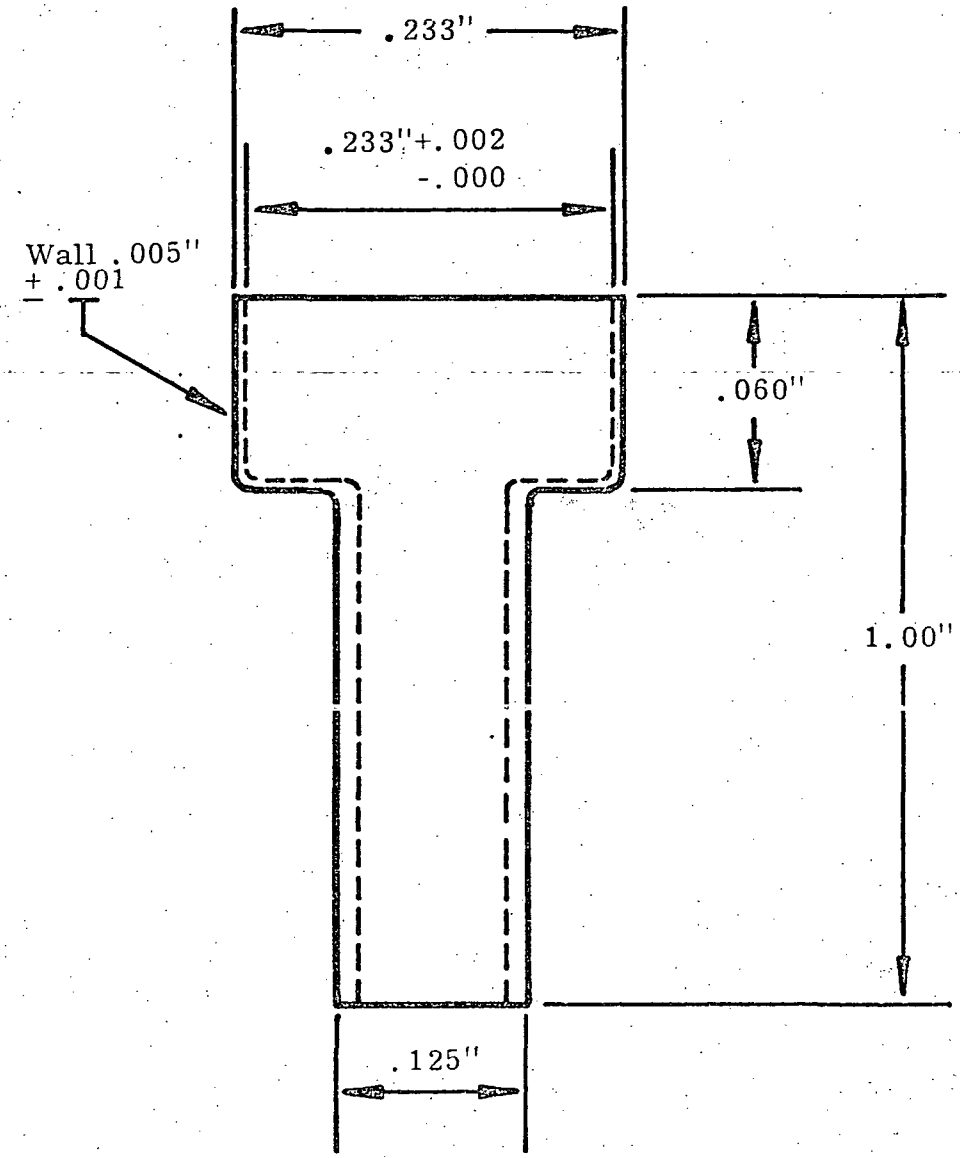

FIGURE 9 FLANGE DETAIL

Also during the program some lamps were made using a new experimental frit which contained no silica binder. However, because of a bad batch of flanges from the vendor, these lamps did not survive any extended life tests and no definite conclusion could be reached. This problem is discussed further in the lamp failure analysis section.

3.3 Final Lamp Processing

The greatest hazard to a lamp during its final stages of processing is the introduction of water vapor. The major purpose of final device processing is the removal of any traces of water vapor within the device prior to sealing off the device. At this point in the fabrication process, the lamp consists of assemblies which have all been subjected to extensive vacuum outgassing and chemical cleaning. But after subassembly processing they have been unavoidably exposed to air for however short the time. Due to normal atmospheric humidity the assembled lamp contains water vapor along with oxygen, nitrogen, hydrogen and CO before the final processing is initiated.

For the final processing the lamp is mounted on a vacuum port by a copper appendage. The vacuum port is attached to an ion pump as shown in Figure 10. The ion pump is attached to the interior of the lamp. The exterior of the lamp is surrounded by an oven and the entire exterior volume evacuated by an oil diffusion pump.

Before the oven is turned on the interior of the lamp is evacuated to 5×10^{-7} Torr. This usually requires several hours. The exterior pressure surrounding the lamp is pumped to at least 1×10^{-6} Torr. Then the oven is activated and the lamp heated to 500°C. The bake out is continued until the internal lamp pressure is reduced to 1×10^{-7} Torr at temperature. Then the oven is turned off. When the lamp temperature reaches ambient the exterior oil pump volume is opened to air. The lamp is then cold weld pinched off the vacuum system when the interior pressure has reached 5 to 7×10^{-8} Torr.

If water vapor is not entirely removed from the lamp interior water vapor cycles are initiated which have been well documented in the electron tube industry. Tungsten participates readily in a water vapor cycle by an oxidation - reduction reaction. During lamp operation the tungsten first reacts with water vapor traces to form tungsten oxide and atomic hydrogen. The tungsten oxide vaporizes from the electrode and condenses on the cooler parts of the envelope. Here it is reduced by atomic hydrogen to metallic tungsten with the reformation of water and the cycle repeats. The following equation describes the reaction.

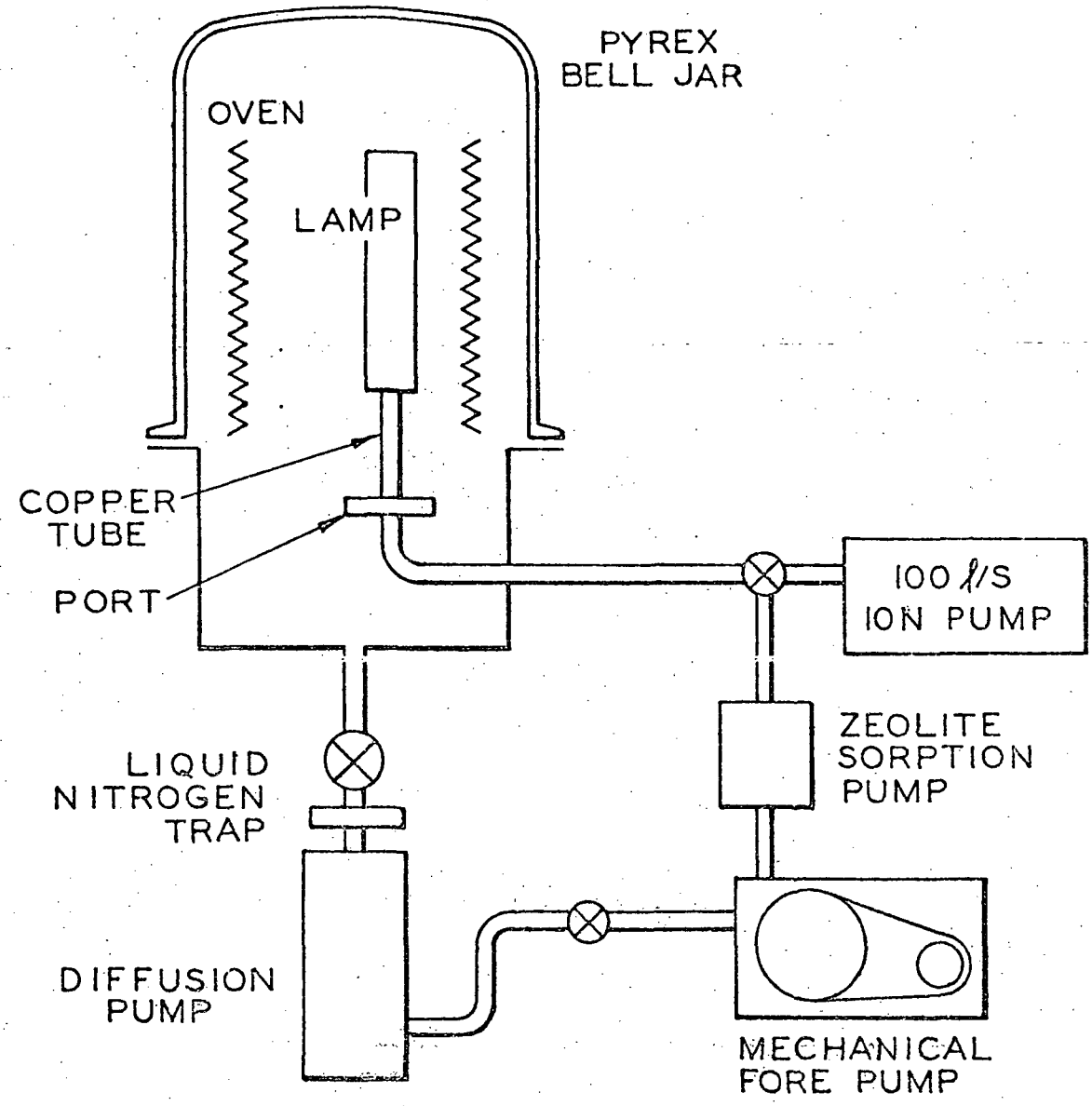

Figure 10

Schematic of Final Processing Station

$$W + 2H_2O \leftrightarrows WO_2 + 4H$$

This reaction often accounts for premature blackening of the envelope walls. Since this is a self feeding repetitive cycle, wherein even water vapor traces in the PPM range can have accumulative effects over a 10,000 hour period the cumulative effect could become significant. After the lamp has been vacuum outgassed it is pinched off the processing station and prepared for alkali metal loading.

3.4 Lamp Loading

During the course of the program, two methods of lamp loading were undertaken. The first method incorporated the use of a double reservoir. In this technique, the material with the higher vapor pressure (in this case rubidium) is placed in one of the reservoirs. The lamp is then heated in a vacuum oven and the temperatures adjusted zonally until the reservoir tip is the coldest point. The temperature of this point is then regulated to provide the proper vapor pressure of the material in the lamp. The lamp is then removed and the reservoir containing the surplus rubidium pinched off. Operation of the lamp in this condition at temperatures above the former reservoir tip temperature will yield a constant pressure (number density) device. As an alternative to this bake, the lamp could be operated and adjusted for desired vapor pressure. Now that a constant pressure rubidium fill is in the lamp, the second reservoir is opened and the potassium is inserted. Operation of the lamp now should result in a device with a constant pressure rubidium and a variable pressure potassium characteristic. Operation of several of these devices yielded spectrums which did not exhibit the above anticipated characteristic. Further analysis into the problem showed that Raoult's Law had to be applied to the mixture of these two materials and that the resultant vapor pressure was dependent on the mole fraction of the components. This analysis also indicated the wide variation which could be obtained using arbitrary amounts in a single mixture. A full discussion of this analysis is presented in Appendix I.

With the above information at hand, the second method of lamp loading was established. Based on preliminary data, the range of vapor pressure operation was selected. Next the reservoir temperature was chosen and the mole fraction required interpolated from the figures in Appendix I. The required weights of the potassium and rubidium were then calculated and the proper mixture was inserted directly into the reservoir.

With these new predictable spectral output lamps, the program now moved into the determination of the optimum fill.

SECTION IV

LAMP PERFORMANCE

The original goal of this program was to examine the performance of 2, 3, 4 and 6mm bore pump lamps with 2, 3 and 4mm Nd:YAG laser rods and optimize the most promising candidates. The work on the 2 and 3mm bore lamps and the 2 and 3mm rods was done in support of another contract and to eliminate conflict and overlap only the larger devices were studied under this effort. The results of the small bore investigation may be found in Reference 9 and in summary in Appendix II.

4.1 Lamp Operation

The lamps tested in support of this program were operated on three DC modular power supplies with series ballast resistors to assist in the control and limiting of lamp current. The first module consisted of a 900 volt power supply with current capability limited to a few milliamps. This supply is only turned on during lamp start. Also, in this supply was a series trigger transformer to break down lamps which would not start with the application of 900 volts.

Connected in series was the second module which contained a 300 volt open circuit DC supply capable of delivering 300 to 400 milliamps. This supply was used during the early warmup of the lamp while the alkali vapor pressure was building up and the arc was becoming established on the electrodes. It is during this portion of the lamp start that the future course of lamp operation is often determined. While operating in this mode, the alkali vapor pressure should build up sufficiently to allow the electrodes to operate as low work function alkali electrodes. Sometimes, however, on initial start or when the lamp has been turned off while operating at very low vapor pressure, there is insufficient alkali material in the lamp body. When this condition is present, the electrodes will become alkali starved and begin to quickly turn red hot. If this condition is not reversed or the lamp is not turned off, often times the sapphire tube will crack due to the high thermal loadings from the hot electrodes. The easiest method of preventing this situation for initial starts or low vapor pressure starts is to turn on the reservoir heater for an hour or so in order to drive some of the alkali material into the lamp. After the initial full pressure operation the lamp has sufficient alkali vapor condensed on the electrode to allow restarts to be simple operations.

Once a stable operation condition is obtained the third supply is turned on and the lamp adjusted to the desired operating power. In order to cover a wide variety of lamp operating parameters, the third supply has the capability of 200 volts open circuit and current adjustment to 25 amperes. Figure 11 is a block diagram of the power supply used during the experimental phase of the program.

Once the desired operating power has been achieved, the next step in the lamp's operation is to obtain reliable vapor pressure control. This is accomplished in the experimental lamps by establishing the tip of the reservoir as the cold spot in the lamp. Operation of the lamps over an extended period of time (usually from several minutes to about an hour) is required to allow for migration of the alkali metal to the reservoir and the lamp vapor pressure becoming a function of the reservoir tip temperature. To facilitate data acquisition from the experimental lamps, the vapor migration was speeded up (from several seconds to several minutes) by pulsing. The lamps tested were pulsed by charging a 100μf capacitor to about 40 volts above the lamp's operating voltage and dumping this energy into the lamp through an SCR firing circuit. Using this technique, spectral, fluorescence and laser power data could be taken over a wide range of operating vapor pressures (reservoir tip temperatures) in a comparatively short time.

A simple criterion to determine if a stable vapor pressure control is obtained is to observe the lamp voltage at a particular reservoir tip temperature. Under stable conditions, the lamp voltage always returns to the same operating point for a particular reservoir tip temperature.

In any space qualified application, the lamps will be filled to operate at a constant optimum vapor pressure and therefore will not have a reservoir. The operation of these lamps will consist merely of turning them on an waiting several minutes until the proper operating ccndition is achieved (similar to commercial mercury and metal halide lamps).

4.2 Spectral Instrumentation

The experimental setup being used to obtain the total lamp spectra and fluorescence is shown in Figure 12. A typical lamp is placed within the integrating sphere shown. Here the total radiation is diffusely reflected within the integrating sphere to produce uniform energy density. A small hole in the sphere samples the energy radiating from the opposite wall. A light baffle is placed between the lamp and exit hole to blank out direct radiation. The light is now mechanically chopped at 33Hz before it enters the 1 meter Jarrell Ash spectrometer and exits either through the side by a 12.5μ slit or through the normal exit slit. Selection of exit slit is made by positioning an internal mirror.

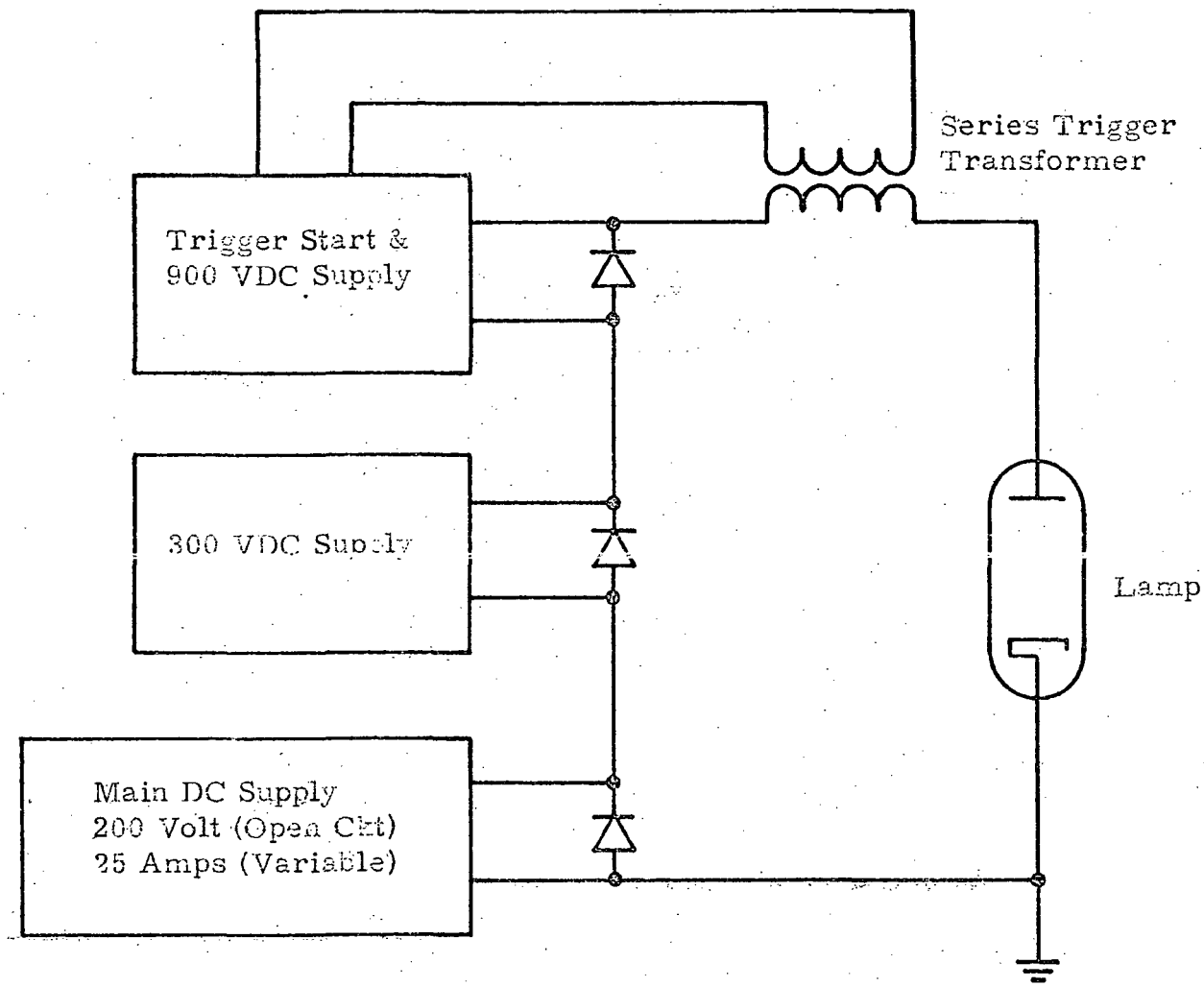

Figure 11

Block Diagram of Experimental Lamp Power Supply

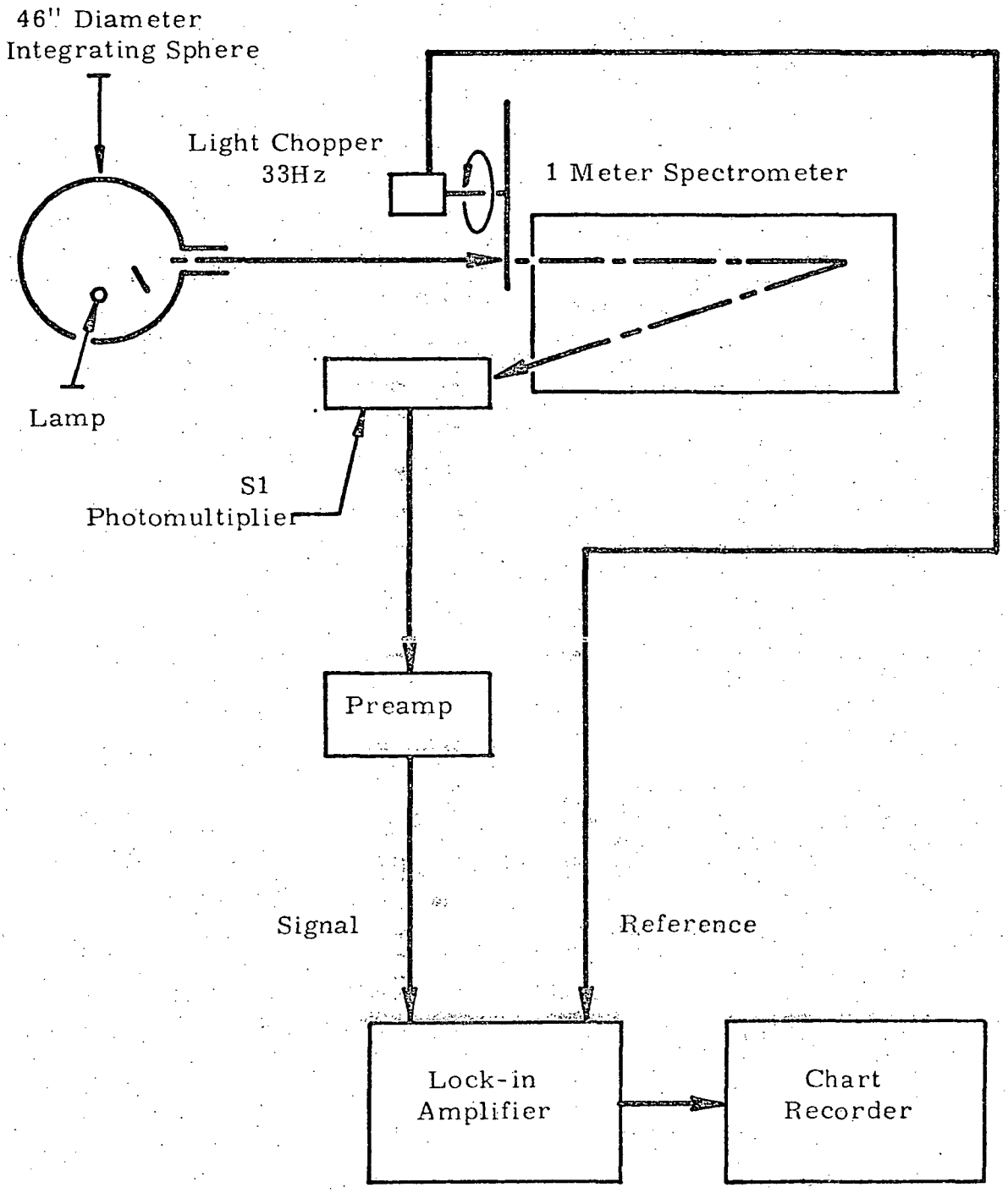

FIGURE 12 BLOCK DIAGRAM OF ELECTRONICS FOR SPECTRAL MATCHING

The light from the side exit is viewed directly by a photomultiplier tube (S-1), measuring the spectral output of the lamps. The light from the normal exit passes through a Nd:YAG crystal where a portion of that light energy within the narrow bandwidth of the spectrometer is absorbed and reradiated as diffuse fluorescence radiation. It is then detected by a S1 photocathode surface of a photomultiplier. The signal is processed through a low noise variable gain preamplifier into the lock-in amplifier where it is synchronously detected against a reference signal derived from the light chopper. This output is then fed to a chart recorder where the data is recorded. Data taken using the above system is presented in Figures 14 through 19.

Light exiting from the normal output slit of the spectrometer passes through the Nd:YAG sample, part being absorbed and the remainder reflected back through the Nd:YAG by the mirror shown in Figure 13. One then has an effective absorption length of twice the thickness of the crystal. The 1.06 fluorescence will be isotropic, and a good portion will be collected by the front reflector and transmitted through the RG1000 filter onto the S1 photocathode surface of the photomultiplier.

All of the non-cavity spectral and fluorescence measurements were made using the above experimental techniques.

4.3 Environmental Effects

As an early part of the long term evaluation of lamp performance it became necessary to determine if there would be any notable effects caused by the surrounding environment. The following sections detail some of the measurements made to determine these effects.

4.3.1 Spectral Output Variations

Because of the possible advantages of operating the system in an inert atmosphere rather than in a vacuum environment it became necessary to determine if there were changes in spectral output based upon the surrounding lamp atmosphere. To conduct these tests, a 6mm by 50mm potassium sapphire lamp was operated in a vacuum and an argon atmosphere. During operation in both cases, the lamp reservoir temperature was adjusted to maintain a constant vapor pressure in the lamp and hence a hopefully constant spectral output. Figure 14 and 15 show the lamp spectral output for vacuum and argon environments respectively. As can be seen there is no appreciable change in line intensity or line width. An additional check was made by examining the fluorescence spectra from a Nd:YAG crystal

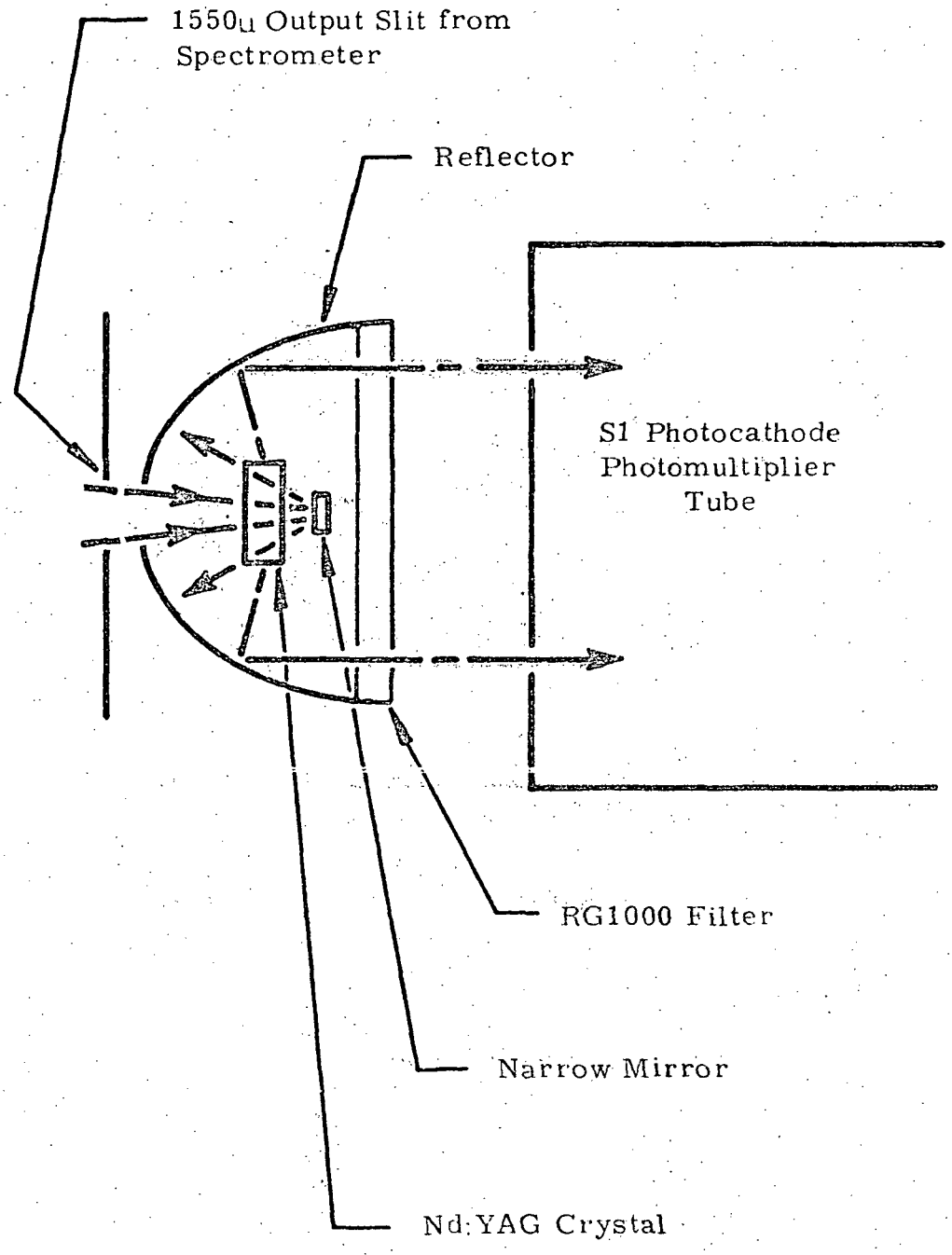

FIGURE 13. Nd:YAG 1.06μ
FLUORESCENCE DETECTION FOR SPECTROMETER

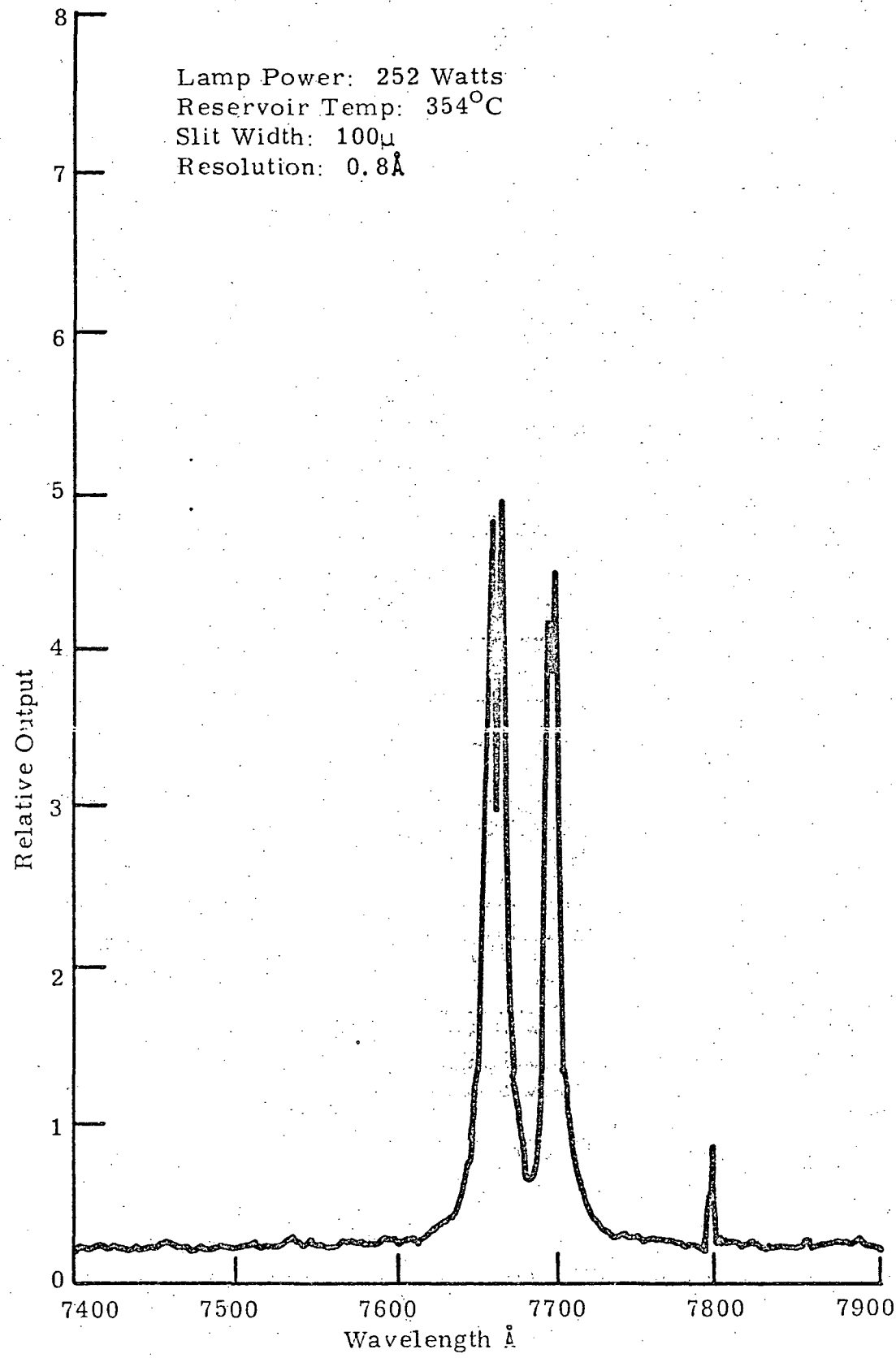

FIGURE 14 POTASSIUM SPECTRA IN VACUUM ENVIRONMENT

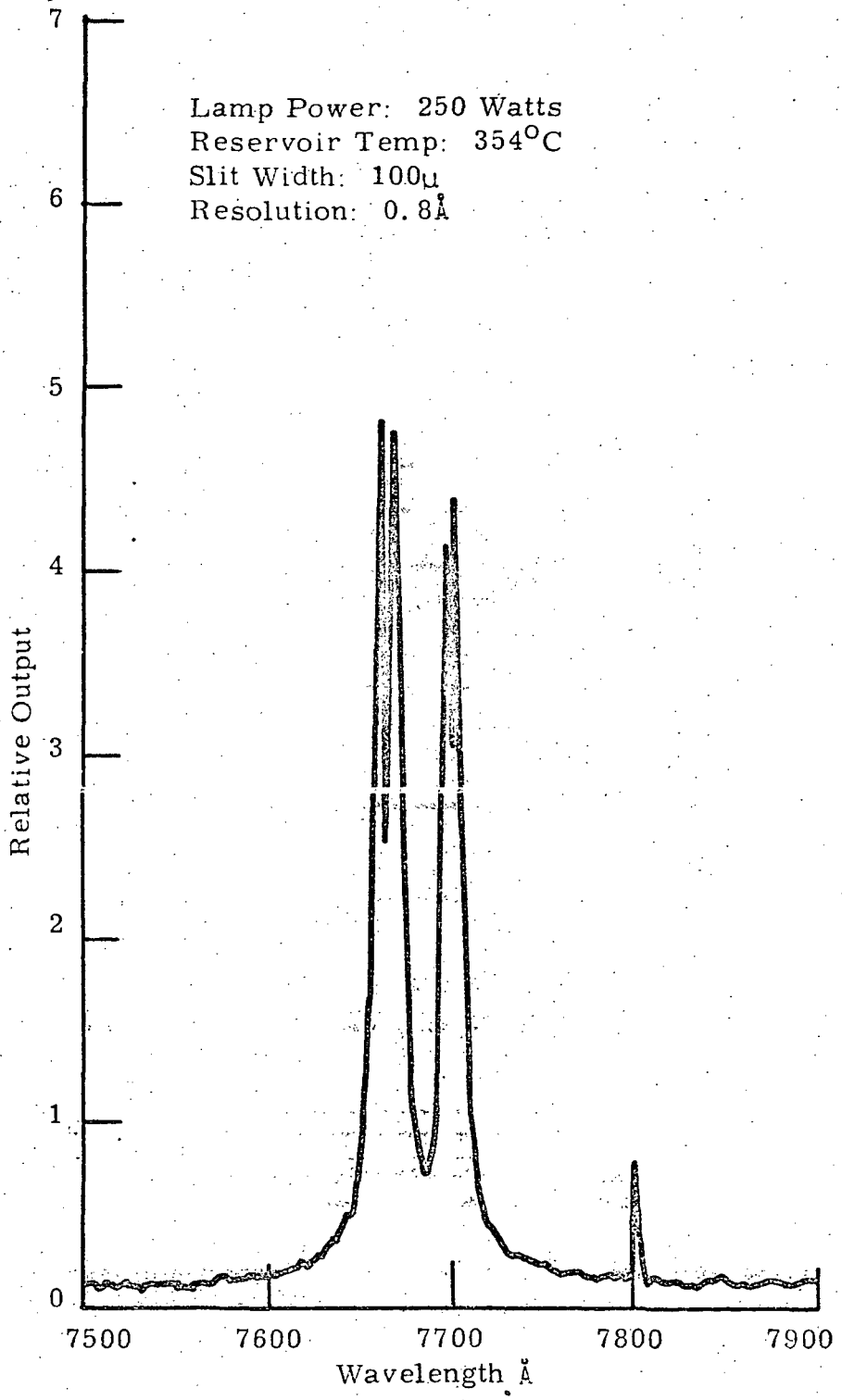

FIGURE 15 POTASSIUM SPECTRA IN ARGON ENVIRONMENT

under both environmental conditions. Figure 16 and 17 show this fluorescence data and as before, there are no significant changes evident. Therefore, it may be concluded that as long as the additive vapor pressure is held constant in the lamp, there should be no change in laser pumping efficiency for either argon or vacuum environments. It was important to establish this independence early in the program so that the data obtained in either vacuum or argon would be mutually interchangeable. The instrumentation described in the previous section was used to obtain the data presented in the above figures.

This conclusion represents a radical change from the accepted thoughts on effects of environment with lamp performance. Previously, the quantity P_o had been the standard of comparison among lamps and that a low P_o meant a low threshold and a potentially efficient laser pump. This basic assumption is still valid but further understanding of P_o is in order.

Previous experiments using mercury-alkali halide lamps were conducted on varying environments with no specific data being taken on spectral output. Since P_o decreased when the lamp was operated in vacuum instead of free air and again for each increase in insulation, it was naturally concluded that the quantity P_o represented nothing more than the heat loss from the lamp. Additional evidence to support this assumption was gathered by observing that water cooled krypton lamps had a high P_o (≈ 410 watts), air operated tungsten and mercury-rubidium iodide lamps both had a P_o of ≈ 200 watts and full vacuum operated mercury-rubidium iodide lamp a P_o of 47 watts.

The particular mercury-iodide lamps used in these experiments had quartz envelopes and moly ribbon seals. An excess amount of fill material is put into the lamp proper and the lamp is then sealed. During operation, the vapor pressure of the fill material is governed by the cold spot in the lamp which is usually at the quartz-moly seal interface. Any variation in this temperature caused by environment or insulation will also change the operating vapor pressure of the lamp. Based on experimental data (to be presented later) a rubidium vapor pressure higher than that associated with the typical quartz-moly seal temperature is required for the optimum match to the Nd:YAG absorption. Therefore, both vacuum and insulation which raises the cold spot temperature will increase the vapor pressure of the device and result in a lower P_o. As a result of this understanding, P_o should now be related to the spectral match of the lamp to the Nd:YAG crystal.

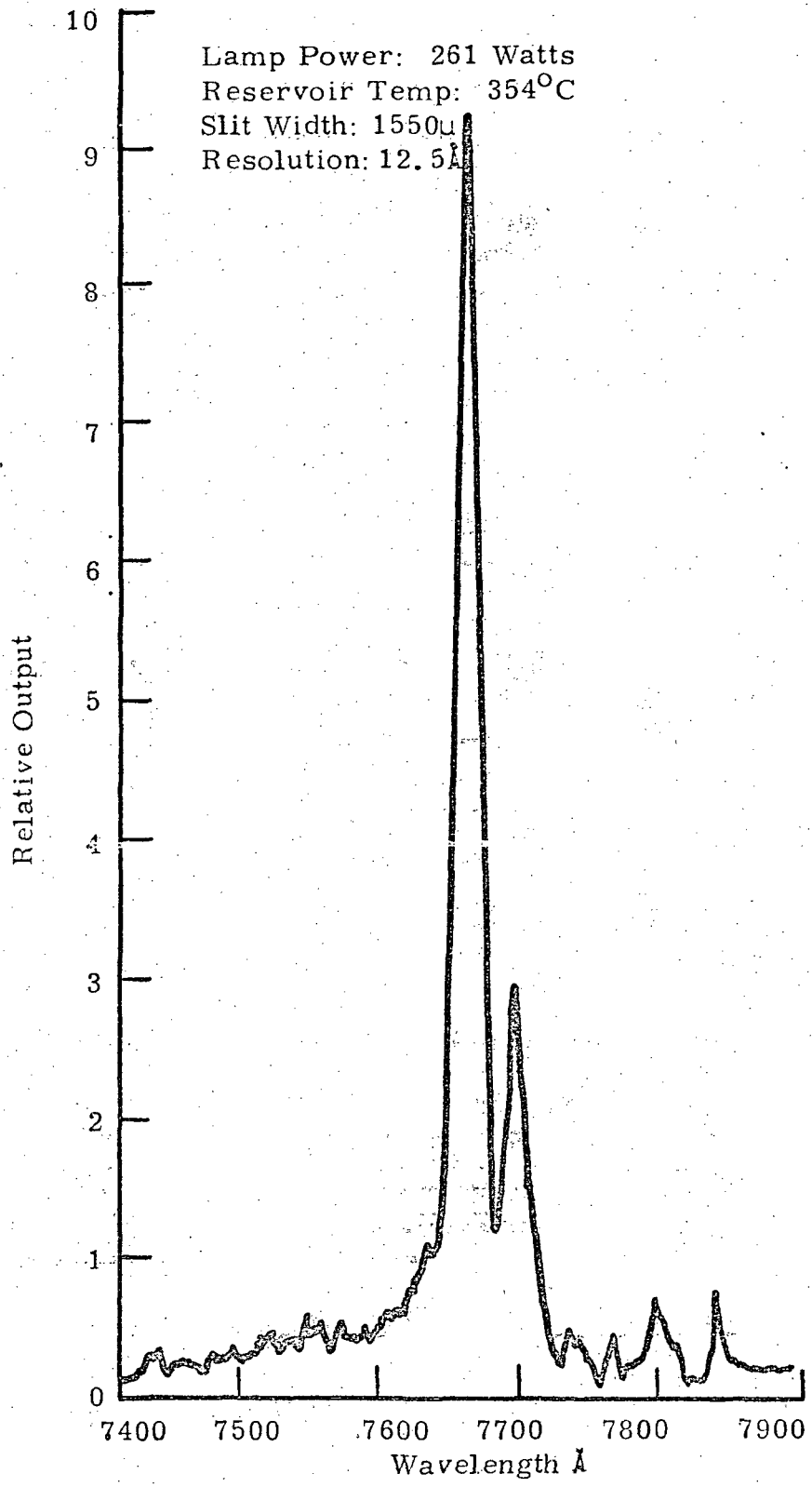

FIGURE 16 Nd:YAG FLUORESCENCE IN VACUUM ENVIRONMENT

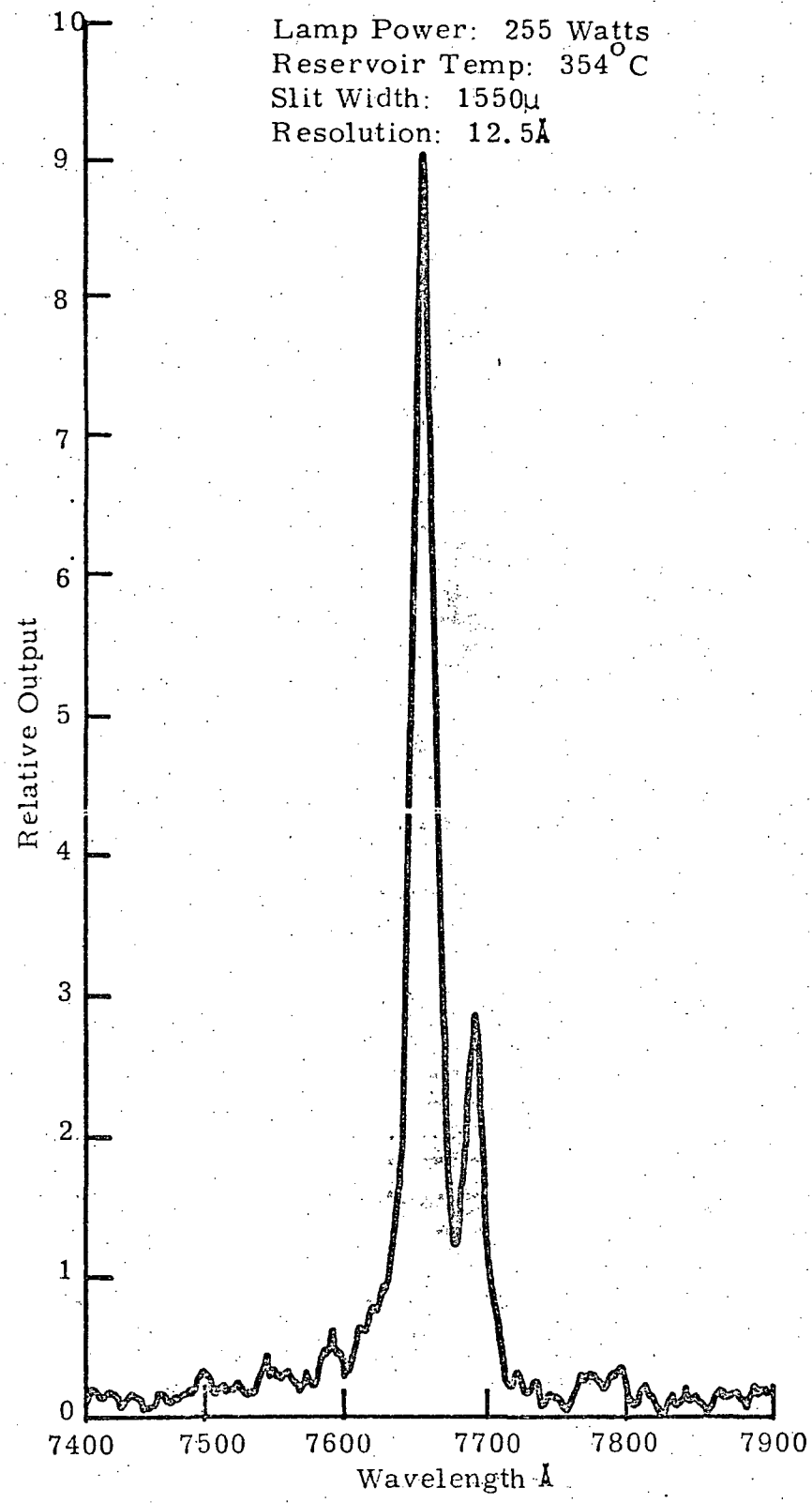

FIGURE 17 Nd:YAG FLUORESCENCE IN ARGON ENVIRONMENT

For lamps operated in support of this program the reservoir (cold spot) is separate from the lamp proper and is independently controlled to maintain a constant vapor pressure of the fill material. Therefore, these lamps maintain a constant spectral output independent of the surrounding environment. Any lamps used in a space qualified laser design should also be constant pressure devices and thereby exhibit the same independence to environmental variation.

4.3.2 Envelope Temperature Variations

To achieve long envelope lifetime, the wall temperature must be maintained sufficiently low to insure maximum strength. Based on 10,000 hour commercial mercury-sodium lamps with polycrystalline alumina envelopes and wall loadings of 32 watts/cm^2 an original criterion was established to maintain the sapphire wall loading below 40 watts/cm^2. Therefore, the next place where the environment would have significant impact is on the temperature of the lamp wall. In order to maintain a high strength in the sapphire, the wall temperature should be maintained below 1000°C. Above this temperature the rupture strength of sapphire decreases rapidly. At 1200°C the strength is a factor of 3-5 lower than at 1000°C. In an inert gas enivornment the wall temperature will be lower than for a vacuum environment because of the increased conductive heat transfer. Data was taken for 2 and 3mm lamps and is presented in Figures 18 and 19. In the data for a 2mm bore lamp (Figure 18) it can be seen that the lamp center temperature is in excess of 1100°C for the argon environment and in excess of 1200°C for a vacuum environment at the estimated 40 watt/cm^2 safe wall loading limit. In the 3mm case however, the lamp center temperature is in excess of 1100°C for the vacuum environment and well below 1000°C for the argon environment. For the larger bore devices, the corresponding temperatures would even be lower.

In order to achieve higher laser output it often became necessary to operate the lamp at powers which produced wall loadings in excess of 40 watts/cm^2. To maintain the wall temperature below 1000°C, an argon flow had to be used. Figure 20 presents lamp center temperature for a 2mm bore device as a function of wall loading when three different argon flow rates were used. It can readily be seen the increase in wall loading which can be achieved while still maintaining the lamp temperature below 1000°C. This data is extrapolated to other lamp bores in Figure 21 and was used as a guide during high power operation.

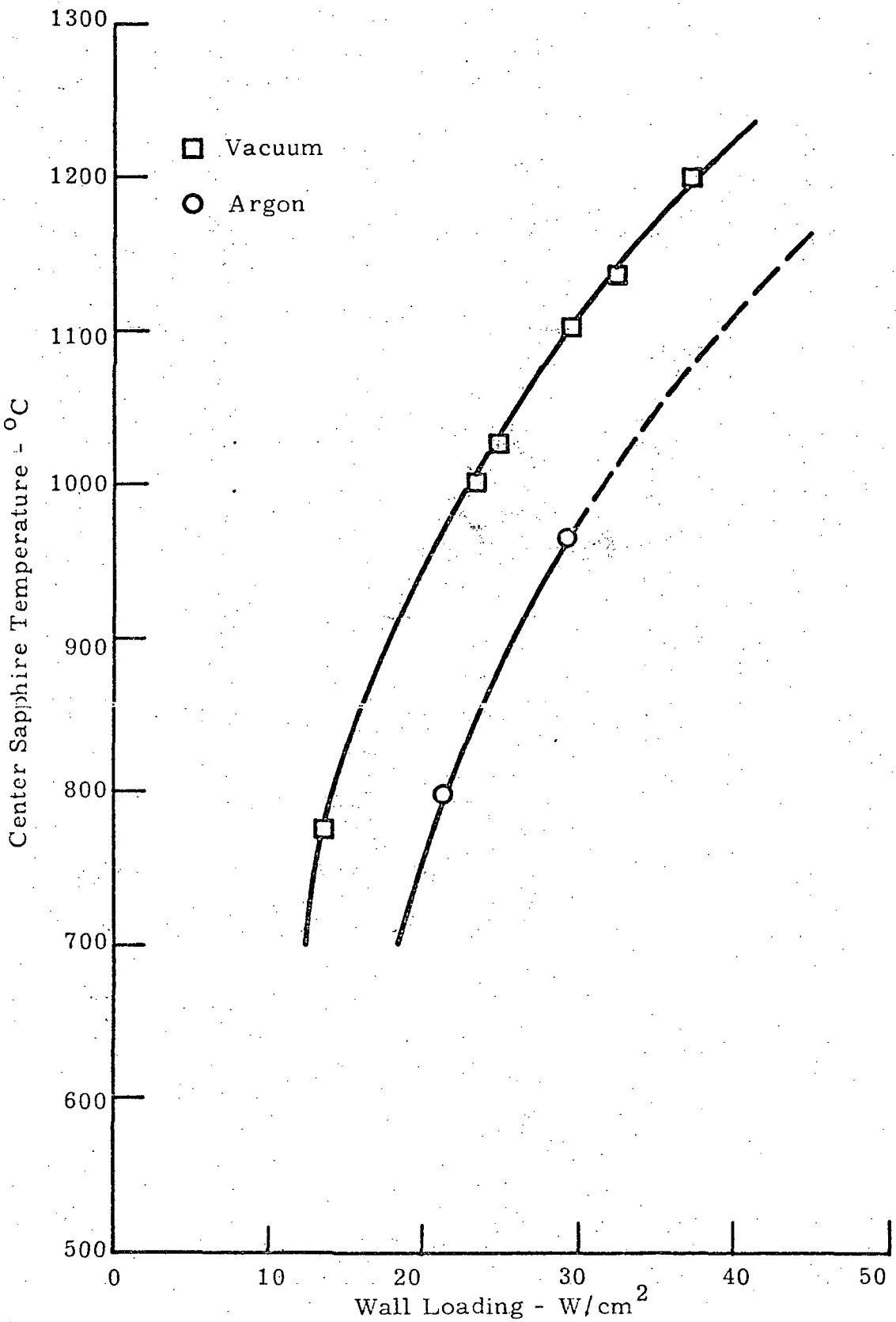

FIGURE 18 SAPPHIRE CENTER TEMPERATURE vs WALL LOADING FOR 2mm BORE LAMP

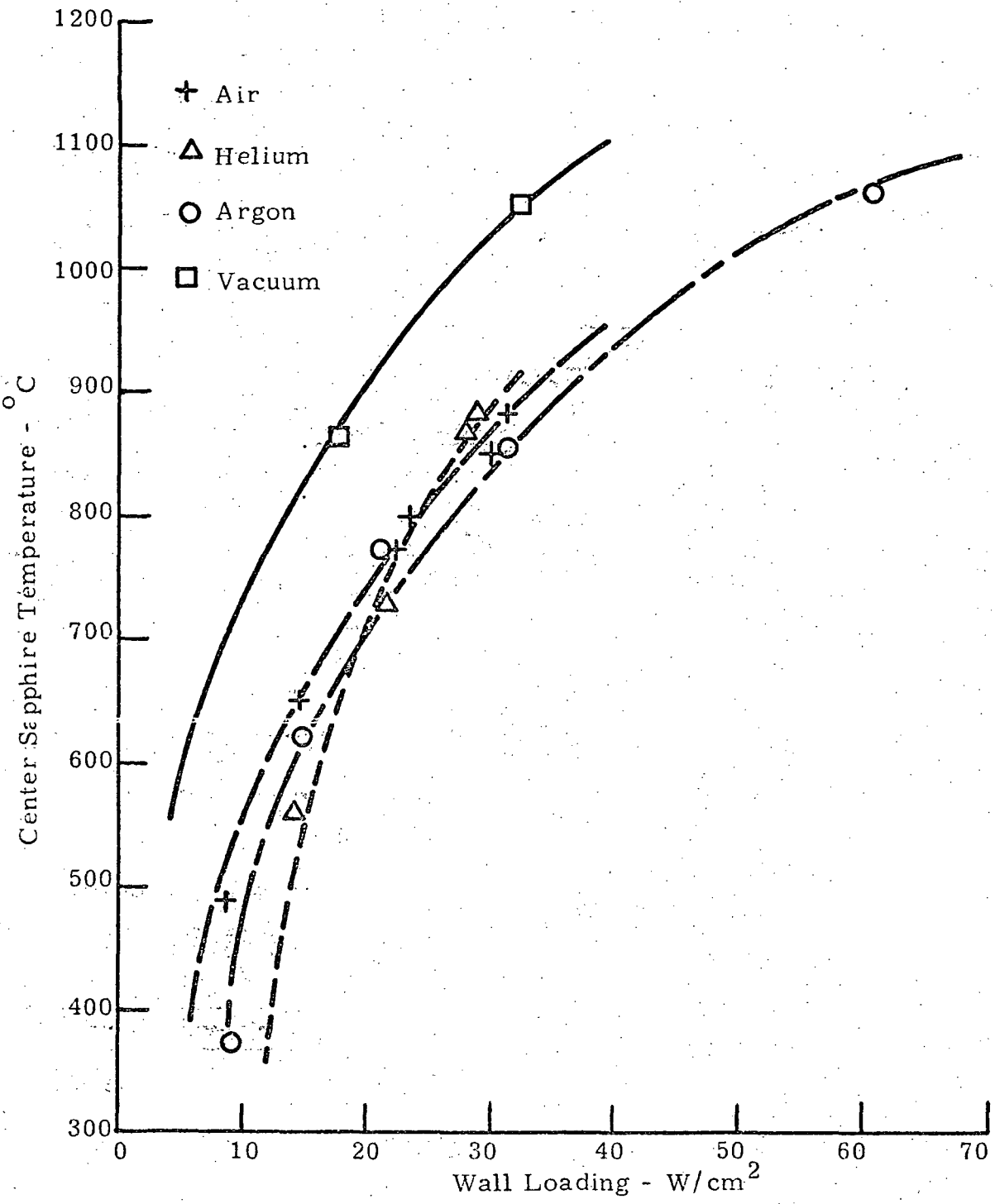

FIGURE 19 SAPPHIRE CENTER TEMPERATURE vs WALL LOADING FOR 3mm BORE LAMP

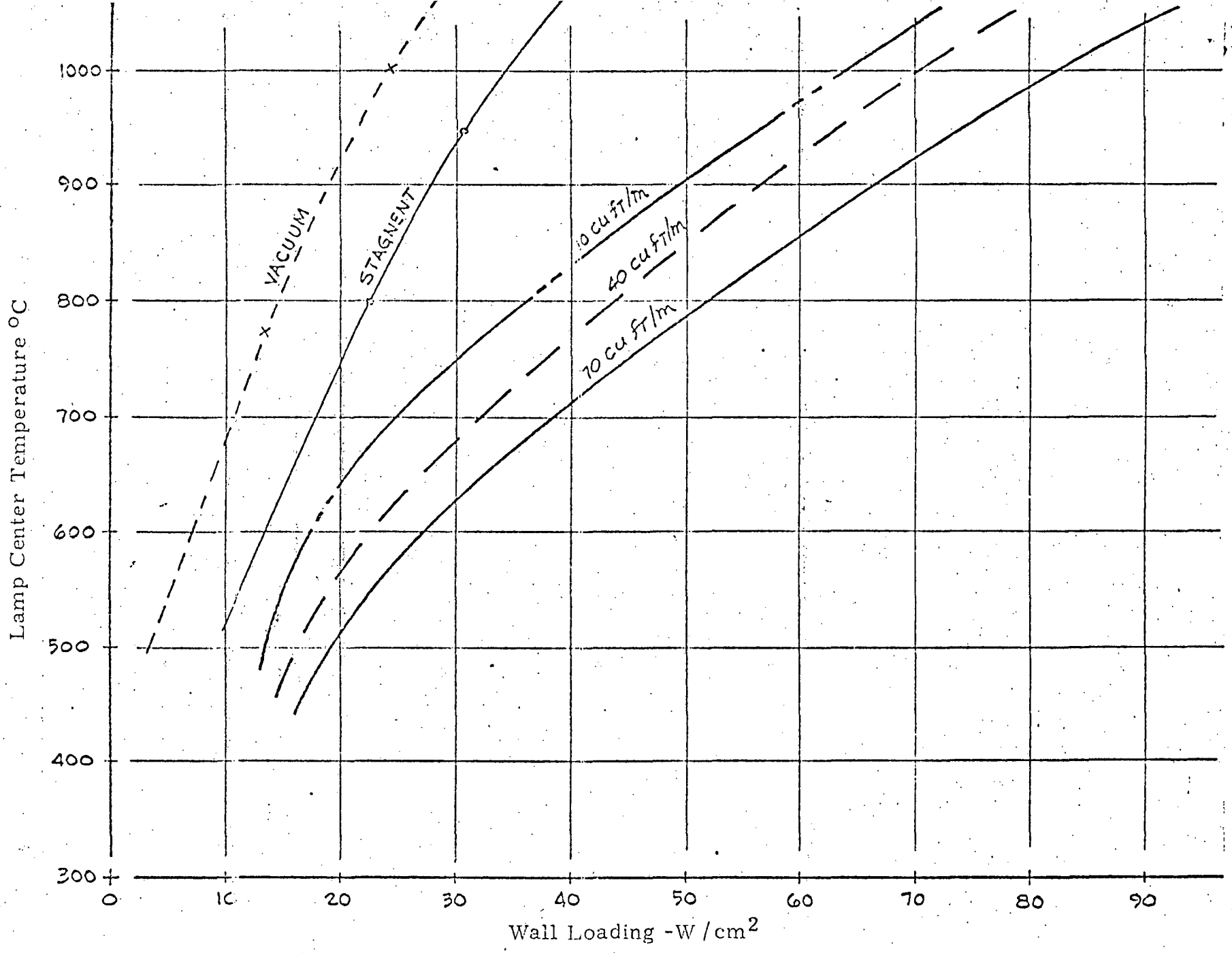

Figure 20 Lamp Center Temperature for 2mm Bore Lamp as Function of Wall Loading and Argon Flow Rate

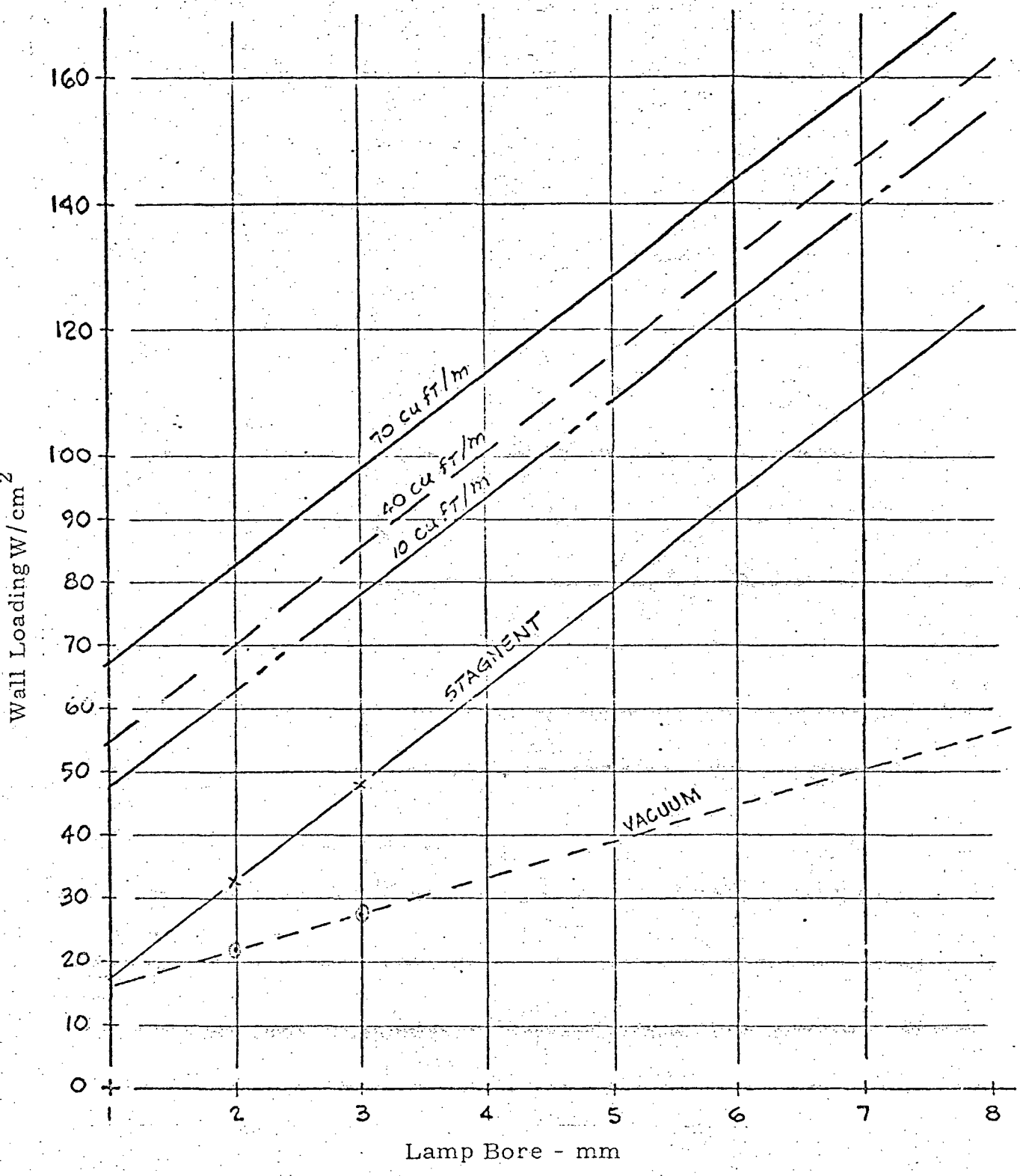

Figure 21 Wall Loadings and Argon Flow Rates which Produce 1000°C Envelope Temperature for Various Bore Diameters

The impact of the ability of operating the lamp in an inert atmosphere environment such as argon has additional implications other than the improvement in sapphire strength discussed above. In addition, the use of an inert atmosphere not only reduces the wall temperature but also reduces significantly the lamp's long wavelength emission spectrum. Since the sapphire has an appreciable emmissivity beyond 4.5 microns, nearly all the long wavelength radiation will result from the hot envelope. Therefore the reduction of the envelope temperature by 200°C or more can result in a reduction of the total blackbody - radiated power by a factor of 2. In space laser systems where there is no water cooling of the YAG rod, the amount of extraneous long wavelength radiation on the rod which causes heating becomes an area of critical concern. Therefore, it can readily be appreciated that a reduction of 2 in blackbody radiation results in a significant improvement.

4.4 Life Testing

The objective of the life testing effort was to determine failure mechanisms associated with extended lamp operation. In order to achieve long lifetime envelope operation, the power loading on the walls should be kept as low as possible and the wall temperature maintained below 1000°C. A thermocouple was placed in contact with the external wall at the center of the lamp and temperatures were measured as functions of both input power and surrounding environment.

The next area of critical concern was the effects of extended periods of operation on the lamp seals. Since the lamp finally developed on this program has frit seals, the majority of attention was directed towards obtaining data on this type of bond. Thermocouples were spot welded to the flanges in the seal regions and temperature histories were kept. Average temperatures in the range of 500-550°C were maintained on both seals during most of the operational time. When a seal did fail, it was subjected to extensive microscopic examination to try to determine the presence of physical changes which may have been responsible for this failure. In addition, when a lamp failed due to other causes, the seal regions were also microscopically examined to ascertain the seal condition and to determine if there was any evidence of early seal deterioration. Lamp seals were maintained between 520 and 535°C. Lifetests of two frit seal lamps with TDS envelopes were conducted in an argon environment. The first of these lamps operated for 70 hours before seal failure occurred. This failure appeared to be an alkali leak at the lower (cathode) seal region. Close examination under a microscope showed that the frit flow seemed to be undisturbed but may have parted from the niobium flange in one small region. The second

lamp also operated in an argon environment before failure occurred at 180 hours. The failure mechanism of this lamp was the same as that in the first lamp - namely a leak at the lower seal region with the same microscopic observations. Since both of these lamps were fabricated with the initial 0.015 inch thick niobium flange, if is believed that this heavy wall is not capable of the flexibility which was required during thermal excursions of the interface. The present design with 0.005 inch niobium thickness should eliminate this failure mode.

Two groups of 0.005 inch wall flanges were ordered and both were delivered with imperfections. These are discussed in the following section.

4.5 Failure Analysis

The failures of lamps tested during this program may be classified into two categories. These are envelope related failures and seal related failures. The following paragraphs elaborate on each of these categories.

4.5.1 Envelope Related Failures

During operation of TDS enveloped lamps, the inside wall on many of the sapphire tubes became frosted. This effect usually occurred after at least 10 hours and before 40 hours of operation. Continued operation of a frosted appearance lamp resulted in the formation of circumferential crazing or cracks on the inside wall. This appearance could be seen along the total length of the tube which contacted the plasma but was mostly noticable in the 1/4-3/8 inch region in front of the electrodes. A lamp with an envelope in this condition fails within several hours.

There are two possible explanations for the formation of the internal frosting. The first is that even though the raw aluminum oxide used in the TD sapphire is absolutely pure it may pick up some form of contamination during the growth into finished tubes. During operation, the hot potassium and rubidium alkali metals are extremely caustic and may react with any impurities. The possible presence of impurities was first evidenced by examintion of photomicrographs taken of sapphire samples. Figure 22 is representative of the I. D. wall structure seen in virgin sapphire material from both the CDS and the TDS process. It should be noted in particular that the TDS material has what appears to be facets (vertical lines in photo) which may be caused by die marks present during the drawing of the crystal.

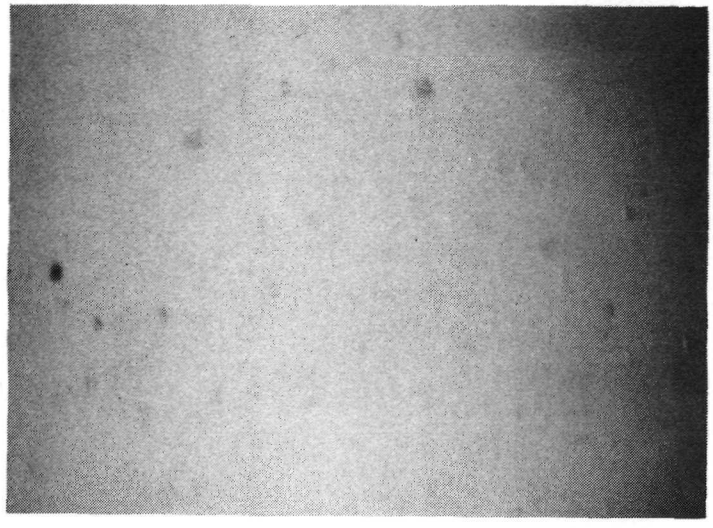

(a) Machined Material

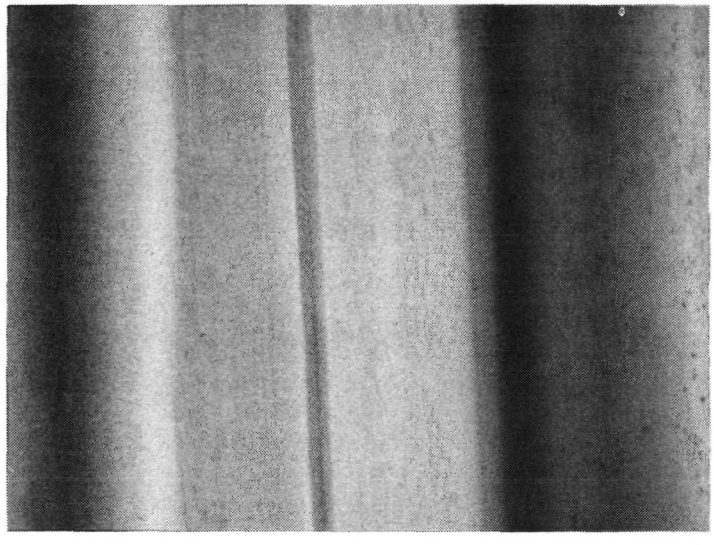

(b) Direct Grown Material

FIGURE 22 ID OF VIRGIN SAPPHIRE MATERIAL x80

However, as will be discussed later, these facets may be the result of dendritic growth within the crystal structure. Also seen in both photographs are dark spots in the crystal. These may be attributed to voids, surface imperfections (pits) or traces of impurities. It should be noted that these spots appear more frequently in the TDS material than in the CDS material.

Next, the O. D. of the materials was examined and analyzed. The O. D. of the CDS material was not photographed since it was highly polished and showed only traces of surface pits which resembled the picture in Figure 22(a). However, the TDS shows a repetitive oscillatory marking seen on the outside surface of a virgin tube. At first it was suspected that these markings were representative either of impurities which had reached the surface or of possible dislocation planes. However, closer examination in Figure 23 (b) showed that these spots were bubbles. This picture, however, does not capture the detail which was visually observed and led to the above conclusion.

According to the manufacturer's analysis, the liquid that arrives through the capillary moves outward being heated or cooled, depending on whether the die is above or below the temperature of the interface between the crystal and the liquid. The outward flowing liquid also tends to sweep the rejected solutes with it. Thus, if the die is a heat-sink, the outer region tends to be cooler and richer in solute than the regions nearer the inlet. Thus, the instability that leads to dendritic growth may develop first at the perimeter; this may cause dendritic growth to begin at or near the outer edge, with faceted growth (observed in Figure 22,) which occurs so rapidly that shrinkage pores are formed. As the crystal is moved upwards, the region of dendritic growth move inwards, producing a "band" of shrinkage voids (observed in Figure 23 as bubbles) on each crystallographically equivalent dendrite as it grows inward. The dendritic growth pattern is self-interrupting because the latent heat evolved by the growing dendrite raises the temperature of the die to the extent that it is no longer as effective a heat sink in the region of contact or near contact. This is an example of the oscillatory mode seen in Figure 23.

The manufacturer also states it is not evident that impurities play any part in either the cellular or the dendritic processes; however, the rejection of dissolved gas may play an important part in the nucleation of bubbles. The significant conclusion of this analysis is that growth occurs with a planar interface and

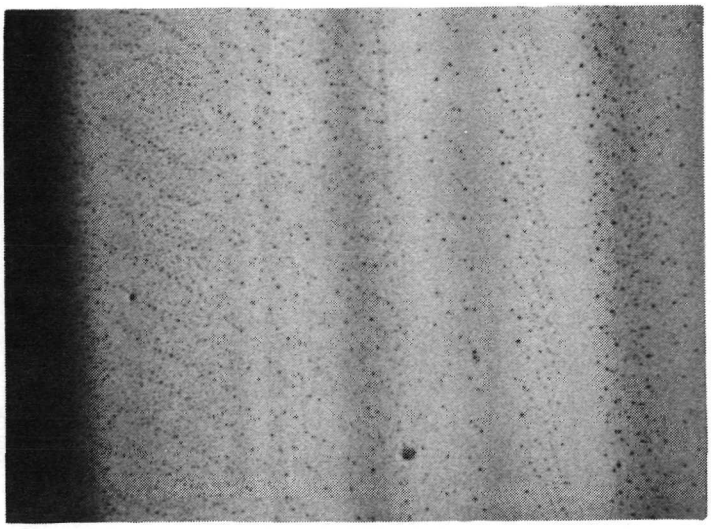

(a) x 80

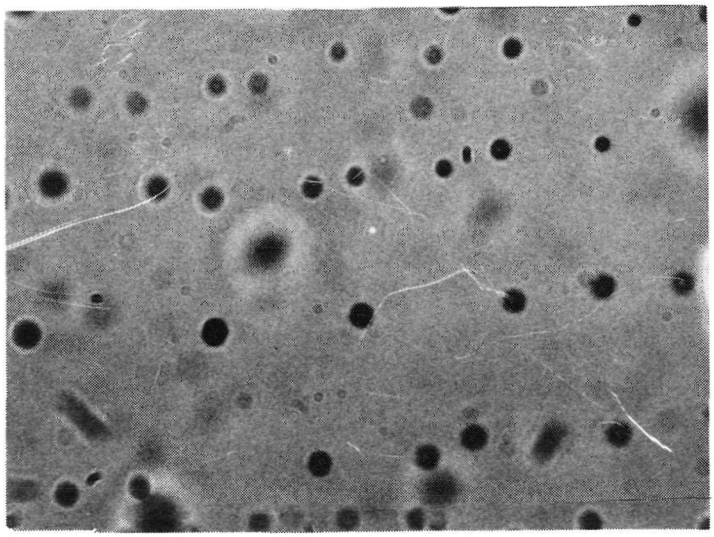

(b) x800

FIGURE 23 OD CF A VIRGIN DIRECT GROWN SAPPHIRE TUBE

without cellular or dendritic growth when there is significant heat flow to the interface. This process is inherently slow, being limited by the radiation of heat at the solid-liquid interface. This is the condition for the growth of crystals that are free from bubbles or other visible defects. When there is heat flow away from the growing crystal, (i.e., the die is the main heat sink) much faster growth is possible but voids and the other imperfections caused by the instability of the interface reduce the optical quality of the crystal.[10]

It now becomes evident from both the above discussion and from the microscopic pictures that the tubes received were grown too fast and therefore of poor quality. These imperfections are significant since all sapphire envelopes which fractured during operation started with cracks on the inside circumference. These cracks follow the bubble formations and the longitudinal facet structure.

A source of impurities which may lead to bubble formation, abnormal crystal growth and the anomalies within the crystal is the molybdenum crucible and dies used in the TDS process. Work by Kingery[11] showed that at sufficiently high temperatures, all refractory metals will react with oxide materials. In the case of molybdenum and alumina, Johnson[12] observed gross changes at a temperature of 2000°C. Since the melting temperature of alumina is in excess of 2000°C and the direct grown process is done at the melting temperature, it becomes reasonable to assume that reactions are taking place between the alumina and molybdenum during the growth of the sapphire tube. The introduction of these impurities into the sapphire whether or not they contribute to dendritic growth or bubble formation can only serve to decrease envelope strength and to help cause premature envelope failure. Except for small scattered surface imperfections which may be caused by impurities, dislocations or other intercrystalline anomalies, the samples machined from Czochralski grown boules showed no signs of the above structure. Therefore, it is this type of tube which should be considered for all long lifetime sapphire enveloped lamps.

The second explanation is that there is water vapor contamination in the lamp which either has not been purged during fabrication or may be present in the fill material. When the lamp is operated, this water vapor produces a small quantity of alkali hydroxides by the reaction $K + H_2O \rightarrow KOH + O_2$. Potassium

hydroxide in particular is extremely reactive and could be attacking the sapphire wall thereby causing the frosted appearance.

This explanation however seems to be the least likely since the four lamps incorporating the CDS envelopes showed no signs of frosting after a comparable time of operation. In fact, these lamps were subjected to wall loadings in excess of 80 watts/cm^2 (using forced argon cooling) with no microscopic evidence of inner wall deterioration. Microscopic examination showed the tubes appearance remained close to the virgin state.

4.5.2 Seal Related Failures

The second area where lamp failures occurred was in the seal region. Initial seal failures resulted from the flange wall being too thick at the seal interface. Under these conditions, the flange is not flexible enough to comply with the expansion variations encountered within the seal interfaces during thermal cycling. Repeated thermal cycles eventually resulted in the frit parting from the niobium flange.

To correct for this difficulty, flanges with a .005 inch wall thickness were ordered. The first group of these new flanges arrived with a .010 inch thickness. Even though they did not meet specification, several lamps were fabricated and tested from this group to provide additional data points. The same type of failure occurred with these lamps as with the first lamp.

Additional flanges were then ordered and carefully inspected for dimensional compliance. These flanges were used on the lamps incorporating CDS envelopes. Failures occurred in these lamps after 3 to 5 thermal cycles or operating periods between 25 and 40 hours. Examination of the seals show no evidence of failure or leaks and subsequent leak detector analysis proved this region was still tight. Helium probling of the lamp on the leak detector shows leaks below the seal interface on the niobium proper. To continue the investigation, new .005" flanges were subjected to metalographic microscopic examination. Figure 24(a) is a view of the interior radius of the flange. Cracks can readily be seen on this surface and are a result of work hardening of the niobium during the spinning process. An exterior view of the same region is shown in Figure 24(b) which shows no evidence of the cracks penetrating completely through the flange. The distortion in the pictures are a result of the curvature of the flange and the depth of focus of the microscope.

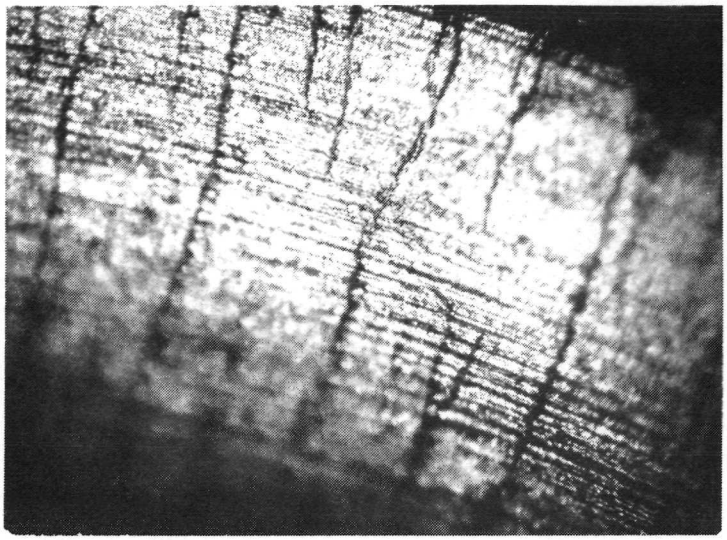

(a)

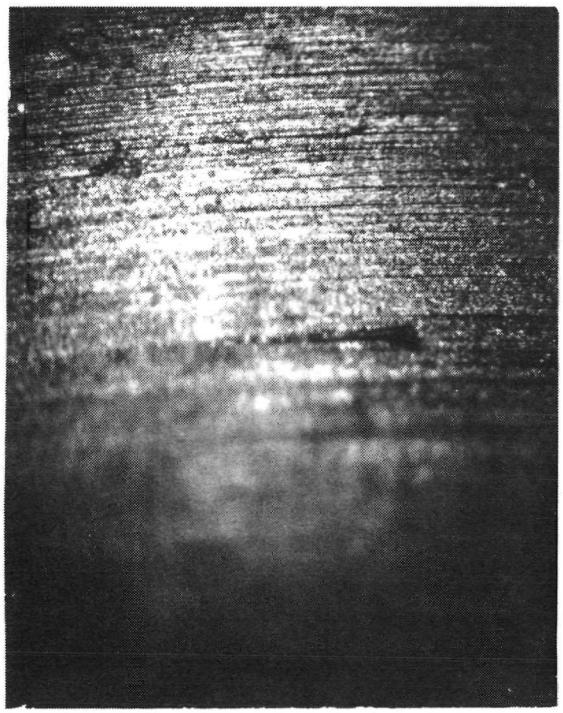

(b)

Figure 24 Flange Wall x 80

Since there are no externally visible cracks, the new flange appears tight on a leak detector check. However, after a few thermal cycles of the lamp, some of the cracks penetrate completely resulting in a slow leak. Failure occurs when a sufficient amount of air has entered thereby preventing restarting of the lamp.

To alleviate the formation of the cracks during the working of the flange, a technique has to be established to insure proper initial annealing of the niobium tube material. The flanges presently are annealed only after they have been spun to their final configuration. The incorporation of intermediate step annealing during the spinning of the flanges should eliminate this problem.

SECTION V

FILL OPTIMIZATION

The optimum lamp design for pumping the Nd:YAG rod is an alkali vapor arc enclosed in a sapphire envelope with an inside plasma diameter equal to the diameter of the laser rod. To obtain maximum output of 1.06 micron radiation from a Nd:YAG, for a given power input, one must not only obtain maximum coupling efficiency between the light source and the laser rod but must also provide this light energy within the proper optical frequency bands. These frequency bands should coincide with the absorption bands of Nd:YAG producing 1.06 fluorescence. The two most prominent bands occur at 0.72 to 0.76 and 0.79 and 0.83 microns as seen from the fluorescence excitation spectra shown in Figure 25. The fluorescence (a measure of the spontaneous emission from the upper energy state to the lower level) is directly proportional to the difference in densities. It is therefore a measure of the population inversion available for laser action.

5.1 Spectral Matching of Quartz Iodine and Krypton Lamps to the Nd:YAG Crystal

The relative fluorescence at 1.06 micron of Nd:YAG, as a function of wavelength, when optically pumped with a Sylvania DXW Tungsten Iodine Lamp, is shown in Figure 26a. Since the Tungsten Iodine Lamp is a black body radiator, there is little one can do to improve its epctral match except by changing its color temperature. When the area under the fluorescent curve in Figure 26 is integrated, one obtains an area proportional to the total fluorescent power. The total area under this curve yields a ratio of the relative fluorescence radiance to input radiance power of .031 relative units. Since this was the first light source used to pump a Nd:YAG laser, to any extent, all efficiencies will be normalized to this relative efficiency.

The 1.06 micron fluorescent radiation, as a function of the wavelength of light output from the Krypton arc discharge, is shown in Figure 26b. The lamp used was a standard Holobeam 2KL3000 operating at 1300 watts. A large percent of the optical pumping comes from the strong spectral lines of krypton near 7510Å and 8020Å and a lesser amount from the other lines from

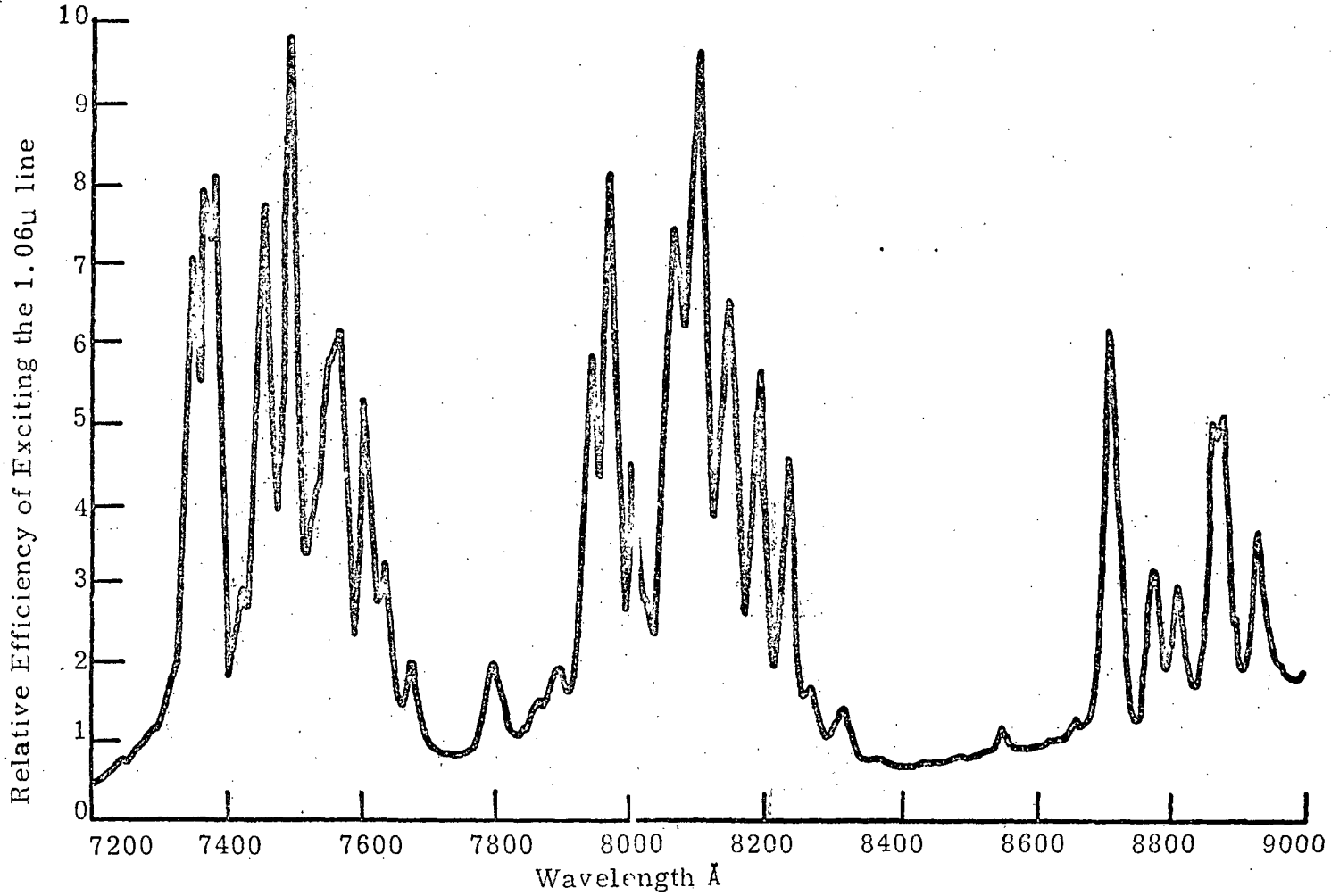

FIGURE 25 EXCITATION SPECTRA FOR Nd:YAG

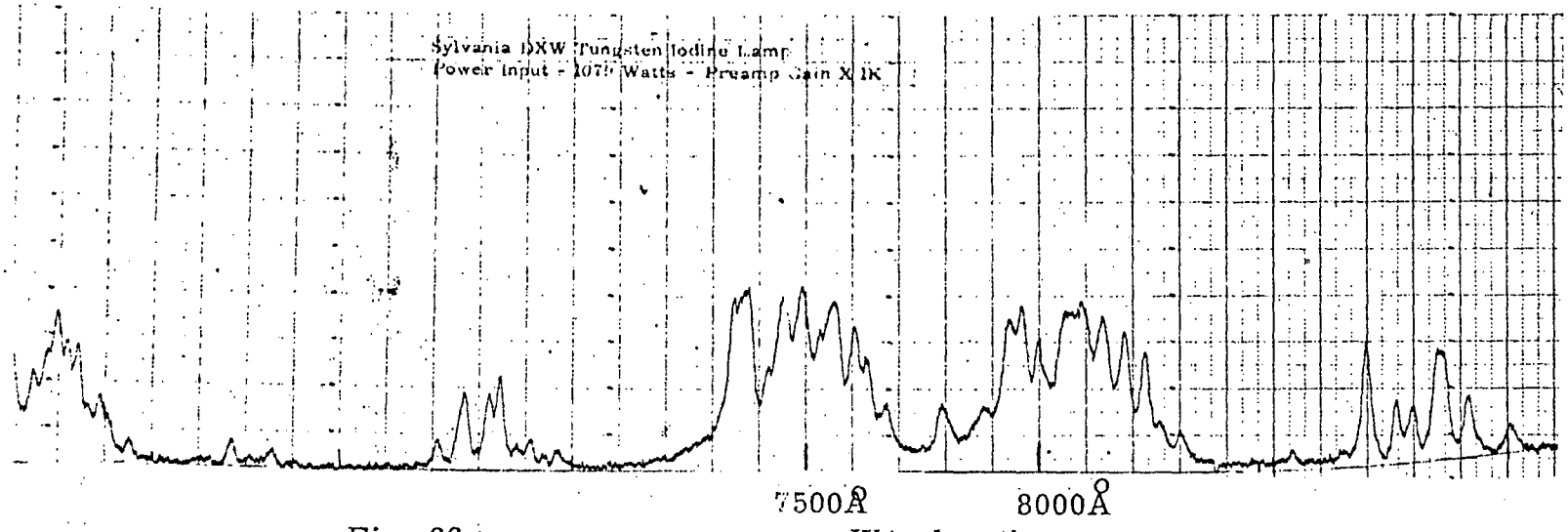

Fig. 26a

Relative Fluorescence from Nd:YAG at 106u
As a Function of Wavelength for Quartz Iodine

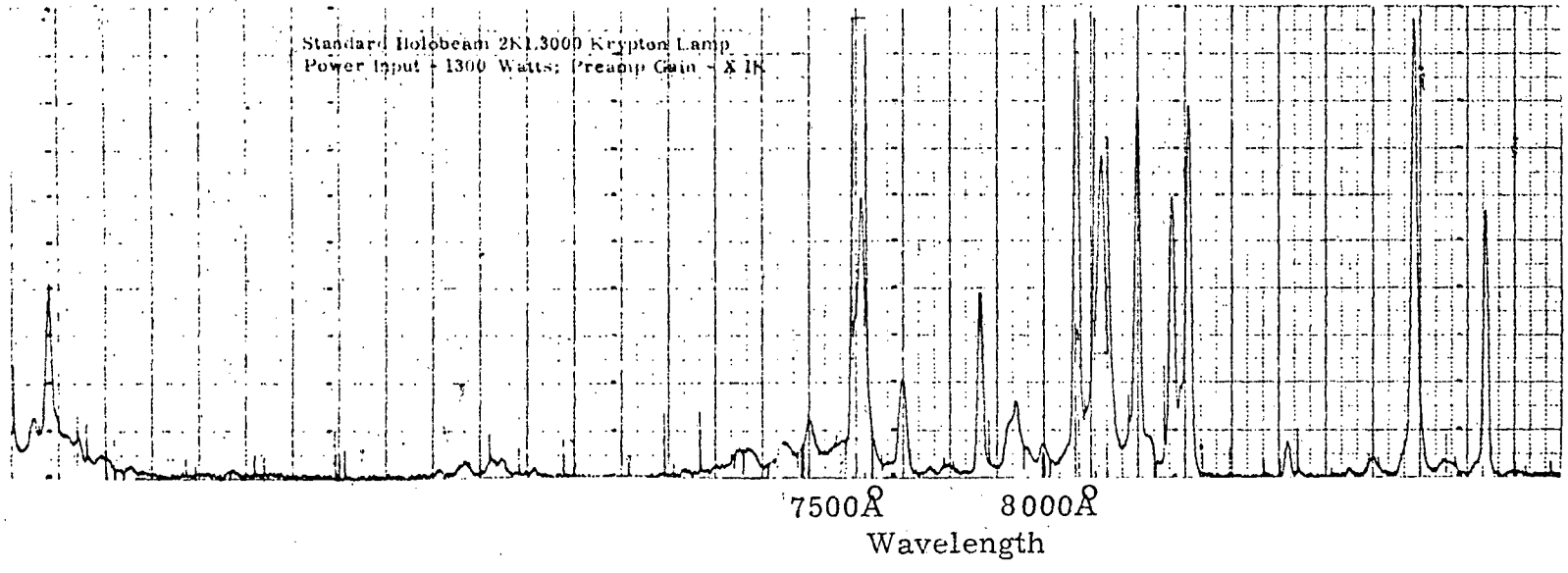

Fig. 26b

Relative Fluorescence from Nd:YAG at 106u
As a Function of Wavelength for a Krypton Lamp

7400Å to 8800Å. When the total area under the curve in Figure 27 was measured and reduced to our common lamp parameters, one obtains a relative radiance pumping efficiency of .035. When this is normalized to the tungsten iodine lamp, it has a relative fluorescent radiance efficiency of 1.13. It is very surprising that the relative efficiency of the krypton lamp, run at 1300 watts input, had an efficiency very nearly equal to quartz iodine. Most reports on the krypton arc lamp show it to be a factor of two to three times better than the tungsten iodine lamp for pumping a Nd:YAG laser. Several other investigators have found similar results to ours in comparing their relative pumping efficiencies. Most likely the reported difference in pumping efficiency is in the efficiency of the pumping cavity and not in the lamp itself. The tungsten lamp is limited to the maximum power for pumping a 50cm long laser rod to about 1000 watts where the upper limit on the krypton is set by the ability to dissipate the heat generated by the lamp and other radiative power that is not absorbed by the crystal.

5.2 Spectral Match of the Alkali Metal Vapor Lamps

The candidate alkali metal lamps have been investigated in three groups to determine their efficiency for pumping the Nd:YAG laser. The groups tested were pure rubidium, pure potassium and potassium-rubidium mixtures. Preliminary evaluations consisted of operating the lamp in the integrating sphere and measuring the spectral and fluorescence characteristics for varying vapor pressures. However, with the infinite number of pressure ratios available from the potassium-rubidium mixture, the quantity of data to be analyzed became overburdening. To reduce the amount of data analysis, a method was then developed for measuring the total fluorescence. Using this technique, the optimum fill for one lamp diamter could be easily determined. A relationship was then developed to calculate the optimum fill ratios for other lamp diameters. It should be noted that this formula did not always yield the absolute optimum fill but did provide an excellent starting point for further experimentation. The experimental work conducted in support of the fill optimization effort is described below.

5.2.1 Preliminary Lamp Evaluations

a) Rubidium Lamps

Preliminary rubidium spectral and fluorescence data were taken in 19.8mm, 7.1mm and 4mm bore lamps.

During these data runs, an optimum match to the Nd:YAG crystal was not determined. Typical data recorded is presented in Figures 27, 28, and 29. This data was chosen since it is representative of three different vapor pressure conditions required to produce similar output spectra in the three diameter lamps (and is also demonstrative of the analytical relationships developed later). To obtain an optimum rubidium match, it will be shown that a higher self absorption and spread of the resonance lines is required.

b) Potassium Lamps

Preliminary potassium spectral and fluorescence data was taken in a 6mm bore lamp. Figures 30, 31 and 32 show typical data for three different vapor pressure conditions. As before, this data was not conclusive to determine an optimum fill but did indicate that a much higher effective line revisal characteristic is required for the optimum potassium match.

c) Potassium-Rubidium Lamps

Preliminary potassium-rubidium spectral and fluorescence data was taken using 4mm bore lamps. Figure 33, 34, and 35 show typical data for three different vapor pressures which again do not represent optimum matching conditions. During testing of these mixture lamps, it became evident that arbitrary fills did not produce repetative data for similar operating conditions. Therefore, to insure lamps with repetative characteristics, the optimization and fill technique presented in the next section developed.

d) Data Analysis (preliminary evaluations)

Even though the above data obtained during preliminary evaluations was not optimum, it does present a basis of comparison between the different types of lamps. Figure 36 summarizes the fluorescence efficiencies measured related to a unity tungsten lamp for krypton and the alkali vapor lamps. The best efficiency obtained during these runs was for a potassium-rubidium fill which yielded a 2.6 times increase in

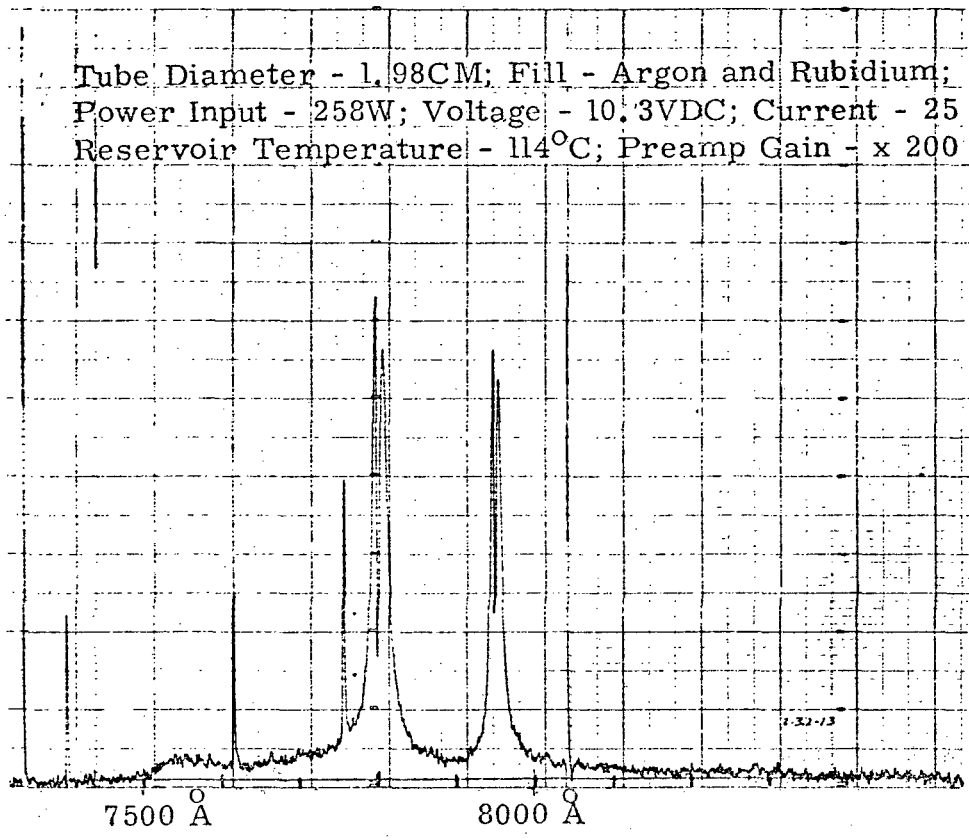

Figure 27a Relative Spectra of Rubidium as a Function of Wavelength

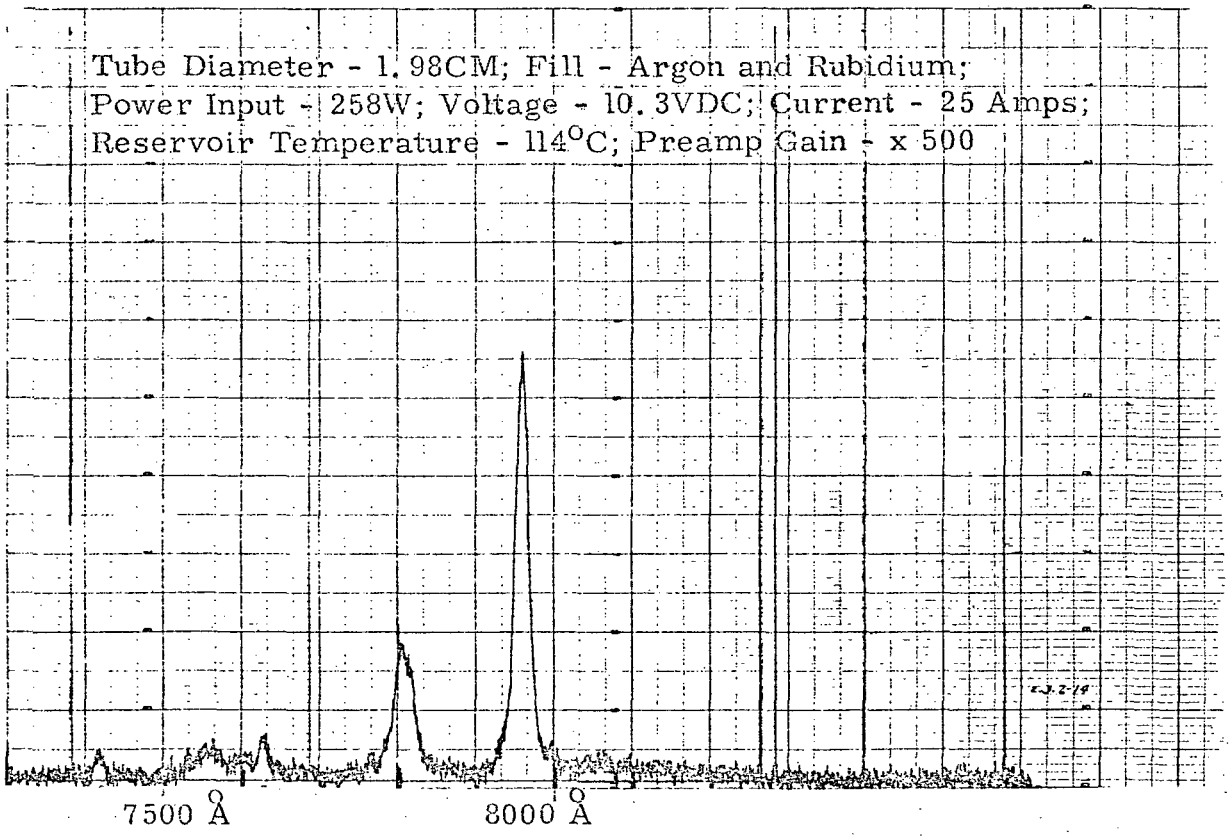

Figure 27b Relative Fluorescence From Nd:YAG at 1.06μ as a Function of Wavelength for Rubidium

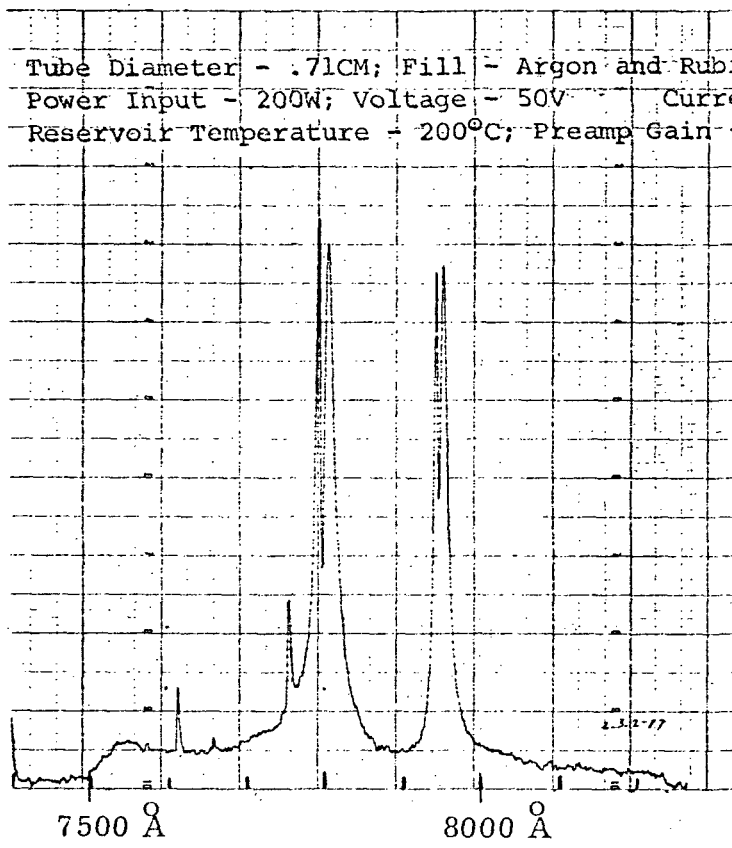

Figure 28a Relative Spectra of Rubidium As a Function of Wavelength

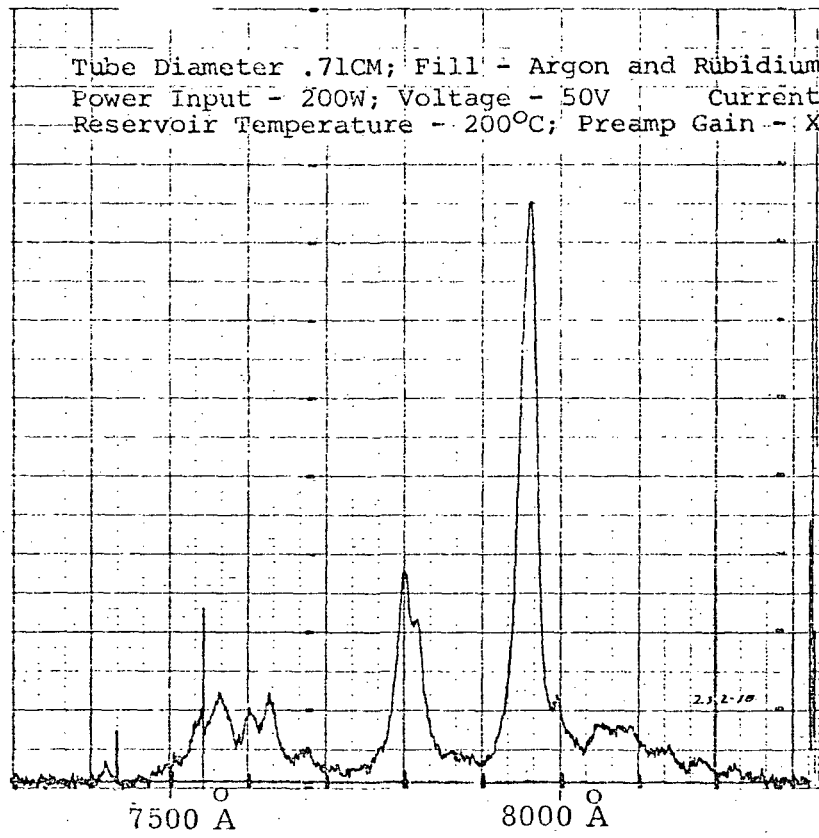

Figure 28b Relative Fluorescence from Nd:YAG at 1.06μ As a Function of Wavelength

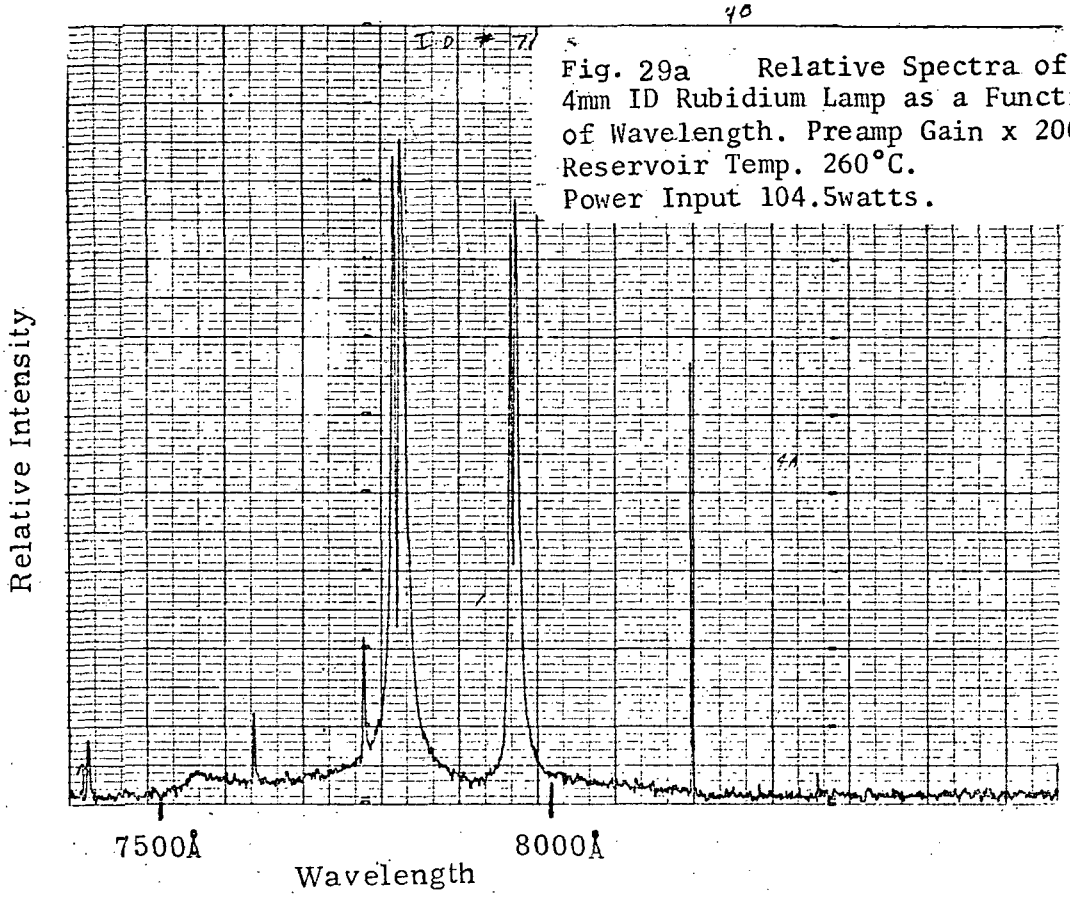

Fig. 29a Relative Spectra of 4mm ID Rubidium Lamp as a Function of Wavelength. Preamp Gain x 200 Reservoir Temp. 260°C. Power Input 104.5watts.

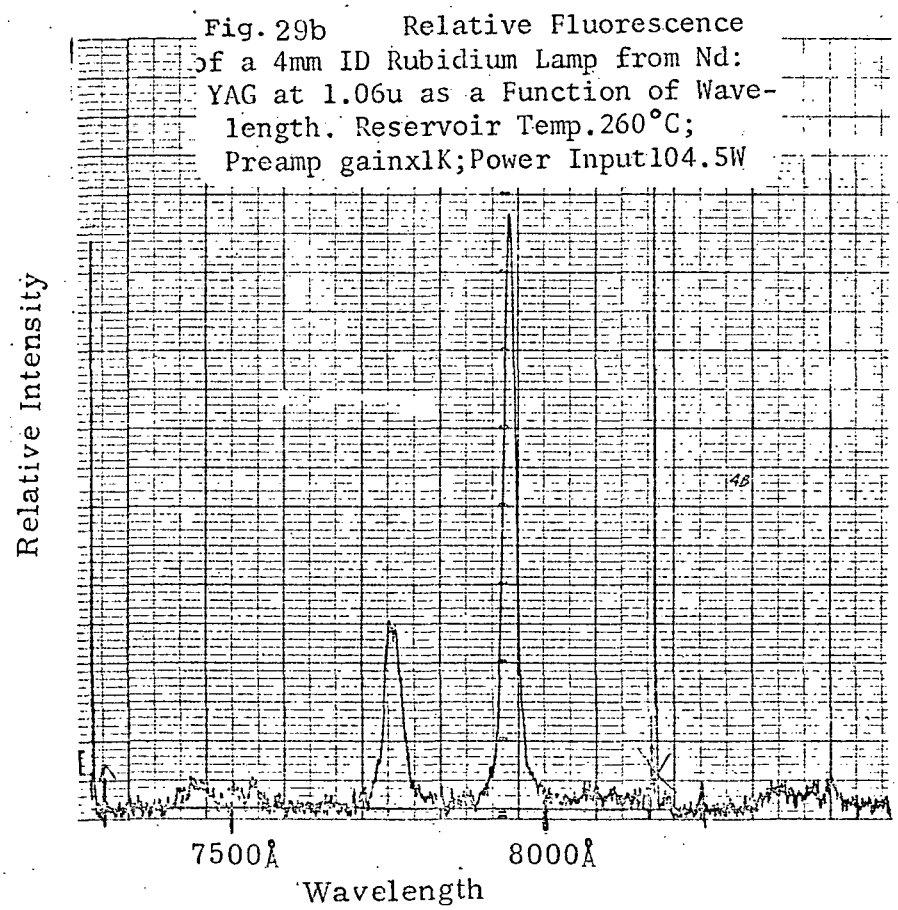

Fig. 29b Relative Fluorescence of a 4mm ID Rubidium Lamp from Nd: YAG at 1.06u as a Function of Wavelength. Reservoir Temp.260°C; Preamp gainx1K;Power Input104.5W

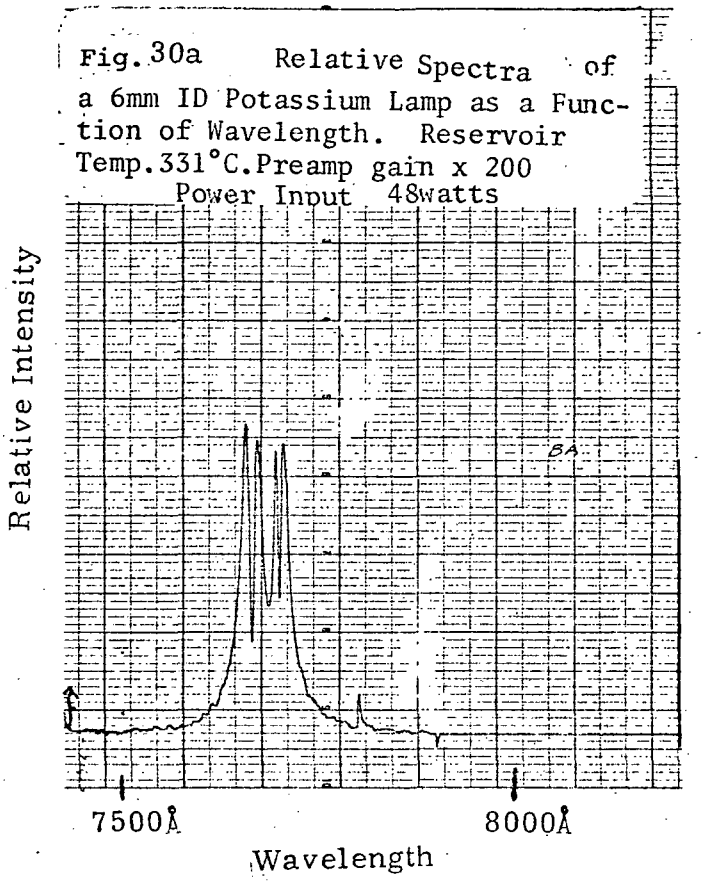

Fig. 30a Relative Spectra of a 6mm ID Potassium Lamp as a Function of Wavelength. Reservoir Temp. 331°C. Preamp gain x 200 Power Input 48watts

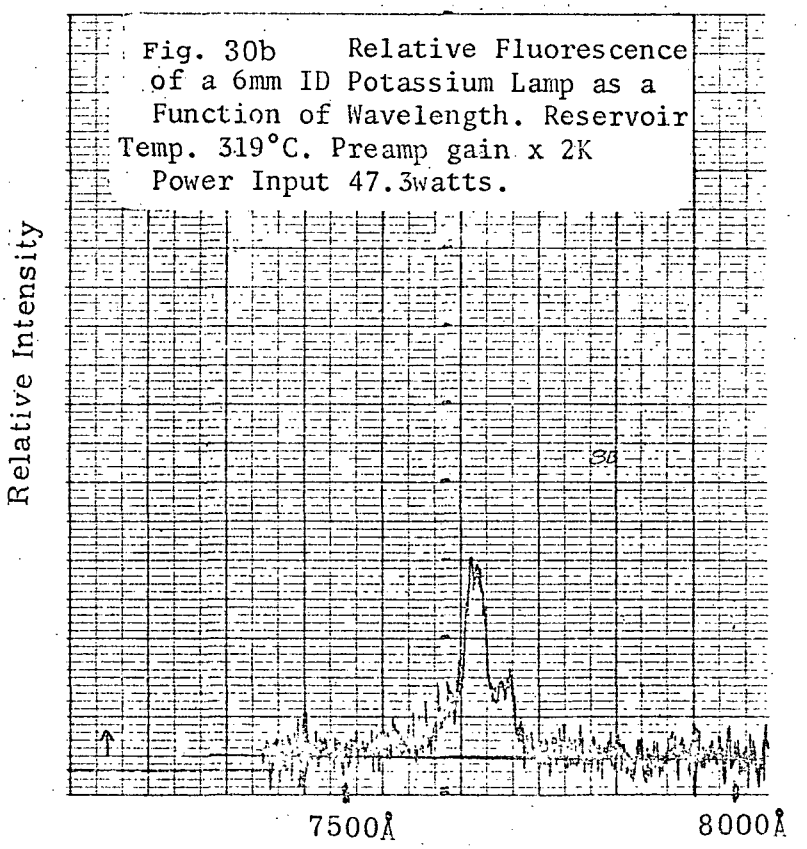

Fig. 30b Relative Fluorescence of a 6mm ID Potassium Lamp as a Function of Wavelength. Reservoir Temp. 319°C. Preamp gain x 2K Power Input 47.3watts.

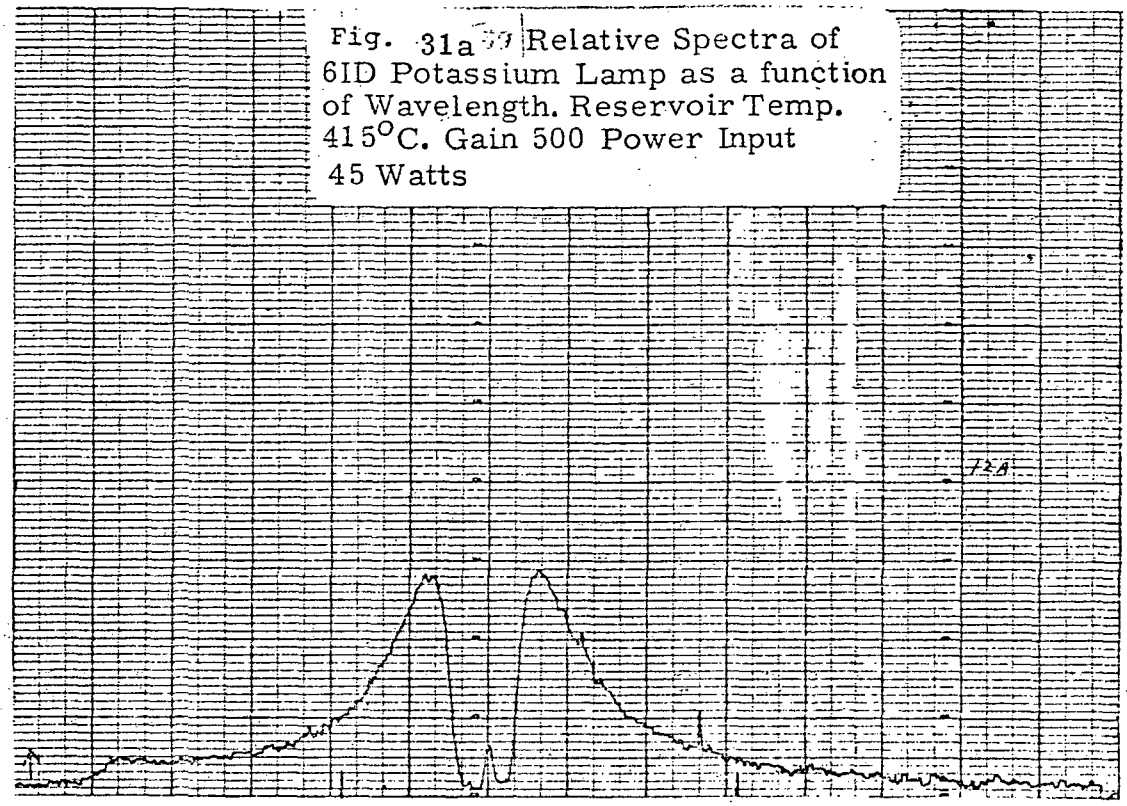

Fig. 31a Relative Spectra of 6ID Potassium Lamp as a function of Wavelength. Reservoir Temp. 415°C. Gain 500 Power Input 45 Watts

7500 8000

Wavelength Å

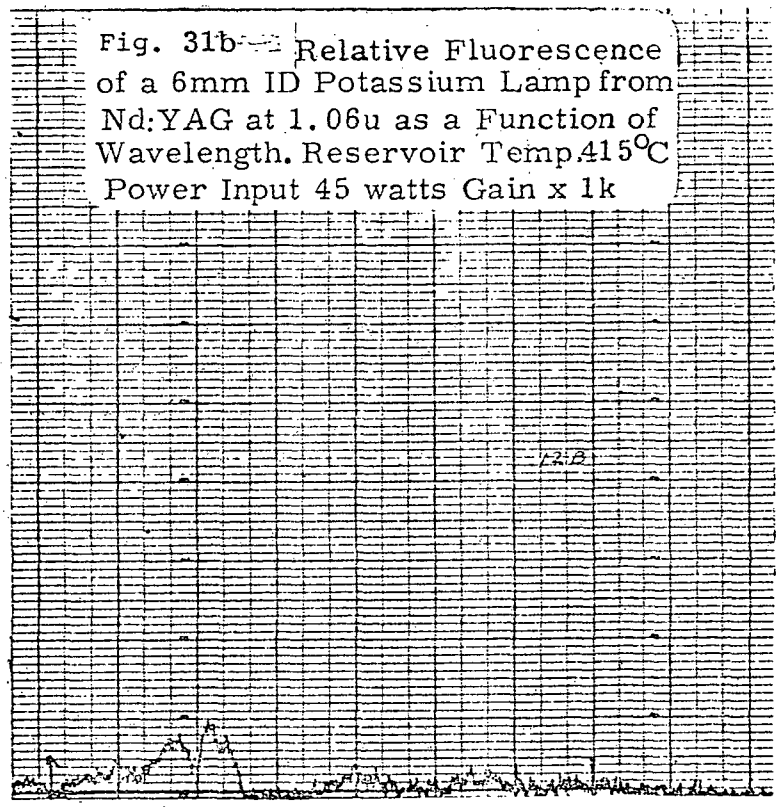

Fig. 31b Relative Fluorescence of a 6mm ID Potassium Lamp from Nd:YAG at 1.06u as a Function of Wavelength. Reservoir Temp 415°C Power Input 45 watts Gain x 1k

7500 8000

Wavelength Å

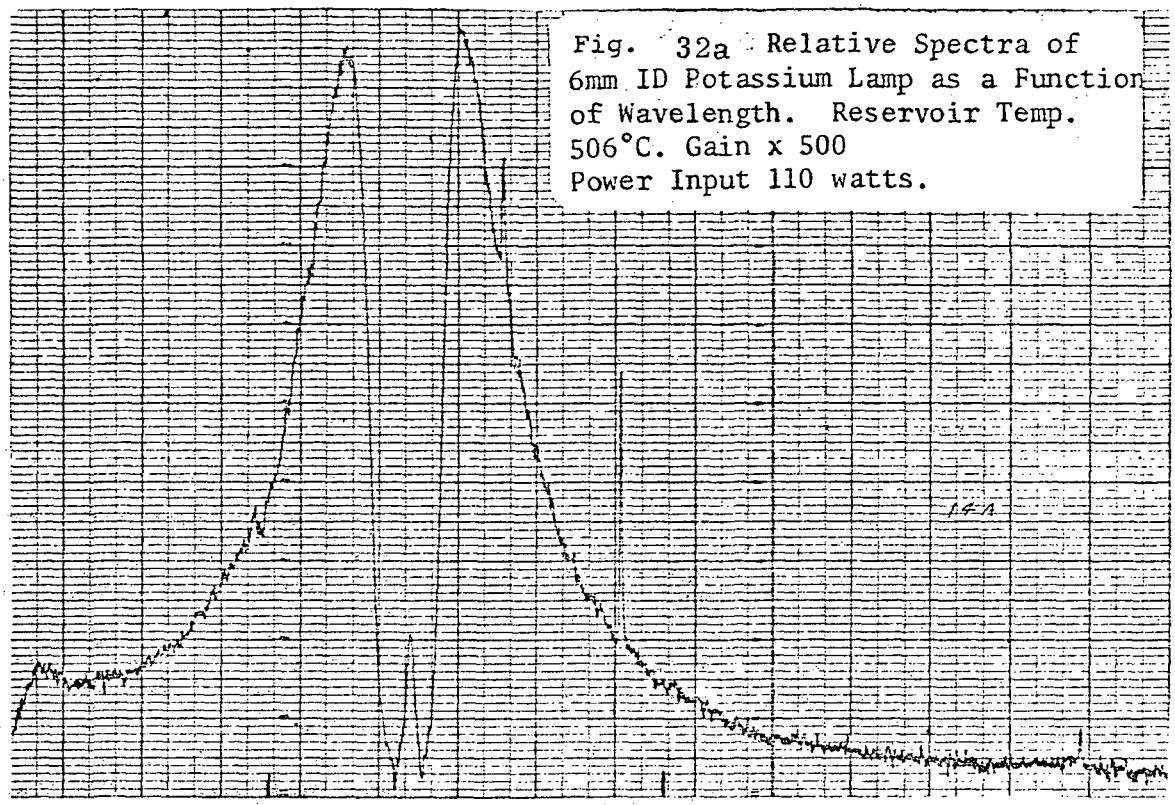

Fig. 32a Relative Spectra of 6mm ID Potassium Lamp as a Function of Wavelength. Reservoir Temp. 506°C. Gain x 500
Power Input 110 watts.

7500 8000

Wavelength Å

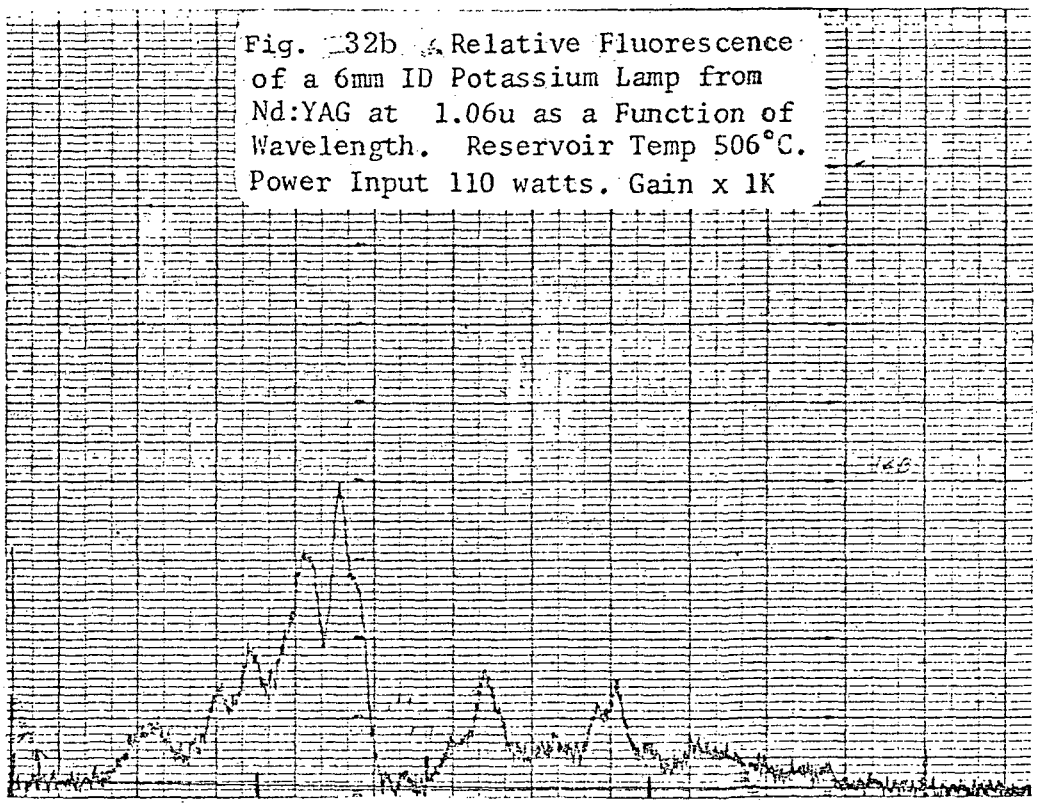

Fig. 32b Relative Fluorescence of a 6mm ID Potassium Lamp from Nd:YAG at 1.06u as a Function of Wavelength. Reservoir Temp 506°C. Power Input 110 watts. Gain x 1K

7500 8000

Wavelength Å

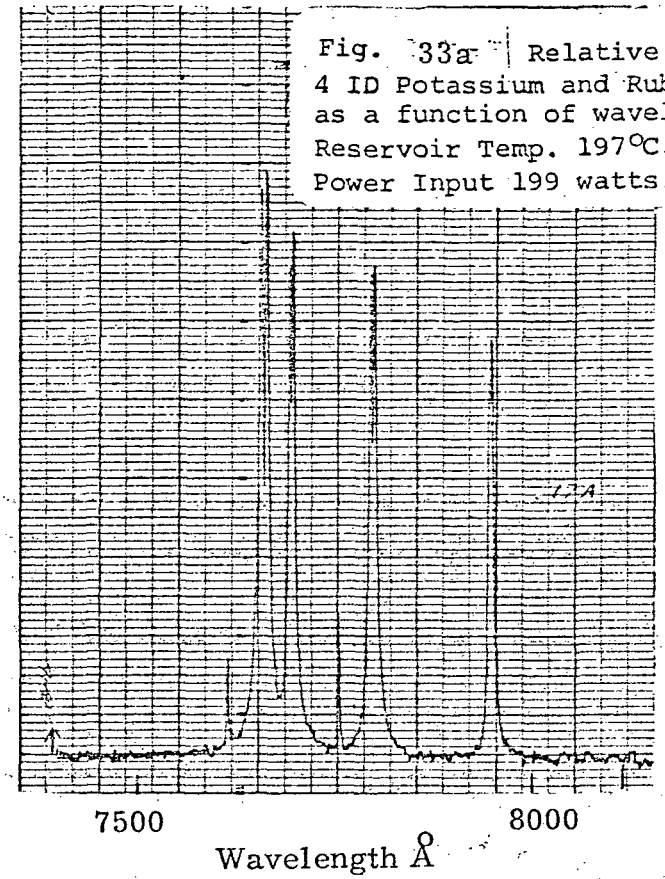

Fig. 33a | Relative Spectra of 4 ID Potassium and Rubidium Lamp as a function of wavelength. Reservoir Temp. 197°C. Gain 100 Power Input 199 watts.

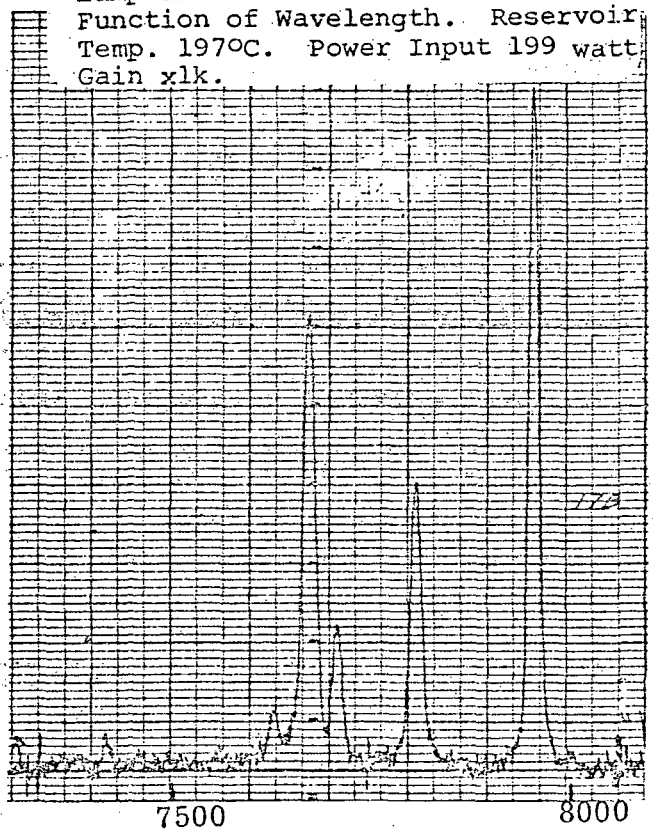

Fig. 33b | Relative Fluorescence of a 4 mm ID Potassium & Rubidium Lamp from Nd:YAG at 1.06u as a Function of Wavelength. Reservoir Temp. 197°C. Power Input 199 watt Gain x1k.

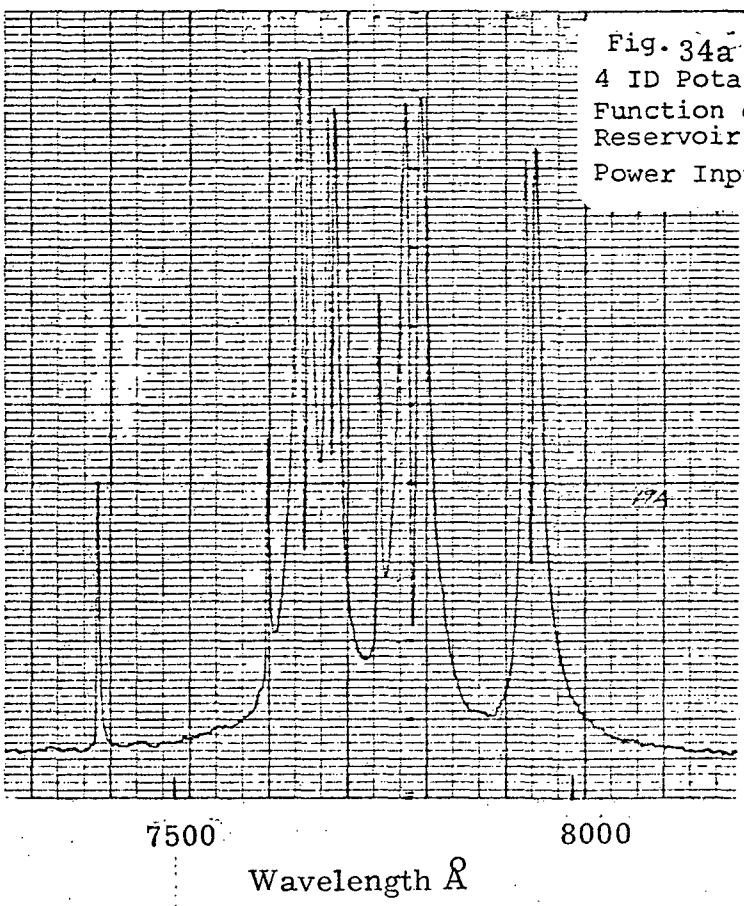

Fig. 34a Relative Spectra of 4 ID Potassium Rubidium Lamp as a Function of Wavelength. Reservoir Temp. 300°C. Gain 100 Power Input 206.4 watts

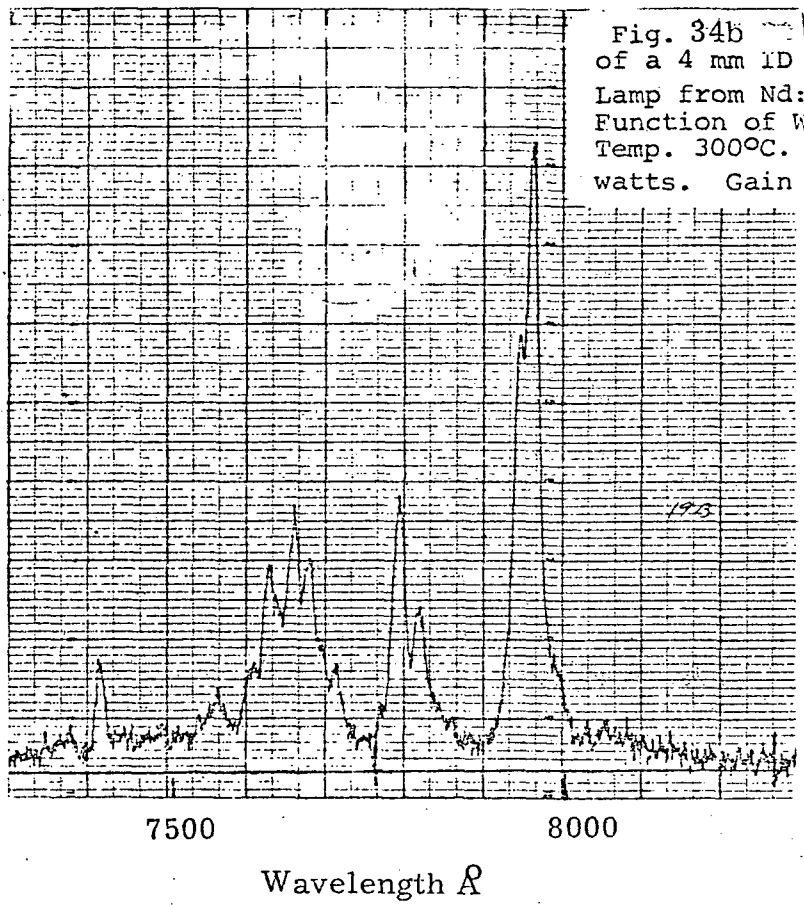

Fig. 34b Relative Fluorescenc of a 4 mm ID Potassium & Rubidium Lamp from Nd:YAG at 1.06u as a Function of Wavelength. Reservoir Temp. 300°C. Power Input 206.4 watts. Gain x1k

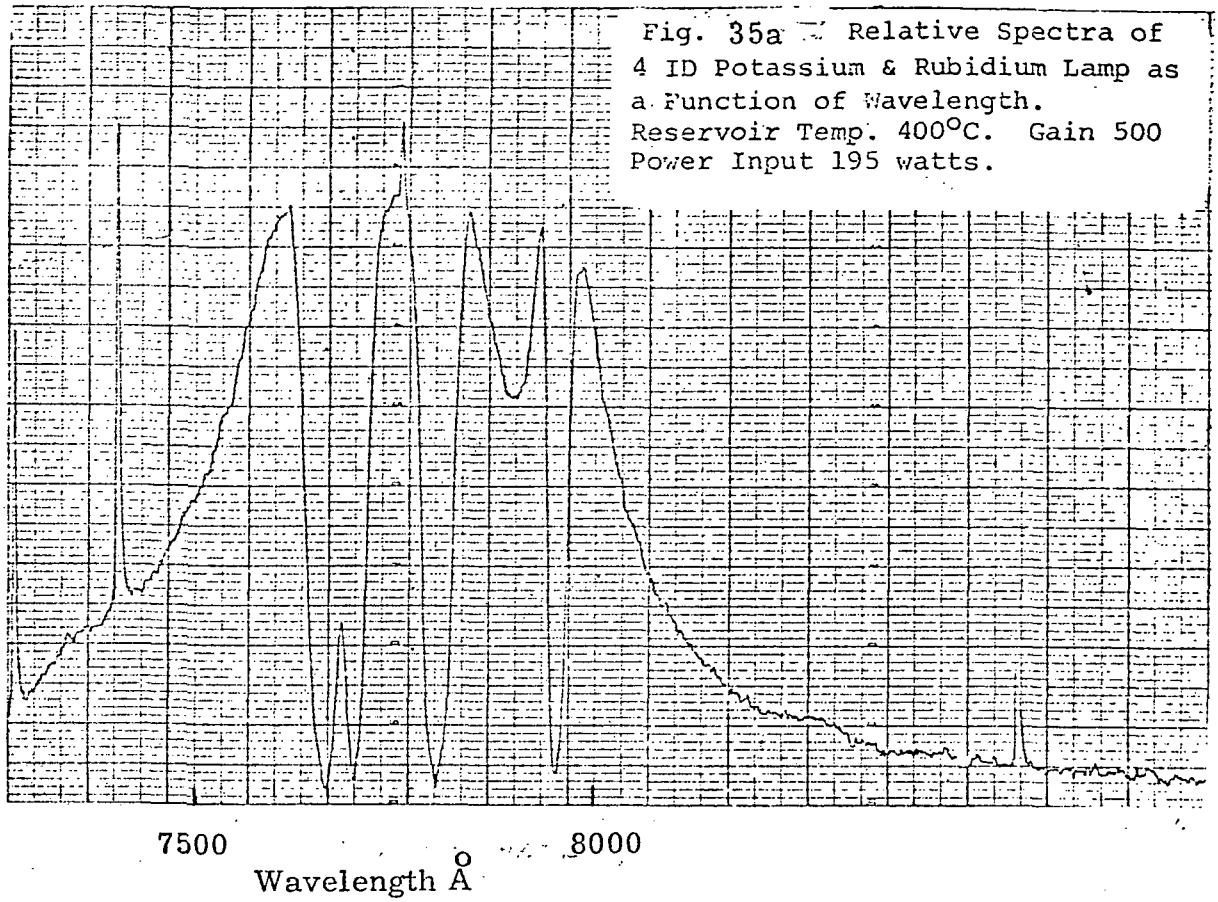

Fig. 35a Relative Spectra of 4 ID Potassium & Rubidium Lamp as a Function of Wavelength. Reservoir Temp. 400°C. Gain 500 Power Input 195 watts.

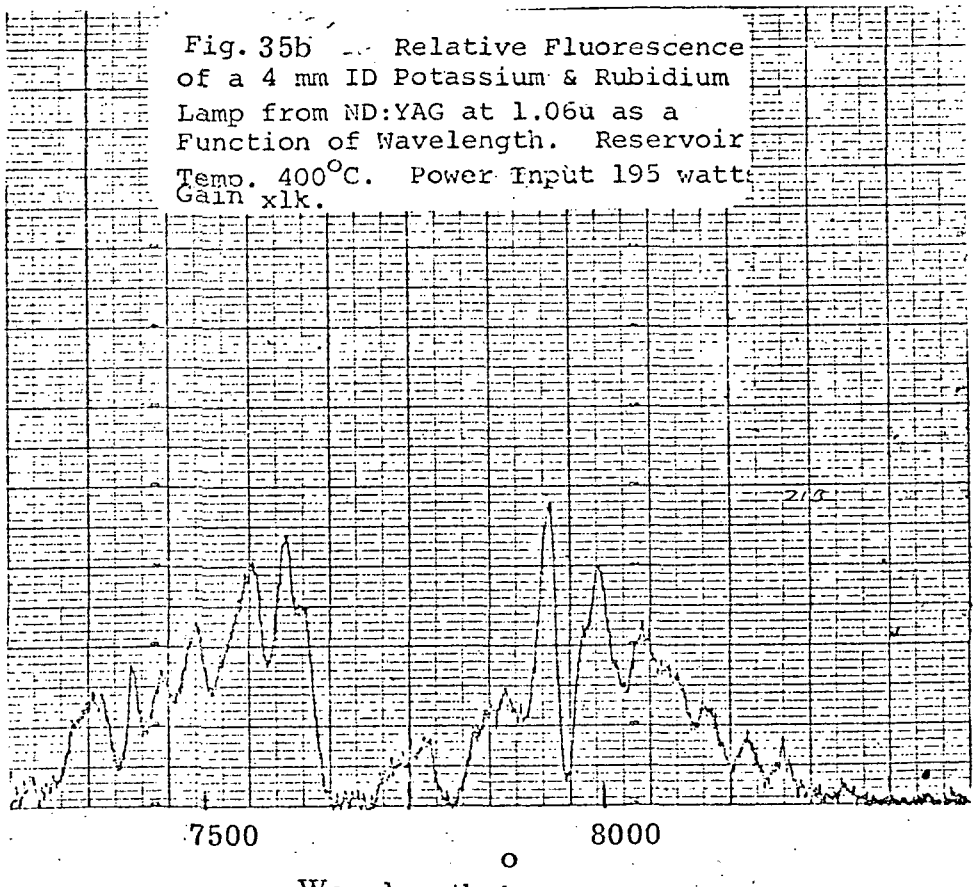

Fig. 35b Relative Fluorescence of a 4 mm ID Potassium & Rubidium Lamp from ND:YAG at 1.06u as a Function of Wavelength. Reservoir Temp. 400°C. Power Input 195 watts Gain x1k.

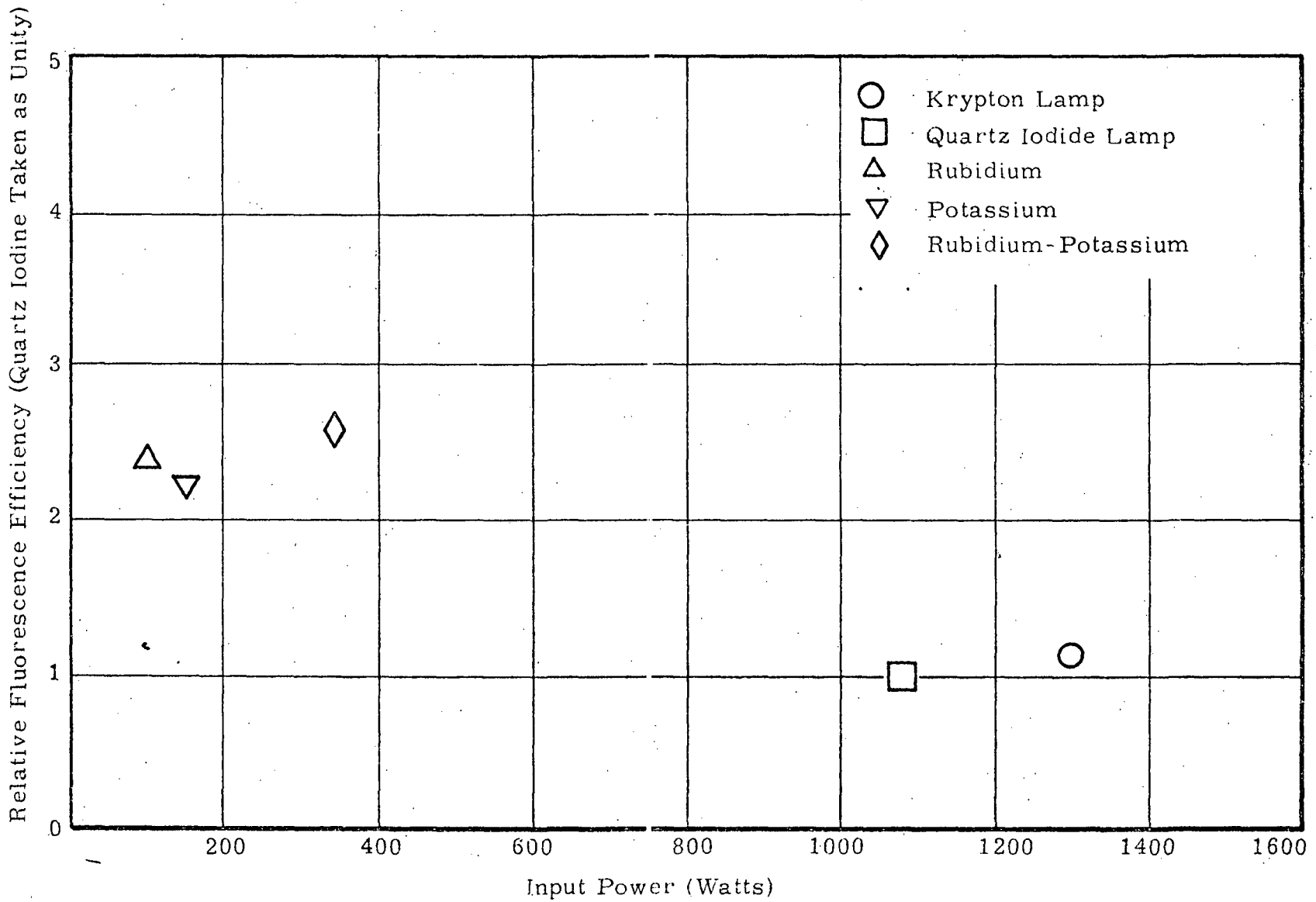

FIGURE 36 YAG 1.06μ FLUORESCENCE EFFICIENCY OF THE ALKALI VAPORS AND KRYPTON RELATIVE TO QUARTZ IODINE

fluorescence efficiency. Based on the above data, the evaluation procedure was modified in order to simplify the optimization task.

5.2.2 Modified Optimization Technique

To facilitate the determination of the optimum spectral match, a simplified approach was undertaken. A lamp with only a single alkali metal (in this case rubidium) was fabricated and operated in the integrating sphere. During these tests, attempts were made to determine the operating condition which yielded the maximum fluorescence output. The previous method was to take complete fluorescence scan and by integration compare the total areas under the curve. The particular method, however, results in a large quantity of data to be both taken and analyzed. In order to expedite the data collection and analysis, a second method was developed. This method consisted of measuring the total fluorescence output by scanning the spectrometer through the zero order. In the zero mode of operation, all the radiation entering the collecting optics of the spectrometer is transmitted into the fluorescence cell. To limit the light entering the collecting optics, a Fish Schurman type 14B filter is used. This filter does not transmit any appreciable amount of radiation beyond 8600Å and therefore limits the total fluorescence measurement to the contributions from the Nd:YAG 7300Å - 7700Å and 7900Å - 8300Å absorption bands. Figure 37 shows the absorption curve of Nd:YAG and the response curves of the RG1000 filter of the fluorescence cell and the 14B filter used in the collecting optics of the spectrometer. It can be seen that the response of the 14B filter is down by approximately 15% for the 7900Å - 8300Å absorption and therefore will result in some error in the total fluorescence measurement. Comparison between the integrated total fluorescence and the total fluorescence measurement agree to within 20% which is more than adequate for the optimization tests.

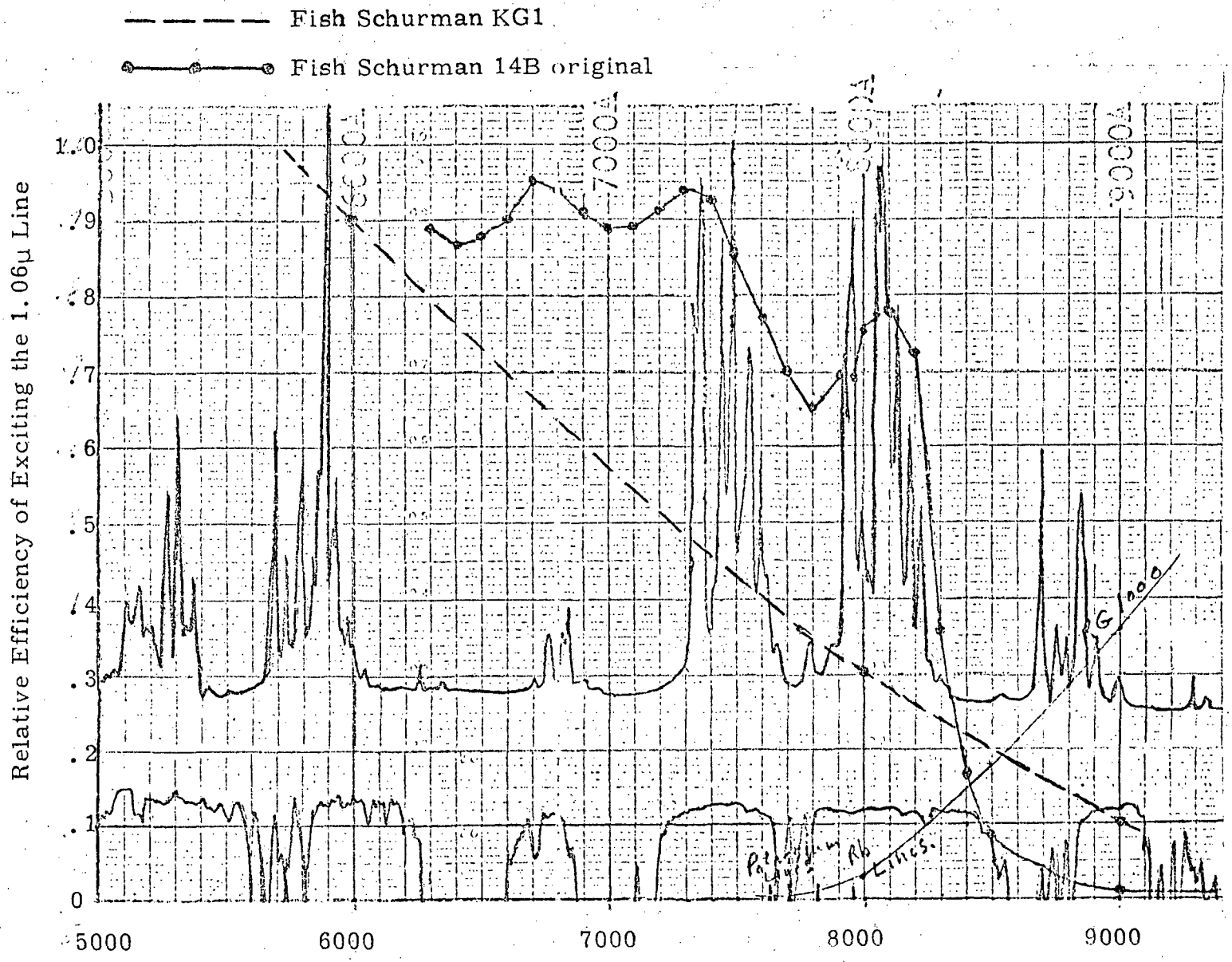

FIGURE 37
Nd:YAG Absorption and Filter Response as a Function of Wavelength

Figure 38 shows a series of total fluorescence output scans taken on a 2mm bore rubidium lamp for various vapor pressures. In these curves, the significant data point is the amplitude of the peak which is representative of the total fluorescence output at zero order. In particular, curve (e) corresponds to the rubidium vapor pressure which resulted in the maximum output. Any increase or decrease in rubidium vapor pressure from this point results in a lower total fluorescence output. The spectrum of the lamp operating at this vapor pressure (43 torr) is shown in Figure 39. Examination of this spectrum in conjunction with the Nd:YAG spectrum shows where it is possible that a high (self absorbed) vapor pressure rubidium spectrum may be more efficient than a low (resonance line) pressure spectrum. In the low pressure spectrum, the fluorescence contribution primarily results from the 7947Å line which closely matches a strong Nd:YAG absorption line. On the other hand, the high pressure spectrum has broadened sufficiently to match several strong absorption lines in the 7900Å to 8100Å region as well as a weak absorption line just below 7800Å. This high pressure match which includes more Nd:YAG absorption lines results in the higher total fluorescence measurement. It should be noted there, that this data was taken for a 2mm bore lamp. For the same spectral output shape in larger diameter lamps, the rubidium vapor pressure will be lower due to the increased absorption length in the plasma.

Now that the rubidium spectral characteristic which produces the maximum fluorescence output is known, the task of optimizing a rubidium potassium lamp becomes greatly simplified. One approach is to use a pure potassium lamp and as before determine the condition which produces the maximum fluorescence. Once this vapor pressure has been optimized, one could then assume that the total optimum lamp fill pressure would be the combination of the individual optimum vapor pressures. However, the technique of filling a lamp directly to the above prescribed optimum values becomes very difficult since at a particular temperature the vapor pressure of the individual alkali fill metals are not readily relatable to the total vapor pressure and hence individual partial

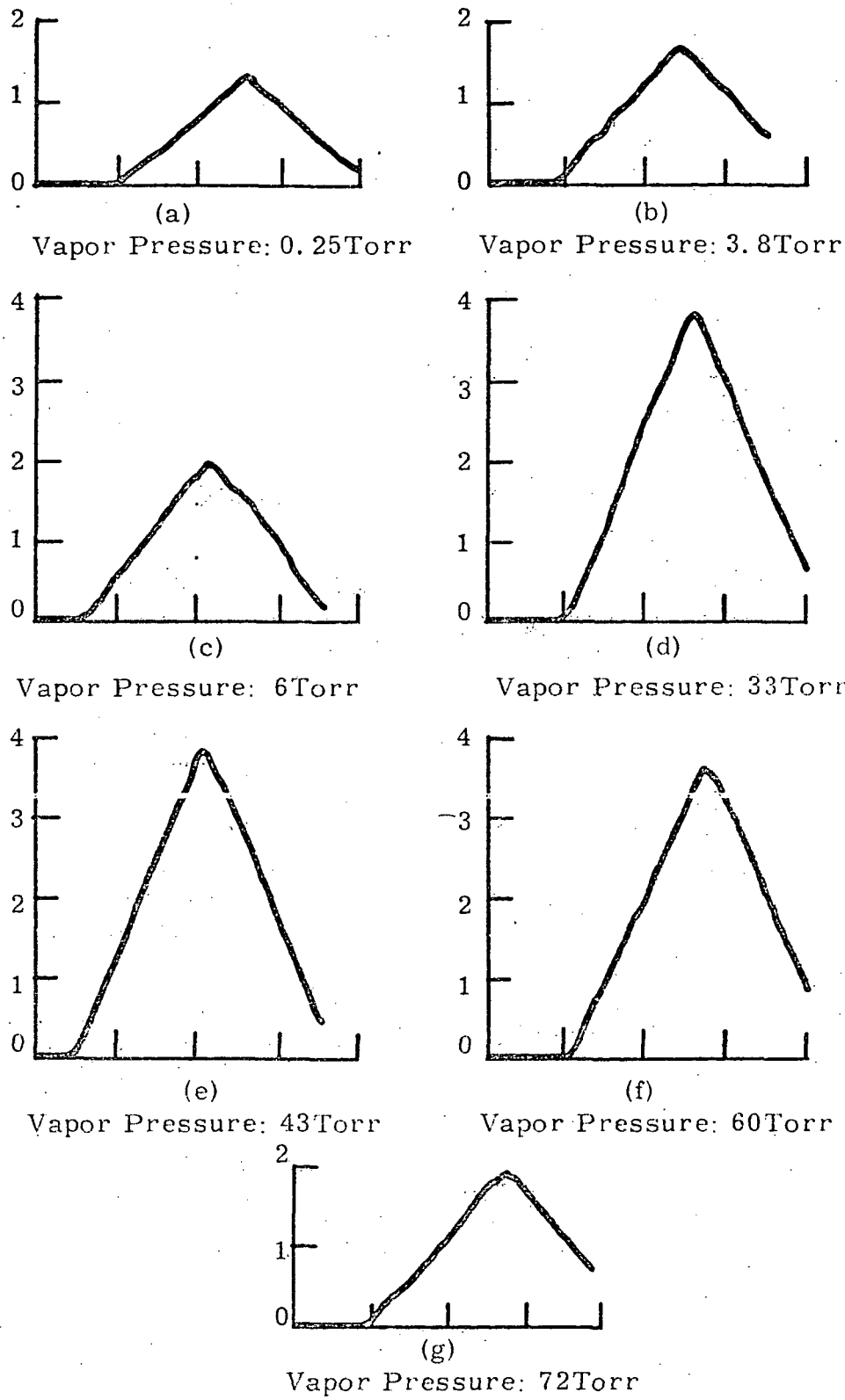

FIGURE 38 RELATIVE TOTAL FLUORESCENCE OF VARIOUS Rb VAPOR PRESSURES (MEASURED BY SCAN THROUGH ZERO ORDER)

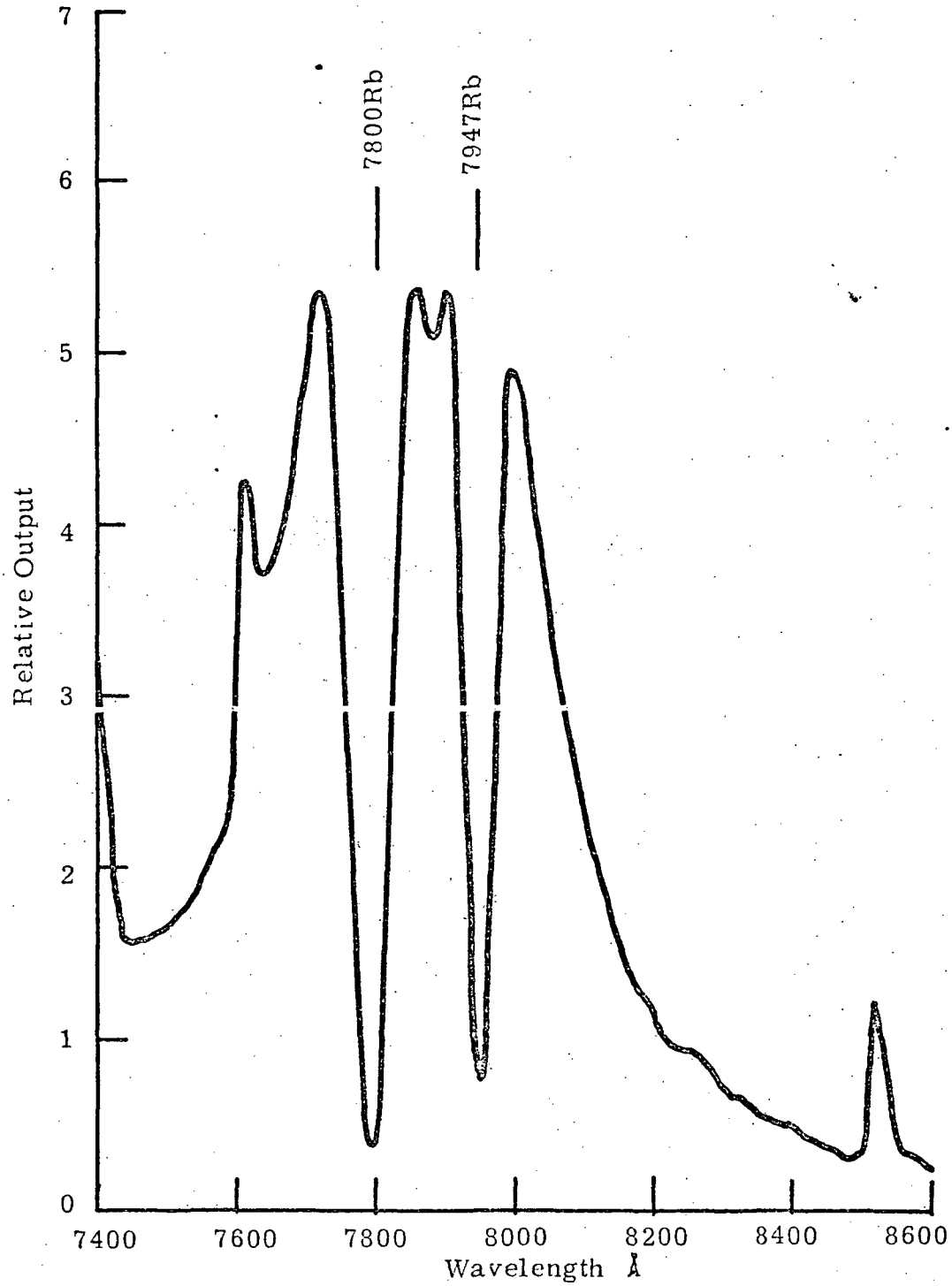

FIGURE 39 RUBIDIUM SPECTRUM
IN A 2mm BORE LAMP OPERATING AT
53.2 VOLTS AND 43 TORR

pressures of an arbitrary mixture. This fact can be understood by an examination of Raoult's Law in combination with an understanding of the statistical mechanics associated with the mixing of liquids. As has been stated earlier, these topics are presented in greater detail in Appendix I. It is for the above reasons that the method of varying the weight ratios and mole fractions of the components was chosen as the method of approaching the optimum fill.

Elenbaas[13] has shown that discharges in different size envelopes exhibit similar properties (i.e., temperature and radiation) if the amount of vapor per unit arc length and the input power densities are identical.

This is equated as:

$$R_1^2 P_1^{-1/2} E_1^2 = R_2^2 P_2^{-1/2} E_2^2$$

$$R_1^2 P_1 = R_2^2 P_2$$

where R is the tube radius, P is the vapor pressure or pressure ratio and E is the discharge potential gradient.

Thus it can be shown that the optimum laser excitation vapor pressure ratio will vary as the ratio of the square of the lamp diameters. The optimum pressure ratio based on the law of similarity is shown in Table I for several lamp diameters.

Table II is a comparison of the data taken on the three pure rubidium lamps which exhibited similar spectral characteristics (see Figures 27 - 29). The table shows that this data tends to follow the above relationships optimized fill approximation. The errors in this table result from two sources namely that the spectrums were not truly identical and in the particular temperature region chosen (104° - 250°C) the vapor pressure curve is very steep, so small temperature variations (errors) result in large vapor pressure differences.

TABLE I

OPTIMUM POTASSIUM-RUBIDIUM PRESSURE RATIOS

Tube Diameter mm	Calculated Pressure Ratio P_K/P_{Rb}	Measured Holobeam	ILC
2	5/1		
3	2.2/1	2.0/1	
4	1.25/1	1.25/1	1/1
5	0.8/1		
6	0.55/1		

These values should be considered as the starting points for any optimization rather than the solution.

TABLE II

Reservoir Temp.	Vapor Pressure	Pressure Ratio	R	R^2	Radius Ratio
^oC	Torr	$P114/P_m$	mm	mm^2	R^2m/R^2_1
114	3×10^{-3}	1	19.8	392	1
200	3×10^{-2}	.100	7.1	50.5	.128
260	2×10^{-1}	.015	4	16	.041

SECTION VI

LASER CAVITY PERFORMANCE

The previous sections have been concerned with the theoretical design (performance) and construction of the laser cavity and the design, fabrication and test of the pump lamp. The testing and performance of the lamp were related to the abstract quantity of fluorescence efficiency which does not predict the performance in laser system. Therefore, with the knowledge gained to date and the emperial relationships developed, the remainder of the lamps fabricated were tested in a laser cavity and performance was measured as output laser power (multi-mode).

The 2 and 3mm data was obtained during investigations in support of a similar program and was reported in Reference 9. It is included here to present a complete analysis.

6.1 2mm System

A 2 x 30mm Nd:YAG rod was placed in the test system described in Section 2.2. In order to establish a reference standard, a 1500 watt tungsten lamp was used to pump the rod. Figure 40 shows the laser power output vs tungsten power for a maximized cavity configuration. As can be seen, the threshold for this rod and cavity configuration is approximately 900 watts. A significant contribution to this high threshold value is the mismatch between the diameter of the tungsten filament and the laser rod. Based on the above performance, it was decided that it would be extremely difficult to obtain CW laser output from a low power alkali pump lamp. Therefore, the 2mm configuration was not given any further consideration as a space qualified system.

6.2 3mm System

Next a 3mm rod was placed in the test system and a tungsten curve was run. This data is shown in Figure 41. It can be seen from this curve that a low threshold value of 430 watts was achieved but was difficult to maintain. The most consistant threshold value was in the region of 575 watts. This value was lowered to 480 watts by upgrading the cooling water system and maintaining the laser rod at 50°F.

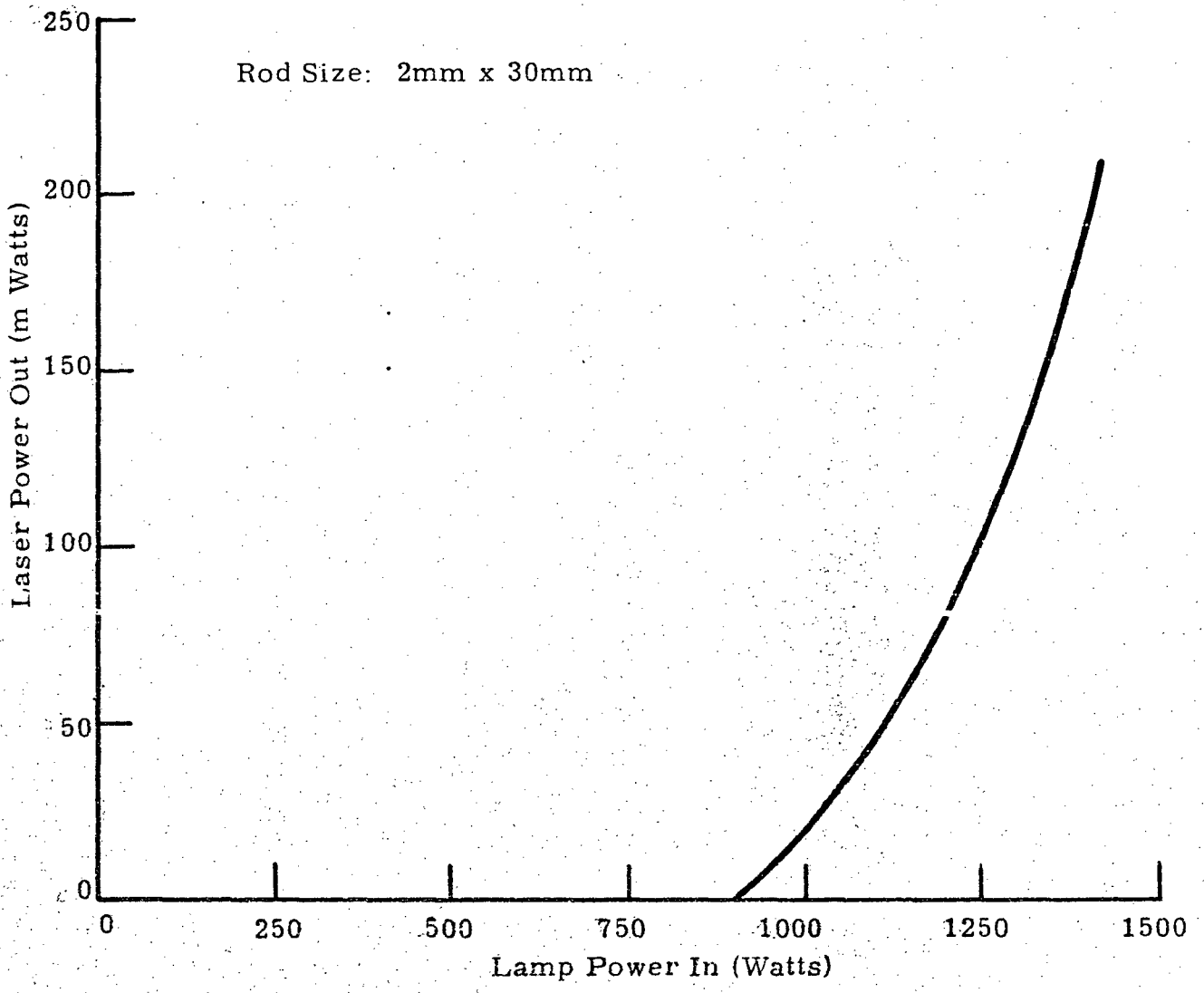

FIGURE 40 LASER TEST CAVITY OUTPUT AS A FUNCTION OF INPUT FOR TUNGSTEN PUMP LAMPS

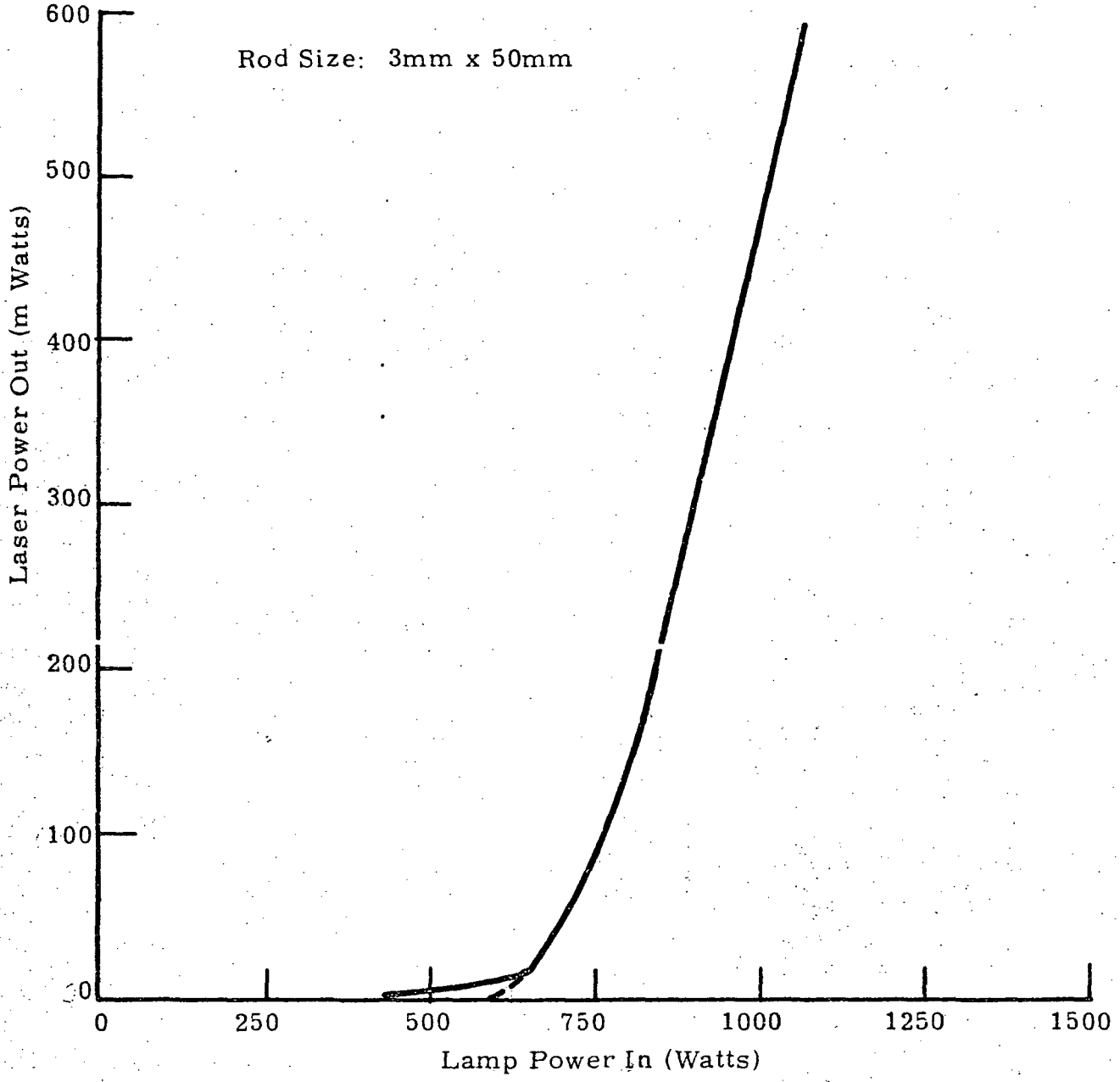

FIGURE 41 LASER OUTPUT AS A FUNCTION OF LAMP INPUT FOR TUNGSTEN LAMPS

The alkali vapor lamp placed in the laser cavity had a 3mm bore and a 2 to 1 ratio by weight of potassium to rubidium. This weight ratio is the starting point for optimization as dictated by preceding discussion. Laser output power data was taken both as a function of DC power input and lamp vapor pressure. Figure 42 shows a summary of the above data taken with a 1% output coupling (99% reflective output mirror). From this figure, it may be seen that typical laser threshold values occurred between 70 and 90 watts. Curve B represents the laser output for the optimum spectral match with the particular fill in this lamp. Extrapolation of this data to higher power levels indicates that 1 watt of laser output power would have occurred at approximately 380 watts. The spectrum of the lamp taken during the condition represented by curve B is shown in Figure 43. This curve was taken of lamp light leakage from the laser cavity before the clearance holes were closed down. In future tests, this data was not available for recording because of the cavity modification. However, future spectra were visually monitored and determined to be of the same order of line spread as this last recorded data.

6.3 4mm System

Since the cavity analysis showed the 4mm rod to be a good performance compromise, the major emphasis on this program was directed towards developing a compatable lamp. Both 4mm and 6mm bore lamps were tested but the fill was not optimized for the latter case.

6.3.1 4mm Lamps

Based on the emperical relationships previously developed, the optimum lamp fill was determined to be in the region of a 1.25-1 weight ratio of potassium to rubidium. Figure 44 shows the laser output power for lamps with a 1.25-1 ratio and a 1 to 1 ratio fill. The latter fill was also evaluated since other investigators (14) have indicated it to be optimum for this lamp-rod combination. For the test cavity configuration with a 3% output mirror, it can be seen that the 1.25-1 ratio lamp has a slope efficiency of 2.25% while the 1 to 1 ratio lamp (evaluated under similar conditions) had a 1.25% slope efficiency. The 1-1 ratio lamp was tested for two vapor pressures and two output couplings with no appreciable change in slope efficiency. The only change

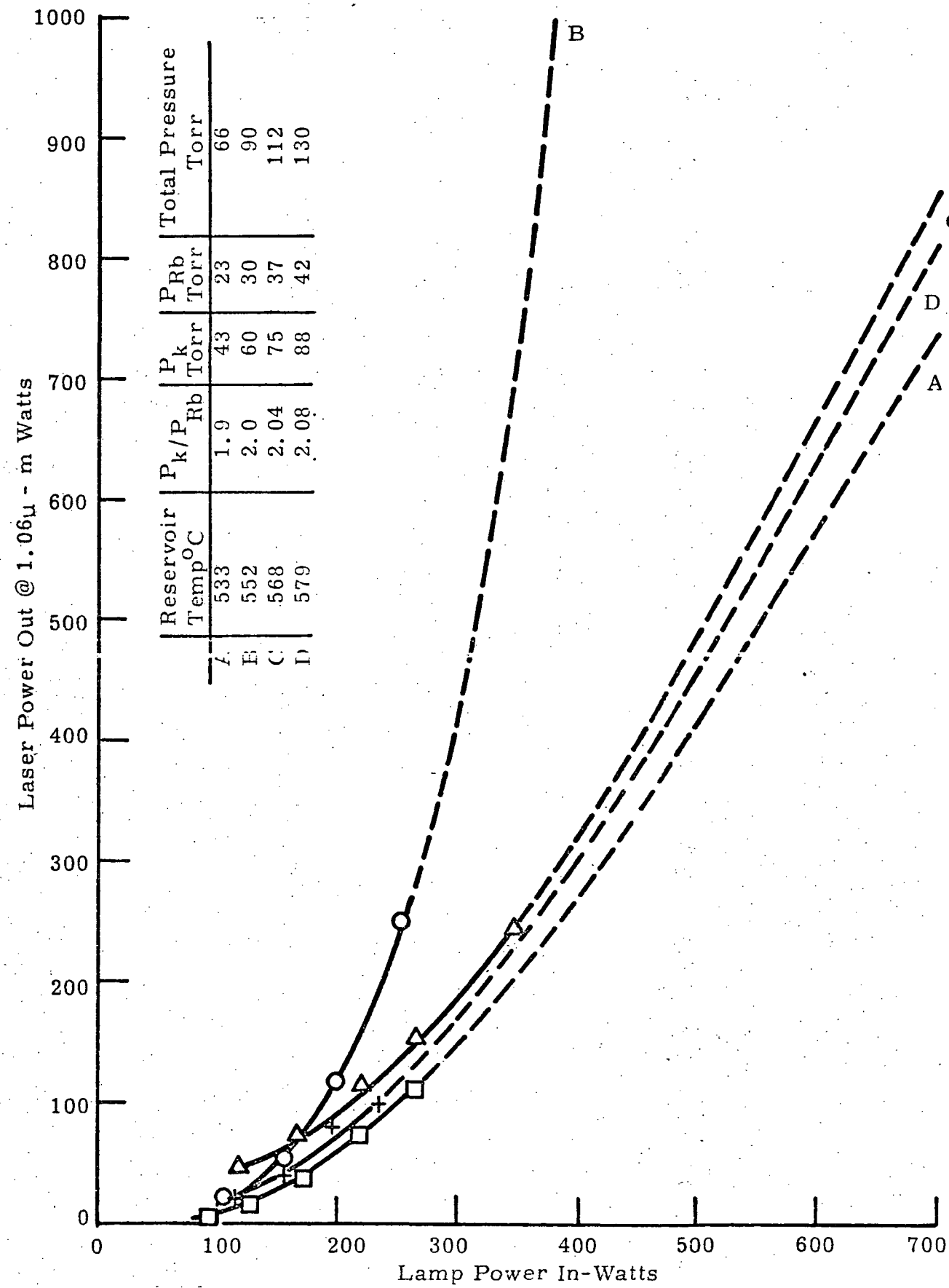

	Reservoir Temp °C	P_k/P_{Rb}	P_k Torr	P_{Rb} Torr	Total Pressure Torr
A	533	1.9	43	23	66
B	552	2.0	60	30	90
C	568	2.04	75	37	112
D	579	2.08	88	42	130

FIGURE 42 LASER OUTPUT POWER vs LAMP INPUT POWER ON ROD FOR 3x67mm LAMP AT VARIOUS FILL PRESSURES

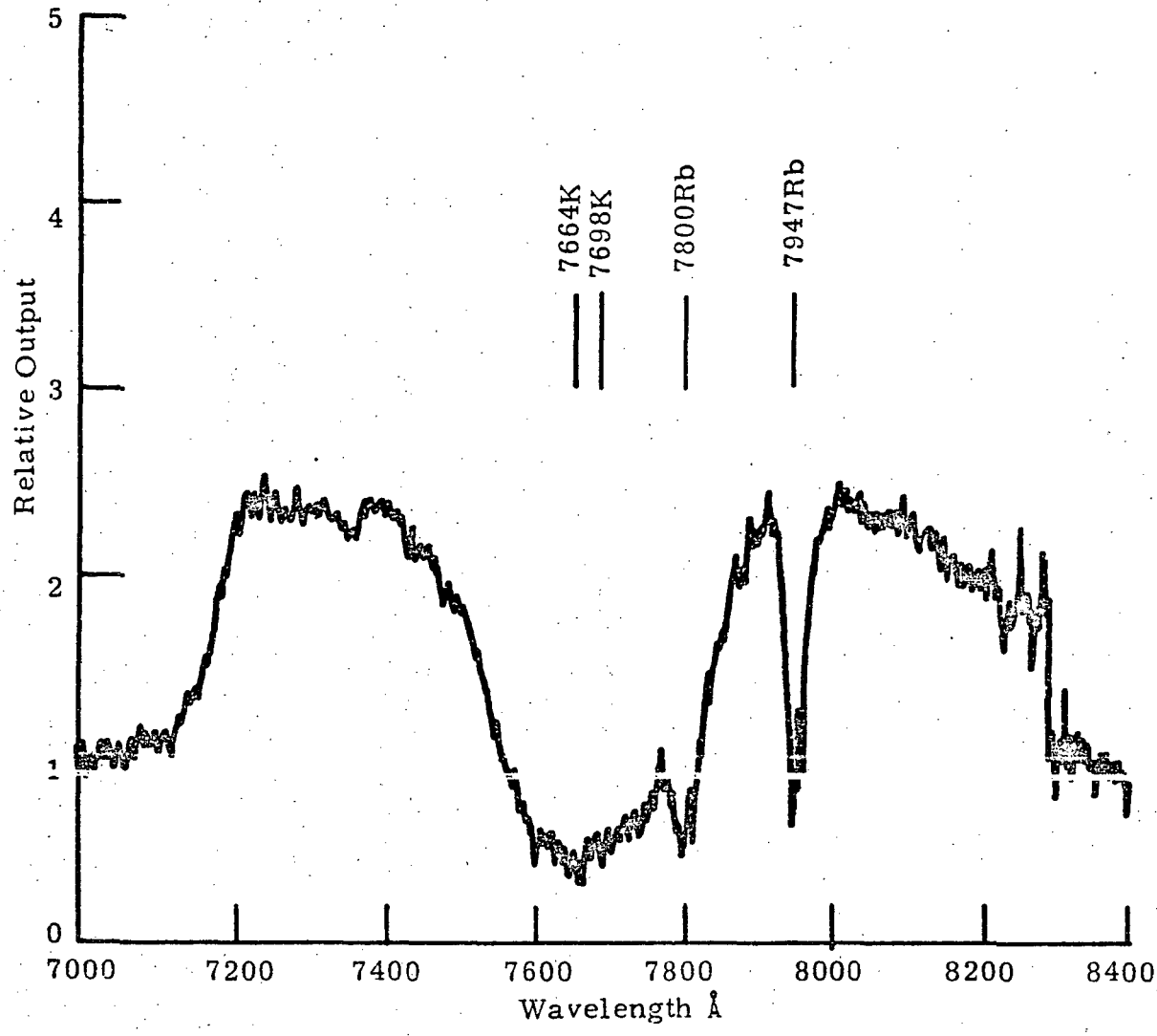

FIGURE 43 SPECTRAL OUTPUT FOR POTASSIUM-RUBIDIUM LAMP OPERATION IN LASER CAVITY

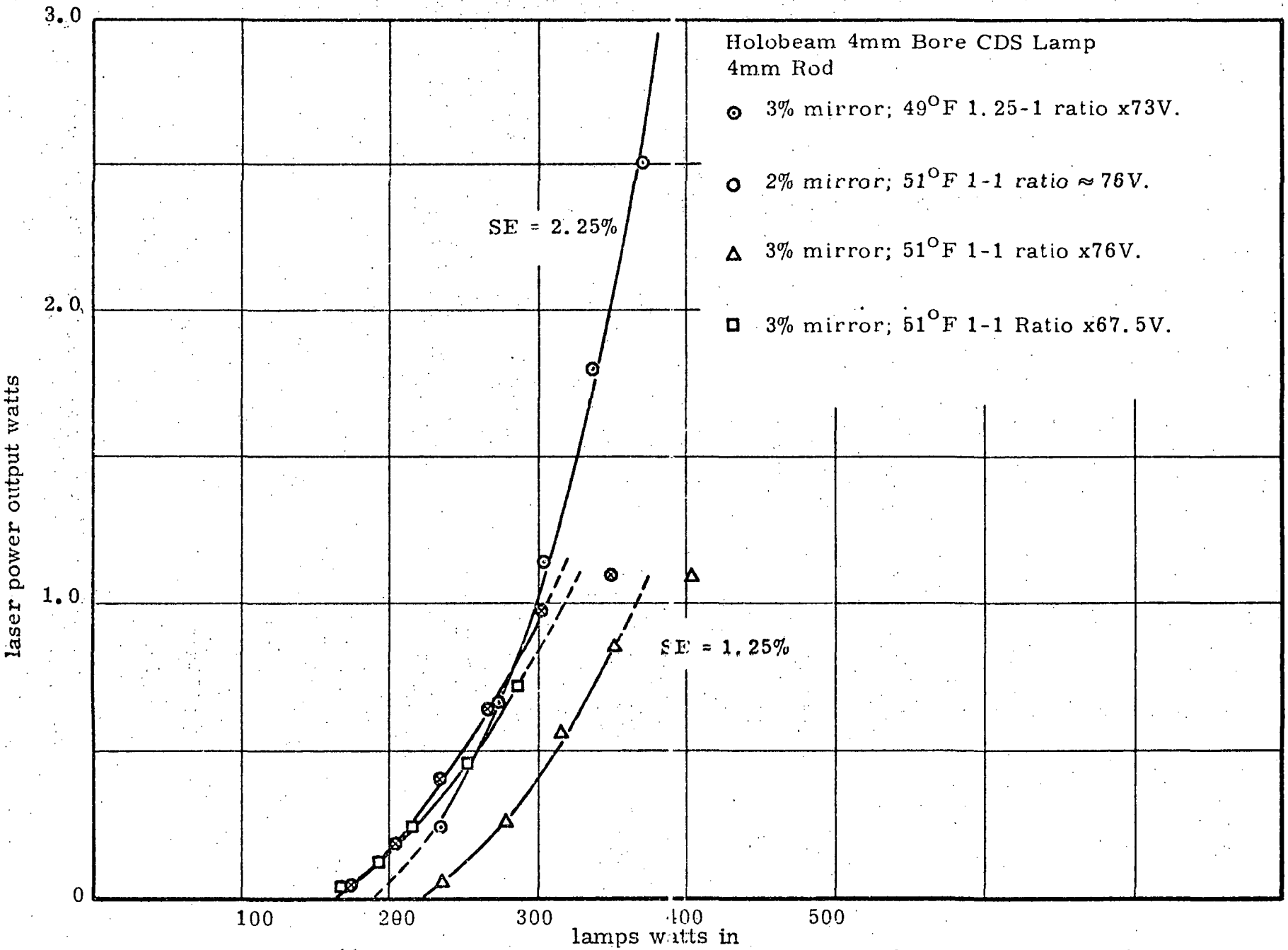

FIGURE 44 LASER POWER OUTPUT FOR SEVERAL LAMP FILL RATIOS AND OUTPUT COUPLINGS

noticed was in the rod threshold power. Based on this data, the 1.25-1 ratio fill was determined to be optimum for the 4mm bore lamp and was used as the fill for all future devices of this size. Both of the lamps used had CDS envelopes.

A second lamp with a CDS envelope and a 1.25-1 ratio K to Rb fill was tested in the laser cavity. During these runs, the output coupling was varied and laser power curves were obtained. These curves are shown in Figure 45 and follow laser theory as anticipated. Table III summarizes the slope efficiency and the threshold data taken. The maximum 1.06mm power output measured during these runs was 3.26 watts at 430 watts of input power.

6.3.2 6mm Lamps

A 6mm bore lamp with a TDS envelope was assembled and filled with a 1 to 1 ratio. The vapor pressure of the lamp was varied by an external heater until the best spectral match to the rod was obtained. This was determined by monitoring the laser output power. A power curve was then taken using a 2% output mirror and the resultant data is shown in Figure 46. Considering this was not an optimum fill (emperical formula predicts a 0.55-1 ratio) it, therefore, becomes significant that a slope efficiency of 1.65% was obtained. Using a 4mm bore lamp with a 2% coupling and a 1-1 ratio, the slope efficiency was only 1.25% and with the optimum fill improved to 1.55%. This improved slope efficiency observed for the 6mm device can probably be attributed to the improved coupling of the radiating plasma into the Nd:YAG rod. This hypothesis will be discussed further in the following section.

Extrapolation of the data to an optimum fill and a 3% output mirror should yield a slope efficiency in the region of 3%. This anticipated value can either be reinforced or increased with the use of a CDS envelope. Data presented in reference (14) indicates that there is approximately a 17% improvement with the use of the CDS envelope instead of the TDS envelope because of improved image projection. Stated another way, approximately 17% less power is required to produce equivalent laser output powers with the CDS lamp.

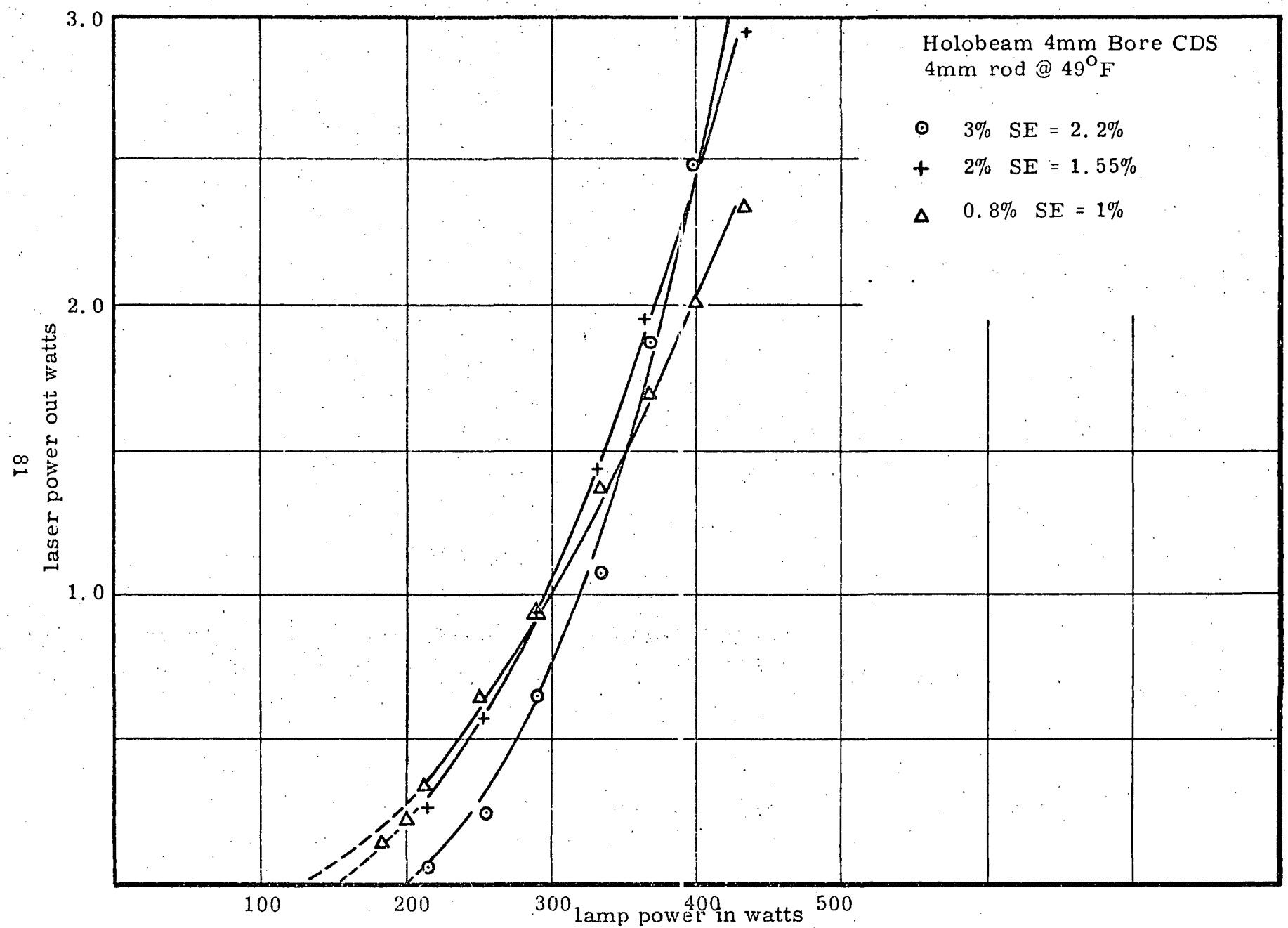

FIGURE 45 LASER OUTPUT POWER FOR AN OPTIMIZED 4mm BORE LAMPS AS A FUNCTION OF INPUT POWER AND OUTPUT COUPLING

TABLE III

Output Coupling	Threshold (Watts)	Slope Efficiency
0.8%	125	1%
2.0%	150	1.55%
3.0%	200	2.2%

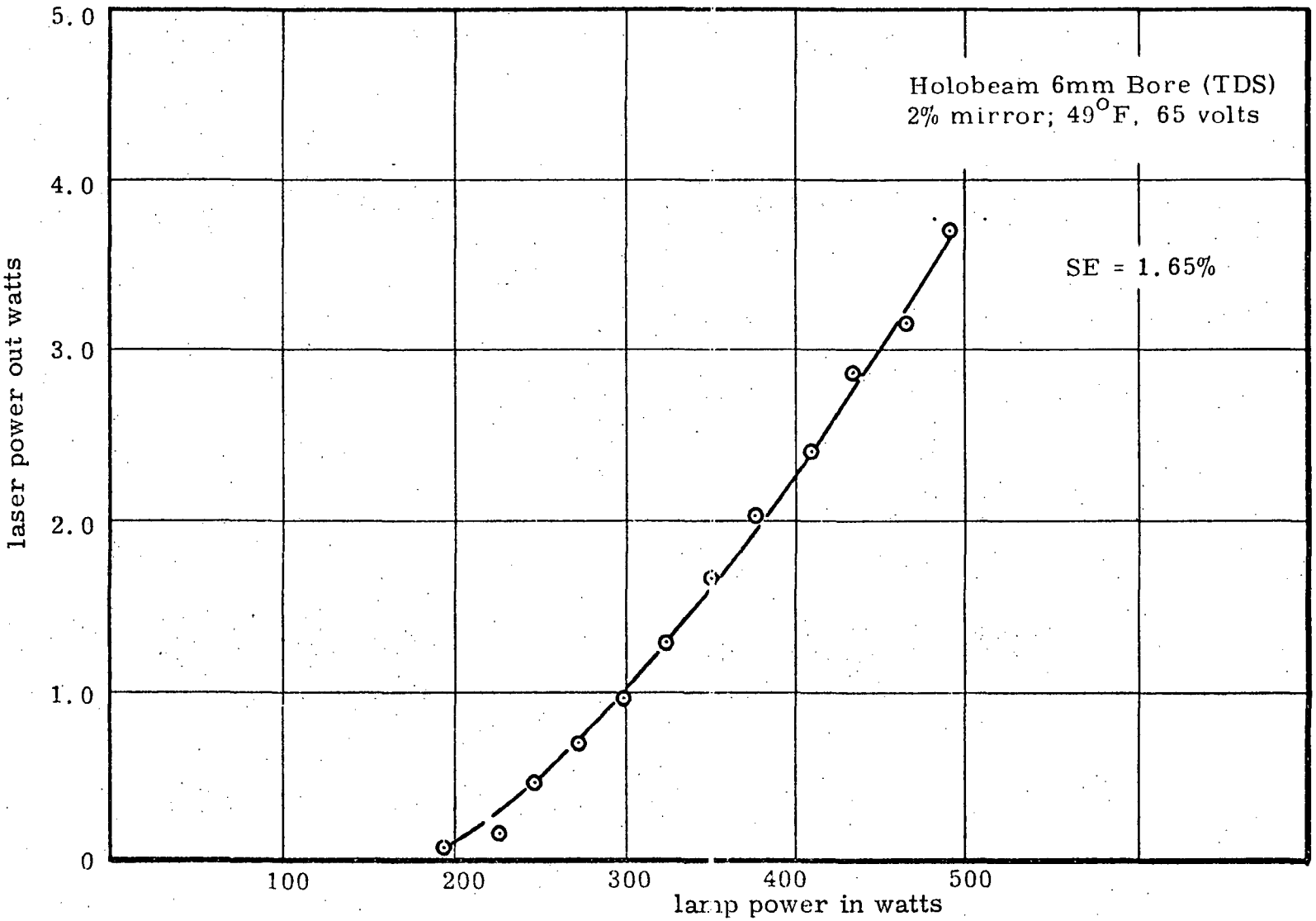

FIGURE 46 LASER OUTPUT POWER vs INPUT POWER FOR A 6mm BORE LAMP

6.4 Calculated Cavity Performance and Improvement

In Section 2.1, cavity performance curves were calculated from the Sylvania formula and were based on extremely ambitious and optimum parameters. These calculations used Po = 23 watts, dk = 0.15 cm/KW and α_o = .006 as the key parameters. Based upon the data shown in Figure 45, these key parameters were re-evaluated.

The first parameter to be changed is the value of P_o. Based on laser cavity performance, this value should probably be increased to between 70 and 90 watts. This value is higher than the one used by Sylvania [8] partly due to the measurement techniques employed to determine the quantity P_o. A comparison of the techniques is presented later in this section.

Using the value of Po = 75 watts, a trial and error approach was taken to fit calculated curves to the data in Figure 45 by varying α_o and dK. Since α_o = .006 was the absolute minimum single pass dissipative loss which could be achieved, it was felt that a higher value would be more realistic. Values of .008 and .01 were tried with the latter yielding the closer fit to the measured data. Based on the above two parameters, a value of dK = 0.06 cm/KW produced the curves shown in Figure 47. Although not a perfect match to the measured data, it does show that the above revised parameters are realistic. Increasing α_o even more would yield a larger value for dK but to do it properly and more accurately, a computer program should be developed.

One method of improving laser performance is to increase the value of dK. The value dK is given by the formula:

$$dK = \frac{\sigma_p \, k_p \, k_r \, \eta N_1 \, \sigma \, \tau \, T}{2h \, \nu_p}$$

where all of the parameters are defined in Reference (8). For the purpose of this discussion, however, it will suffice to say that all parameters on the right are dependent upon the laser material or the pump lamp with the exception of k_p which is the pump cavity efficiency. This parameter is therefore the easiest to maximize. The first step to increase the value of k_p to maximize the lamp coupling into the rod which requires that the radiating plasma fill the rod volume. Table IV shows

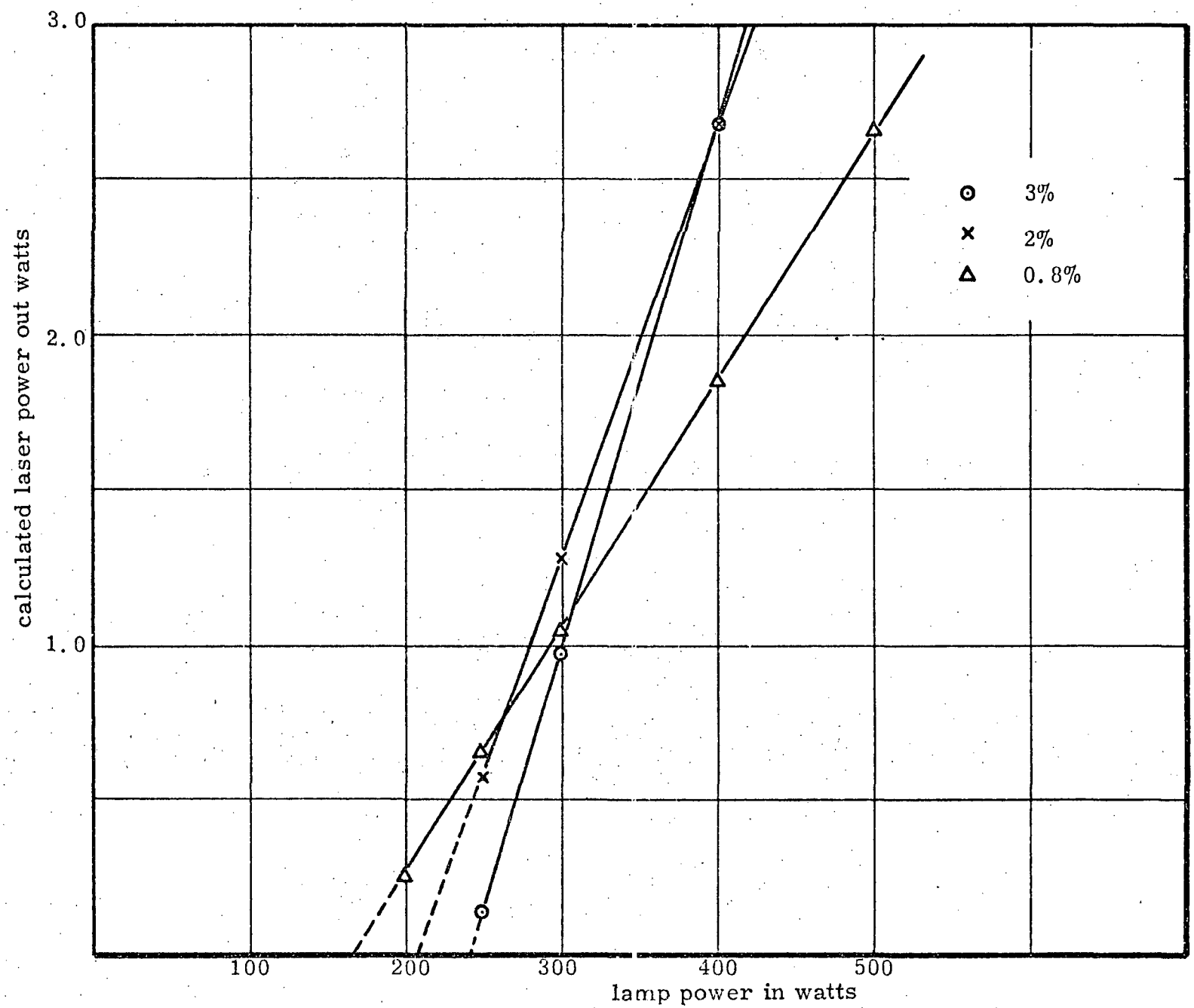

FIGURE 47 CALCULATED MATCH TO MEASURED LASER PERFORMANCE DATA

TABLE IV

Lamp bore dia mm	Luminescent Plasma dia mm	% Lamp Volume Luminescent	Lamp Voltage
3	2.05	47%	135
4	2.65	44%	80
6	3.80 *	40% *	65

* estimated

typical luminescent plasma diameters for various bore lamps. It can be seen that a 4mm lamp does not efficiently pump a 4mm rod while a 6mm bore lamp nearly fills the rod. This is probably the reason that the 6mm bore lamp resulted in a high slope efficiency than the 4mm lamp for 2% output coupling even though the fill was not optimized. The second parameter to be optimized is k_r which is the efficiency of converting input power into the desired radiation. For final lamps, this value is maximized by the optimization of the fill. In the case of the 6mm bore lamp, this parameter can still be increased by optimizing the fill ratio.

Data in the Sylvania report (Reference 8) gives measured values of dK for potassium iodide-mercury lamps. The value for potassium is 0.08 cm/KW and for rubidium is 0.046 cm/KW. In the theoretical analysis a value almost twice that of potassium was used for dK. However, with the measured value on a 4mm bore lamp being in the region of 0.06 cm/KW the original 0.15 cm/KW value needs correction. Based on observed lamp performance and expected improvements in k_p and k_r it is felt that the value of dK for the potassium rubidium lamp will lie between 0.10 and 0.11 cm/KW. Because of spectral overlaps in the broadened line structure, the above value is less than the sum of the individual potassium and rubidium values.

The next parameter which can be improved is α_o the single pass dissipative loss. The measured value was in the region of 0.01. The maximum improvement which can be achieved by use of high quality external mirrors and a high quality rod is a reduction of this loss coefficient to 0.006. A lower value could be achieved if the mirrors were on the rod ends.

The last key parameter which could be altered to improve performance is P_o. Using optimum lamp fills and fluorescence measurement techniques the P_o of the potassium-rubidium lamp was determined to be in the neighborhood of 75 watts. Since the fills were optimum, it is felt that improvements in this value would be difficult to achieve.

Based on Sylvania data (Reference 8) a lower value of P_o may have been expected from the potassium-rubidium lamp. They reported values of 23 watts for potassium and 47 watts for potassium and 47 watts for rubidium individually. The difference can be accounted for by examining the measuring techniques. Sylvania's method considered the radiation from the lamp in the

0.73 to 1.0μm band while the fluorescence technique only considers the radiation in this band which actually contributes to pumping of the Nd:YAG crystal. The effective pumping radiation is less than the total radiation from the lamp in the 0.73-1.0μm region, therefore, a higher more meaningful value of P_o is determined from the latter technique.

To summarize this section, consider the calculated curves shown in Figure 48. Curve A presents the optimistic performance which would have been achieved if the original key parameter assumptions were valid. Curve B presents the calculated representation of the measured data while the dashed curve presents the actual data. Based on analysis of the lamp/cavity performance, Curve C presents the revised estimate of achievable performance. It is believed that Curve C represents a realistic performance level for a carefully assembled system using state-of-the-art components and an optimized alkali pump lamp.

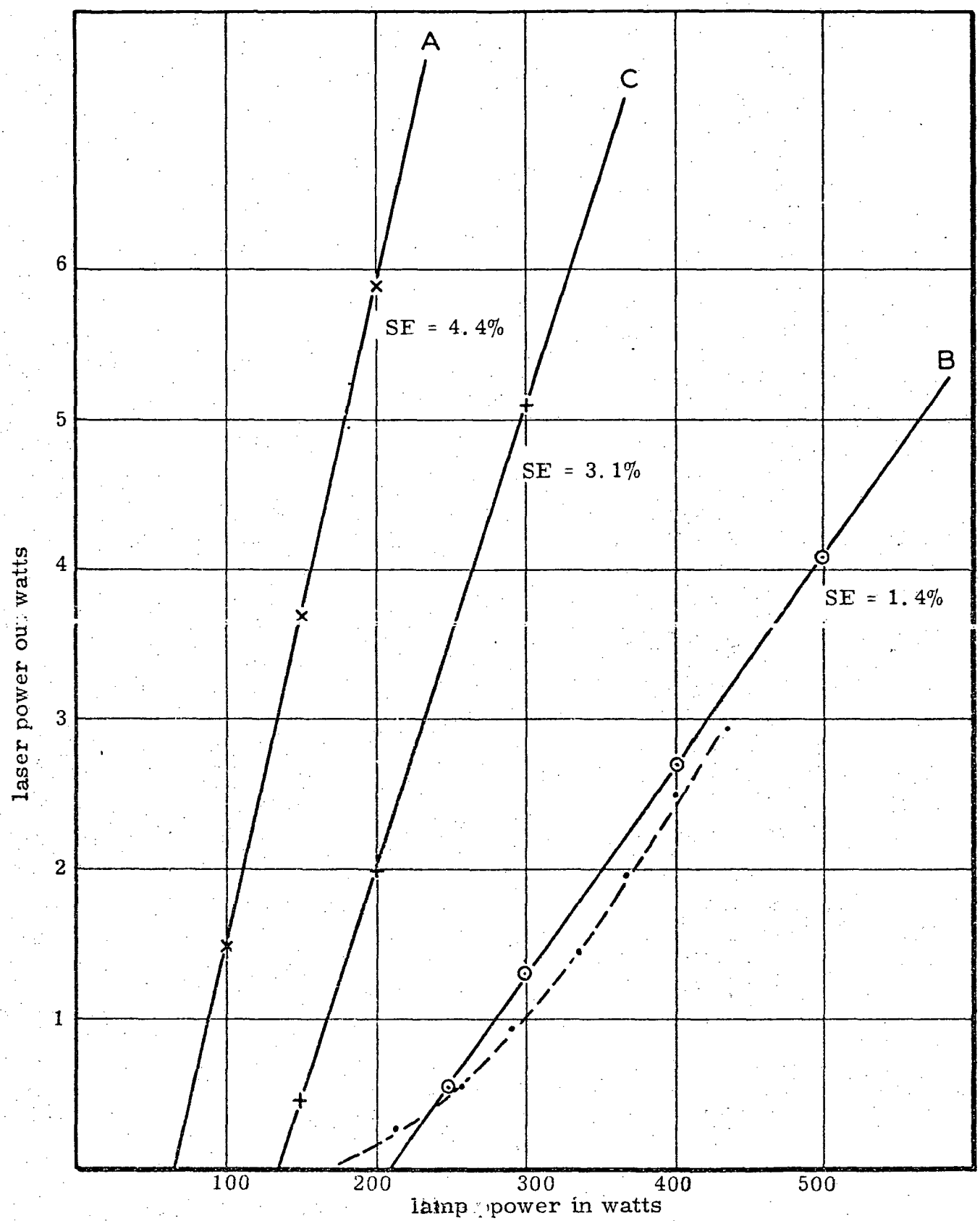

FIGURE 48 CALCULATED LASER PERFORMANCE

SECTION VII

CONCLUSIONS AND RECOMMENDATIONS

The lamp development program reported herein has resulted in the following conclusions and recommendations.

7.1 Conclusions

The data taken in support of the program allows the following conclusions to be made:

1) Lamp envelopes made from CDS instead of TDS sapphire show no signs of cracking or frosting even when subjected to wall loadings in excess of 70 Watts/cm^2 (with forced cooling).

2) The ability of the lamp to operate in an inert as well as a vacuum environment was demonstrated in Reference 9. This principle was extended under this contract to the use of flowing argon to permit wall loadings in excess of 70 Watts/cm^2. Extrapolation of the data indicates that a 4mm bore lamp should be capable of operation in excess of 100 Watts/cm^2 and a 6mm bore lamp in excess of 140 Watts/cm^2. However, wall loadings of this magnitude should never be required in the space qualified system.

3) For input powers between 200 and 300 watts, a 2% mirror offers the best output coupling.

4) The quantity P_o used in cavity parameterization and previously related to the thermal losses from the lamp has been redefined as a measure of spectral match to the Nd:YAG pump bands with the introduction of constant vapor pressure lamps.

5) A 6mm bore lamp offers a better match to a 4mm laser rod than a 4mm bore lamp since its radiating plasma closely matches the rod diameter.

6) A slope efficiency of 1.55% was achieved with an optimized 4mm bore lamp and 2% output coupling. With an unoptimized 6mm bore lamp, and the same output coupling the slope efficiency increased to 1.65%. Calculations indicate that for both an optimized 6mm bore lamp and an improved laser cavity the slope efficiency should be around 3% with multimode power of 1 watts for 170 watts input and 4 watts for 265 watts input.

7.2 Recommendations

Based on the accomplishments of the present program the recommendations may best be presented as task areas for additional investigations. These areas are as follows:

1) Lamp Life Improvement

The investigation has shown that the use of CDS envelopes over TDS envelopes results in longer envelope life with no signs of cracking, or frosting even at wall loadings of 70 Watts/cm^2 (with forced cooling). The area which needs additional improvement is the seal interface. Because of flange material failures reported on, the silica free frit has not had sufficient evaluation and life-test. Future programs should continue with these investigations.

2) Fill Optimization

At this time, the optimum fill ratios are known for 3 and 4mm bore devices. The optimum fill for the 6mm bore device has not been experimentally optimized as yet. Theory indicates that it should be around a 0.55 to 1 ratio of potassium to rubidium. Since a 6mm bore lamp provides a better pumping match to a 4mm rod than a 4mm bore lamp, this optimization becomes necessary.

3) IR Rejection

In a space qualified system, the laser rod will not be water cooled and therefore subject to degradation from this unfiltered radiation.

Figure 49 presents relative spectra for a rubidium lamp. It is interesting to note the relative magnitude of the radiation beyond 1.0μm compared to the useful radiation in the pump bands. Similar observations can also be made for a potassium lamp and for a combination potassium-rubidium lamp. Future efforts should both measure the degradation in laser performance due to this radiation and investigate methods to prevent the radiation from reaching the laser rod.

4) Mode Locking

As part of this program, several attempts were made to achieve single mode output. Because the $Ba_2NaNb_5O_{15}$ crystal was not optically perfect (had burn marks and surface scratches) it was too lossy when inserted into the low output laser cavity. With this crystal in place, laser threshold could not be achieved at input powers compatible with the pump lamp. Threshold and

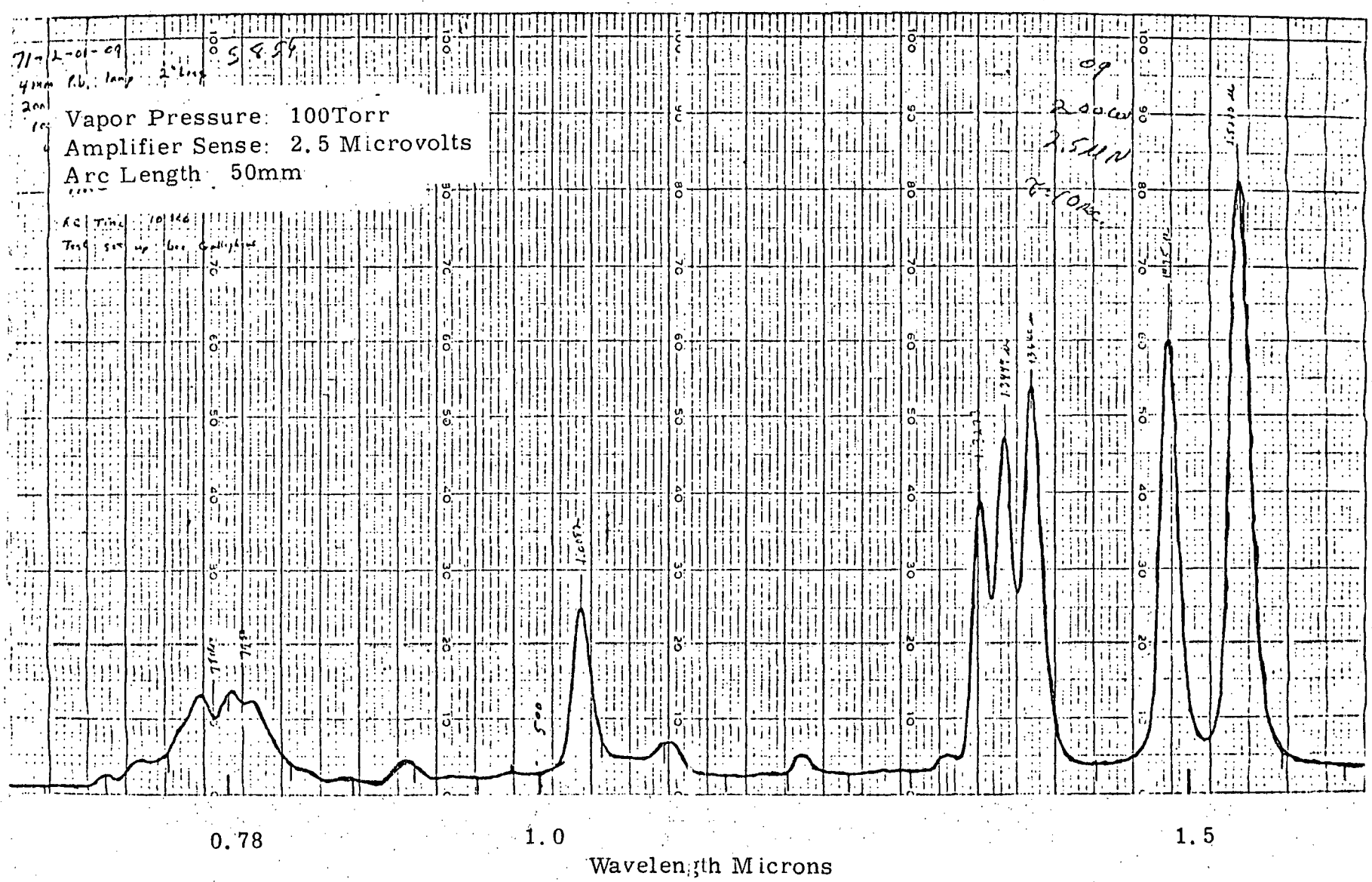

Figure 49 Relative IR Spectrum of a 4mm Bore Rubidium Lamp at 200 Watts

mode locking was achieved however using this crystal in a Krypton pumped system. In a future program, the methods of mode locking should be investigated for use in a low power low gain laser system with the most promising one being selected for optimization. An improved cavity configuration could then be designed and optimized to interface with an alkali pump lamp. Mode locking should then be readily achievable.

APPENDIX I

VAPOR PRESSURE OF THE K-Rb MIXTURE

The initial approach to the filling of lamps in this program was to take an arbitrary mixture of potassium and rubidium and controlling the reservoir temperature determine the operating vapor pressure. Another method utilized two reservoirs. In the first reservoir, rubidium was placed and the lamp baked until the desired vapor pressure is achieved. The surplus rubidium and first reservoir was then removed and the potassium was placed in the second reservoir. The lamp was then ready to be operated above the rubidium bake temperature with the characteristic of a constant rubidium vapor pressure device with a variable potassium pressure. However, both of these methods yielded results which were not anticipated. In the first case, the lamp performance varied greatly between lamps. In the second case, the constant rubidium vapor pressure state was not achieved. To explain these discrepancies, Raoult's law and the laws governing the mixing of solutions was explored in greater detail.

A solution is by definition, any phase containing more than one component; this phase may be gaseous, liquid or solid. For the purpose of this analysis, the potassium-rubidium mixture will be considered as an ideal solution. A solution is ideal if the vapor pressure of each component is proportional to the mole fraction (α) of that component in the solution.

Consider a mixture of potassium and rubidium with the mole fraction of potassium (α_K) being given by:

$$\alpha K = \frac{n_K}{n_K + n_{Rb}}$$

where n_K = number of moles of potassium
n_{Rb} = number of moles of rubidium

Since the solution is ideal, an atom of potassium will have the same tendency to escape into the vapor, whether it is surrounded entirely by other potassium atoms, entirely by rubidium atoms, or partly by potassium and partly by rubidium atoms. The partial pressure of the potassium in the mixture is therefore the same as that of the pure liquid potassium proportionately reduced on account of the lowered fraction of the potassium atoms in the solution. Expressed mathematically the relationship is

$$P_K = \alpha_K \; P_K^{\circ}$$

where: P_K is the partial vapor pressure of potassium above the solution
P_K° is the vapor pressure of pure potassium at the same temperature.

Similarly, $P_{Rb} = (1 - \alpha_K) \; P_{Rb}^{\circ}$

The above relationships are known as Raoult's Law. (15) (16)

The next step in the investigation is to develop mathematical relationships for the vapor pressures of pure potassium and pure rubidium. (17) Plotting ($\log_{10}$) vapor pressure against 1/T and fitting by method of least squares yields for potassium

$$\log_{10} P_K^{\circ} = 4.09537 - 4205.78/T + \log_{10} 760$$

and for rubidium

$$\log_{10} P_{Rb}^{\circ} = 4.046261 - 3880.02/T + \log_{10} 760$$

where: P_K° and P_{Rb}° are given in torr by using correction factor $\log_{10} 760$
T = temperature in $^{\circ}K$.

Taking the antilogs of the above expressions, relationships can then be found for P_K° and P_{RB}°.

The total vapor pressure is given by

$$P_T = P_K + P_{Rb} = \alpha_K P_K^{\circ} + (1-\alpha_K) \; P_{Rb}^{\circ}$$

A computer program was then developed to print values of P_K; P_{Rb}; P_T and P_K/P_{Rb} for varying values of temperature and α_K. The data resulting from the computer analysis is presented in graphical form in Figures 50 and 51. In Figure 50, the pressure ratio (P_K/P_{Rb}) is plotted against temperature ($^{\circ}K$) for mole fractions ranging from 0.05 to 0.95. In the second Figure 51. the total pressure is likewise plotted against temperature for values of α_K. Using these two graphs, the behavior of the potassium-rubidium mixture becomes predictable.

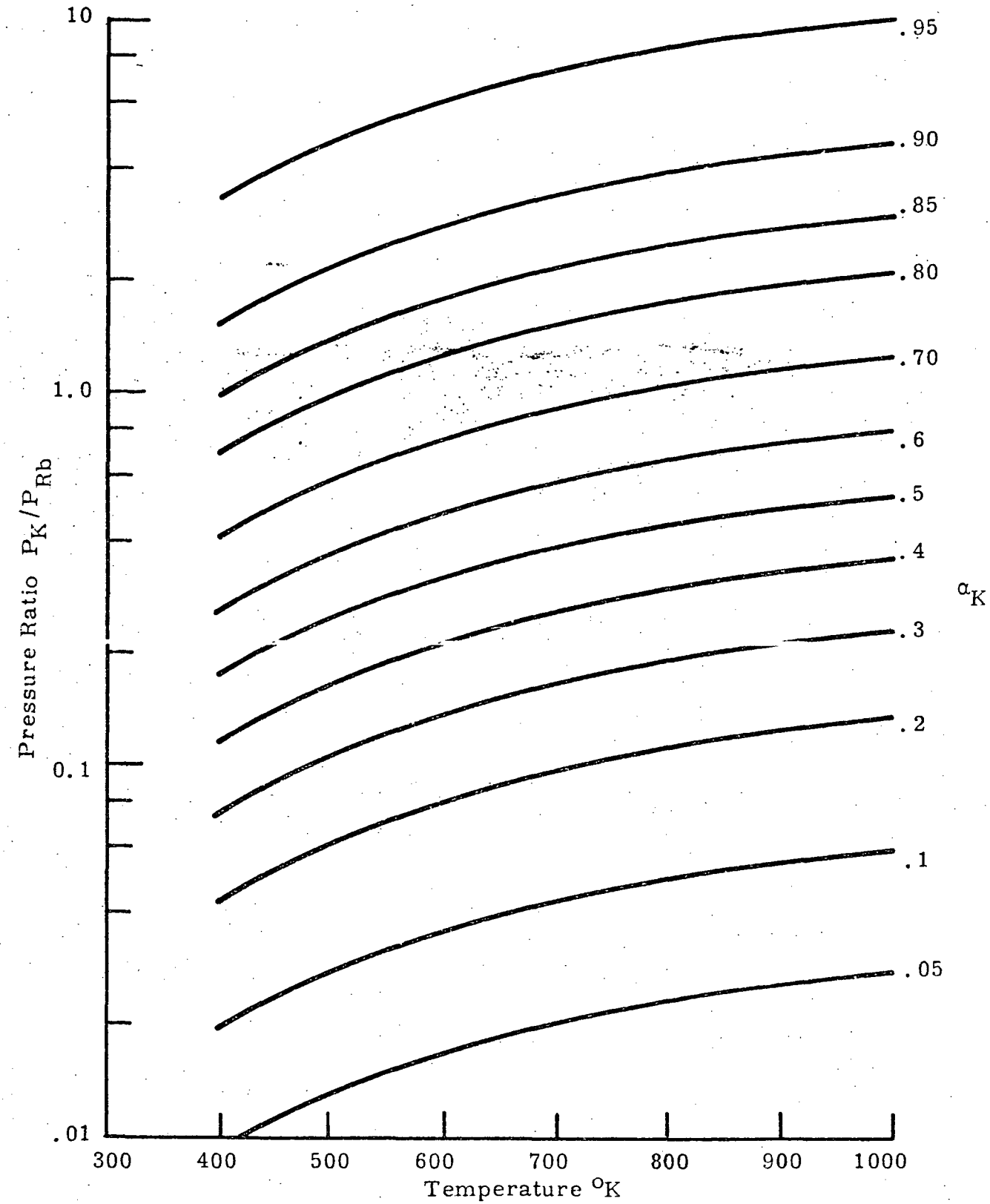

FIGURE 50 PRESSURE RATIO vs TEMPERATURE FOR VARIOUS MOLE FRACTIONS IN THE K-Rb MIXTURE

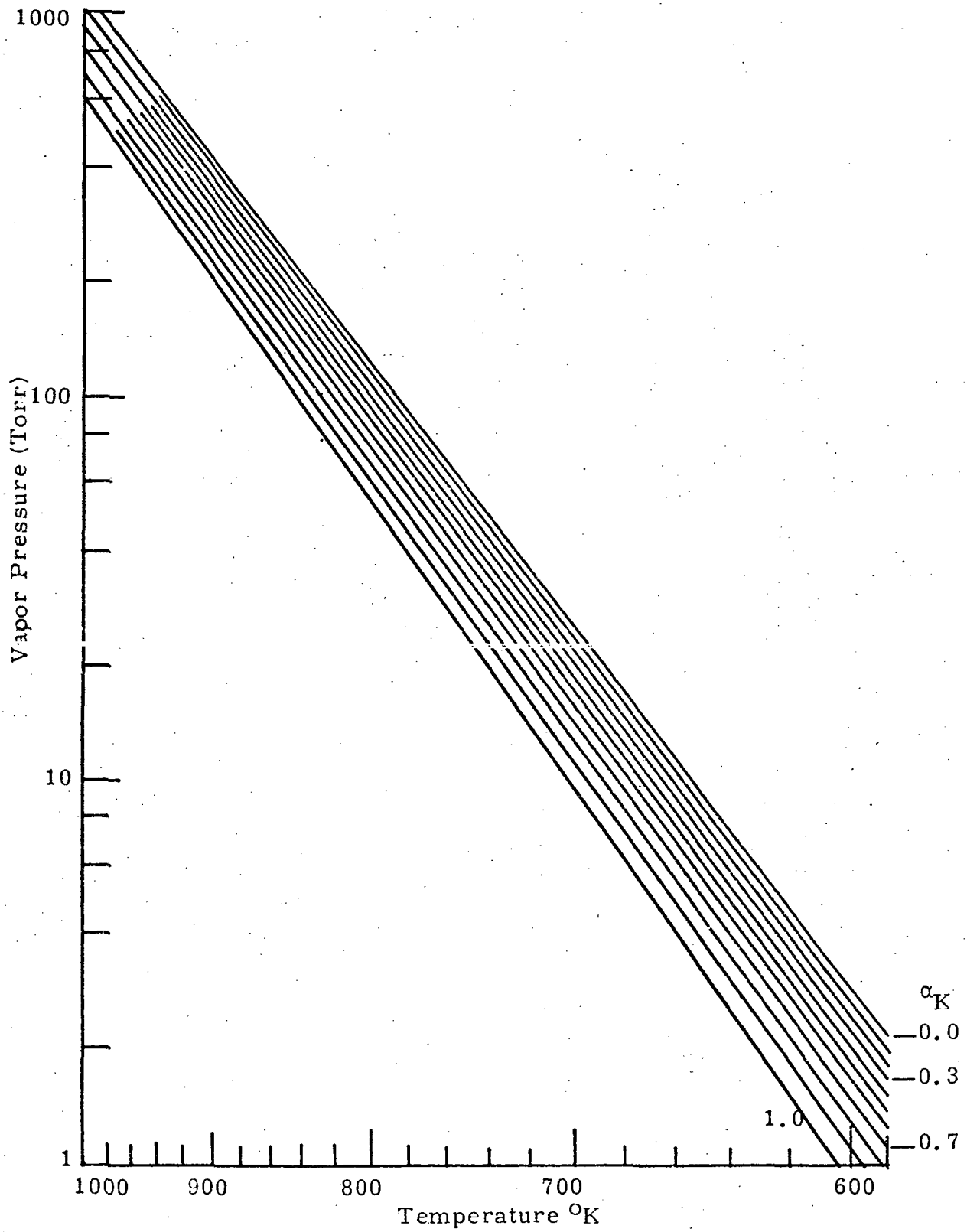

FIGURE 51 TOTAL VAPOR PRESSURE vs TEMPERATURE FOR VARIOUS MOLE FRACTIONS IN THE K-Rb MIXTURE

As an example, consider a 2 to 1 ratio by weight of potassium to rubidium. Let the potassium be the solute and the rubidium be the solvent. The mole fraction is given as the number of moles (grams/atomic weight) of solute per the number of moles of solute plus the number of moles of solvent. As a matter of definition, the number of moles of solvent is always based on 1000 grams of solvent. Therefore, for the 2 to 1 ratio take 2000 grams of potassium and 1000 grams of rubidium. α_K then becomes $\frac{2000/39.1}{2000/39.1 + 1000/85.48} = 0.81.$

From Figure 50, one can see that an α_K of 0.81 yields a pressure ratio of 0.73 to 2.3 over the temperature range of 400°K to 1000°K. Since the lamps are designed to operate with a typical reservoir temperature of from 450°C (723°K) to 550°C (823°K) it can be seen that the pressure ratio ranges approximately from 1.7 to 1.9 and the total pressure (from Figure 51) approximately from 18 to 90 torr.

The 2 to 1 ratio by weight of potassium to rubidium may also be expressed as having a pressure ratio of 0.73 to 2.3 (a function of temperature), a mole ratio of 4.4 to 1 and since the materials exist as atoms and not molecules an atomic ratio also of 4.4 to 1. Table V further illustrates these relationships for typical weight ratio fills of potassium to rubidium.

TABLE V

K-Rb RELATIONSHIPS

Weight Ratio (K/Rb)	Atomic (Mole) Ratio (n_K/n_{Rb})	α_K	Temp ^oK	Pressure Ratio (P_K/P_{Rb})
1-2	1.1-1	0.52	500	0.27-1
			600	0.35-1
			700	0.41-1
			800	0.47-1
1-1	2.2-1	0.64	500	0.55-1
			600	0.71-1
			700	0.86-1
			800	0.97-1
2-1	4.4-1	0.81	500	1.07-1
			600	1.38-1
			700	1.66-1
			800	1.88-1
3-1	6.6-1	0.87	500	1.70-1
			600	2.10-1
			700	2.70-1
			800	3.00-1
5-1	11-1	0.92	500	3.00-1
			600	4.00-1
			700	4.85-1
			800	5.50-1

APPENDIX II

SUMMARY (from Reference 9)

In summary, this program has again demonstrated that the use of lamps filled with carefully tailored ratios of potassium and rubidium result in efficient low power Nd:YAG laser pumps. Even more significant however, is the demonstration that the lamps can be operated in an inert or controlled atmosphere environment without significant degradation of lamp spectral output. A direct result of ability to operate in a non-vacuum environment is the significant reduction of envelope temperature (>200°C). This lower temperature improves lifetime due to increased wall strength and decreases the effects of long wavelength blackbody radiated energy. Based on lamp performance data the criterion for optimum device performance is to maintain the envelope temperature below 1000°C or for a 3mm bore lamp the wall loading about $40 W/cm^2$.

It is the constraint of maintaining the wall temperature below 1000°C which indicated that the 2mm bore lamp would have at best a limited lifetime. Table VI shows that for 120 watts input power the wall loading on a 2 x 3mm lamp is $64 W/cm^2$ and on a 2 x 50mm lamp $38.3 W/cm^2$. For stagnant argon cooling, it is shown in Figure 18 that the 2 x 30mm lamp would have a wall temperature well in excess of 1200°C and the 2 x 50mm lamp would have a wall temperature of 1080°C. Therefore, the input power specification for the lamp and the envelope temperature became incompatible requirements.

As in most R&D programs there are still some areas which need additional investigation. In this program these areas are seal improvement and envelope material performance. In the first area, thisprogram investigated three basic sapphire to metal sealing systems. They are copper seals, active alloy seals and frit seals. The copper seal was first attempted to provide a rugged test device for initial fill experiments. However, after the first few weeks it became apparent that there was difficulty in achieving successful metalization of the direct grown sapphire tubes without a high spoilage rate. In addition it was also known that due to both long term hydrogen diffusion through the copper and long term alkali attack on the copper that the 10,000 hour lifetime goal could not be attained by this device. Therefore additional efforts were not expended to improve this device.

At the same time, parallel efforts were being conducted to develop a successful active alloy braze. In these attempts, two methods of active alloy preparation were used. The first consisted of using prepared transfer tapes with various ratios of the ternary alloy (V, Zr, Ti) in combination with a organic binder.

TABLE VI

INTERNAL WALL LOADING (W/CM^2) FOR SEVERAL TUBE SIZES

Tube Size mm	Wall Area cm^2	Wall Loading (W/cm^2) @ 120 Watts	@ 150 Watts
2 x 30	1.88	64	80
2 x 50	3.14	38.3	48
2 x 75	4.7	25.5	32
3 x 30	2.72	42.5	55
3 x 50	4.7	25.5	32

No leaktight sapphire to niobium or sapphire to sapphire bonds were achieved using the transfer tape approach. Next, the use of three braze washers made from each of the braze metals was used. In these attempts a leaktight bond was achieved only between sapphire and sapphire but not between sapphire and niobium. At this point, the active alloy seal investigation was discontinued and full efforts were directed to frit seals.

The use of frits as a method of achieving the required sapphire to metal seal is well founded since there are in existence commercial sodium-mercury lamps using PCA to niobium frit seals. These lamps have lifetime ratings of 10,000 to 15,000 hours which is the goal of this program. During the course of investigation, both 1731 frit containing a small percentage of silica and an experimental type of silica free frit were used. A lamp incorporating the 1731 frit operated for 180 hours before a seal failure occurred. This failure was attributed to a parting of the frit caused by the thick (.017") flange. To correct this problem the final lamps had .005" flanges in the region of sapphire contact. At the end of the program there was insufficient data taken to predict the anticipated lifetimes of the silica free frit.

In conclusion, this program has shown the ability of frit materials to provide relatively reliable metal to sapphire seals in an alkali environment under high thermal conditions (seals $\approx 600^{\circ}C$).

In the area of envelope material, additional investigation is needed to fully characterize the performance and the degradation processes associated with the direct grown sapphire. The program showed that many of the envelope failures occurred along the striations present in the sapphire material. These envelopes also acquired an internal frosting after varying periods of operation. It is necessary to determine if this frosting is a processing related effect or due to contaminants or irregularities present in the sapphire material.

The lamp-laser performance may be summarized by indicating the achievements attained.

1) Lamp operation in an inert environment does not have any significant degradation effect on laser performance.

2) The ability to achieve low laser threshold in the order of 70-90 watts with the use of alkali lamps has been demonstrated.

3) Laser output in excess of 250 milliwatts has been demonstrated and extrapolated to yield 1 watt at approximately 380 watts input. The output power can be increased by optimizing the laser cavity design to the lamp and closing the lamp clearance holes in the end plates.

4) Operating lifetime of 25 hours has been demonstrated inside the laser cavity.

5) The optimum spectral match for a 3mm bore lamp occurs for a fill ratio of approximately 2 to 1 by weight (4.4 to 1 molar ratio) of potassium to rubidium. It is estimated that a slightly better match may be achieved with a 1.85 to 1 ratio by weight of potassium to rubidium.

REFERENCES

1. I. Liberman, D.A. Larson, C.H. Church, "Efficient Nd:YAG Lasers Using Alkali Additive Lamps", IEEE J. Quant. Elect. Vol. QE-5, No. 5, p. 238, May 1969.

2. T. H. Read, "The CW Pumping of Nd^{3+}: YAG by Water-Cooled Krypton Arcs", Applied Physics Letters, Vol. 9, Nov. 1966.

3. G. Reiling, "Characteristics of Mercury Vapor-Metallic Iodide Arc Lamps", JOSA, Vol. 54, No. 4, Apr. 1964.

4. J. F. Waymouth et al, "A New Metal Halide Arc Lamp," Illum. Engr., 85 (Feb. 1965).

5. I. Liberman, et al, "Optical Pumps for Lasers - Phase II, Final Report", Contr. DA-28-043-AMC-02097 (E) 1968.

6. C. H. Church, et al, "Arc Discharge Sources - Final Report", Contract Nonr. 4647 (00), AD 65718 Mar. 1967.

7. R. G. Schlecht, C. H. Church and D. L. Larson, "High Efficiency NaI Pumping of a Continuous YAG:Nd^{3+} Laser, IEEE J. Quant. Elect. Vol. QE-2, pp. xlvii-xlix, April 1966.

8. J. D. Foster and R. F. Kirk, "Space Qualified Nd:YAG Laser (Phase I-Design)", Contract NAS12-2160, Report No: NASA CR-1771, Oct. 1971.

9. K. B. Ward, "Low Power CW Alkali Pump Lamps" Final Report AFAL-TR-72-40, Contract No. F33615-71-C-1798, May 1972.

10. La Bell, H. E. Jr. et al, "Growth of Controlled Profile Crystals from the Melt-Part III, Mat. Res. Bull., Vol. 6, Pergamon Press, Inc. (1971),

11. Proceedings of an International Symposium on High-Temperature Technology, McGraw-Hill Book Co., Inc., New York (1960).

12. Johnson, P.D., J. Am. Ceram. Soc., 33, 168 (1950).

13. Elenbaas, W., "The High Pressure Mercury Vapor Discharge", Inter Science Publishers, N.Y., 1951.

14. Nobel, L., "Pump Lamps for Nd:YAG Lasers" Final Report AFAL-TR-72-50, Contract No. F33615-71-C-1812, Feb. 1972

15. Lay, J. E., Thermodynamics, Merril Books, 1963.

16. Hutchinson, E., Chemistry-The Elements and Their Reactions, Saunders, 1959.

17. Bonilla, C. F., Sawhney, D. L., and Makansi, M. M., "Vapor Pressure of Alkali Metals", Transactions of the ASM, Vol. 55, 1962.